STUDY OF RADIOACTIVITY LEVELS IN DIFFERENT KINDS OF FOOD STUFF GROWN ON THE BANK OF RUPSHA RIVER AND ITS IMPACT ON HUMAN HEALTH

M. Sc. Thesis

MST. NUR NAHAR

DEPARTMENT OF PHYSICS
KHULNA UNIVERSITY OF ENGINEERING & TECHNOLOGY
KHULNA-9203, BANGLADESH
APRIL 2016

STUDY OF RADIOACTIVITY LEVELS IN DIFFERENT KINDS OF FOOD STUFF GROWN ON THE BANK OF RUPSHA RIVER AND ITS IMPACT ON HUMAN HEALTH

M. Sc. Thesis

MST. NUR NAHAR
ROLL NO: 1555501
SESSION: JANUARY-2015

A THESIS SUBMITTED TO THE DEPARTMENT OF PHYSICS, KHULNA UNIVERSITY OF ENGINEERING & TECHNOLOGY, IN PARTIAL FULFILLMENT OF THE REQUIREMENT FOR THE DEGREE OF MASTER OF SCIENCE

DEPARTMENT OF PHYSICS
KHULNA UNIVERSITY OF ENGINEERING & TECHNOLOGY
KHULNA-9203, BANGLADESH
APRIL 2016

DEDICATED

TO

MY BELOVED PARENTS

Acknowledgements

My very first gratitude goes to the omnipotent, omniscient Allah for enabling me to complete the synchronized study by His grace.

I express with due respect my deep sense of gratitude and indebtedness to my Supervisor **Professor Dr. Jolly Sultana**, Department of Physics, Khulna University of Engineering & Technology, Khulna, for her indispensible guidance, keen interest, constructive and constant inspiration throughout suggestions close supervision and fruitful discussion during the research work.

I take the privilege to express my gratitude and deep respect to my Joint-supervisor **Dr. Md. Idris Ali**, Chief Scientific Officer (CSO), Health Physics & Radioactive Waste Management Unit (HPRWMU), Institute of Nuclear Science and Technology (INST), Atomic Energy Research Establishment (AERE), Savar, Dhaka, Bangladesh for his continuous efforts guidance and direction towards the successful completion of the work. I am grateful to **Dr. Debasish Paul**, CSO, HPRWMU, INST, AERE, Savar, Dhaka for his keen interest, encouragement and whole-hearted co-operation in connection with the present work.

I am also grateful Mr. Md. Abu Haydar, SO, HPRWMU, INST, AERE, Savar, Dhaka for his all out efforts and continuous help in the conduction of this study. In absence of this kind of help from them, the work could never be completed. I am thankful to Dr. S. M. Yunus, Director, INST, AERE, Bangladesh Atomic Energy Commission (BAEC) for giving me the opportunity to work at the laboratories of HPRWMU, INST, AERE, Savar, Dhaka.

I gratefully acknowledge Prof. Dr. Shibendra Shekher Sikder, Prof. Dr. Mahbub Alam and Prof. Dr. Md. Abdullah Elias Akhter Department of Physics, Khulna University of Engineering & Technology, for their co-operation and inspiration during this work. My thanks are also for Md. Kamrul Hasan Reza, Md. Asaduzzaman, Mr. Sujit Kumar Shil, Md. Alamgir Hossain Assistant Professor & Suman Kumar Halder, Md Ashiqur Rahman, Sumon Deb Nath, Lecturer, KUET, for their moral support.

I would like to express my heart full obligation thanks to my parents, brother, sister, and all others family members for their multifaceted support and love no matter distance.

I would also like to thank to all of my friends and well-wishers. I am grateful to the authority of KUET for providing me the relevant facilities and financial assistance for the research work.

Mst. Nur Nahar

ABSTRACT

The natural environment around us is the prime source of radiation. The activity concentrations of radionuclide have been investigated in the human food-chain. To determine the radioactivity level in the Paddy, Arum, Papaya &Leafy vegetables samples collected from different locations on the Bank of Rupsha River at Rupsha upazialla in Khulna of Bangladesh.

In the present study, a total of 6 Paddy, 7 Leafy vegetables, 8 Arum and 7 Papaya samples have been collected from 8 locations of the area under investigation. The samples have been analyzed by gamma-ray spectrometry system using a 'Hyper-Pure Germanium' (HPGe) detector of 20% relative efficiency to identify the probable radionuclides, activity concentrations and the radiological risks to human from intake of these crops and vegetables. Natural radionuclides such as ^{226}Ra, ^{232}Th and ^{40}K have been found in the samples and no artificial radionuclide has been detected in any of the sample.

The activity concentrations of ^{226}Ra, ^{232}Th and ^{40}K in Paddy samples have been found to be varied from 17.59±4.44 Bq/Kg to 42.32±4.48 Bq/Kg, average 24.43±5.16 Bq/Kg, BDL to 3.745±2.99, average 2.048±2.798 Bq/Kg and 35.97±150.34 Bq/Kg to 170.12±135.49 Bq/Kg, average 93.96±133.75 Bq/Kg, respectively. In Leafy vegetables activity concentrations have been found to be varied from 25.97±11.28 Bq/Kg to 49.11±13.48 Bq/Kg, average 34.22±12.55 Bq/Kg, BDL to 17.075±11.515 Bq/Kg, average 9.84±10.63 Bq/Kg and 626.88±176.34 Bq/Kg to 1378.25±225.93 Bq/Kg, average 1110.50±200.24 Bq/Kg. In Arum samples activity concentrations have been found to be varied from BDL to 8.78±3.08 Bq/Kg, average 5.77±2.97 Bq/Kg, BDL to 2.53±4.32 Bq/Kg and 426.91±107.23 Bq/Kg to 1280.71±133.89Bq/Kg, average 758.298±109.66 Bq/Kg. The activity concentrations in Papaya samples have also been found to be varied from 13.295±9.64 Bq/Kg to 77.96±22.01 Bq/Kg, average 43.31±15.28 Bq/Kg, BDL to 26.2±17.27 Bq/Kg, average 15.44±11.28Bq/Kg and 1112.65±202.33 Bq/Kg to 1712.47±221.96Bq/Kg, average 1490.27±226.27 Bq/Kg, respectively.

The annual effective dose of all samples (Paddy, Leafy vegetables, Arum and Papaya) have been found that intake high effective Dose of ^{226}Ra of 349.23 µSv y^{-1} by Papaya samples and 344.92 µSv y^{-1} by Leafy vegetables samples. ^{232}Th of 248.29 µSv y^{-1} by Paddy samples & ^{40}K of 454.90 µSv y^{-1} by Arum samples. The maximum effective dose of ^{226}Ra (0.39mSv) is high than world safe value (0.12mSv) in Papaya, The effective dose of ^{40}K (0.45mSv) is high than world safe value (0.17mSv) in Arum and ^{232}Th (0.24mSv) is slightly than world safe value(0.12mSv) in Paddy samples. The natural radioactivity concentrations of ^{226}Ra, ^{232}Th and ^{40}K for all samples are higher than the worldwide average values. The current result is slightly higher compared with the results of similar studies undertaken in other countries and in different places in Bangladesh. However, these values of doses are much below the permissible level set by ICRP, and, therefore, there is no immediate health risk on workers and public due to natural radioactivity present in the samples of the study area.

Therefore, the results on radionuclide concentrations and annual effective dose have been obtained from this study may provide with interesting information to evaluate the extent, degree and routes of the radiological impact. This study would also be useful as a base line data on radiation exposure and environmental impact caused by crops and vegetables on the Bank of Rupsha River in Khulna of Bangladesh.

CONTENTS

		Page
Title Page		i
Declaration		ii
Certificate of Research		iii
Dedicated		iv
Acknowledgement		v
Abstract		vi
Contents		viii
List of Tables		xi
List of Picture		xii
List of Figures		xiii
Abbreviation		xv
CHAPTER I	**Introduction**	**1-25**
1.1	General introduction	1
1.2	Radioactivity and Radiation	4
1.3	Discovery of Radioactivity	4
1.4	Classification of Radiation	5
1.4.1	Ionizing Radiation	5
1.4.2	Non - ionizing Radiation	8
1.5	Radioactive Decay	8
1.6	Classification of Radioactivity	10
1.6.1	Natural Radioactivity	10
1.6.1.1	Origin of natural radionuclide	11
1.6.1.2	Origin of Potassium	16
1.6.2	Artificial or Induced Radioactivity	16
1.7	Sources of Radiation	18
1.9	Objective of Present study	24

CHAPTER II Literature Review 26-46

2.1 Introduction 26
2.2 Review of the previous work 26
2.3 Information on the effects of Radiation 29
2.4 Energy, Activity, Intensity and Exposure of radiation 29
2.5 Biological effect of radiation 31
2.6 Cell Radiosensitivity 32
2.7 Health Effects from Exposure of Radiation 34
1.7.1 Stochastic Effect 36
2.7.2 Non-Stochastic Effect or Deterministic Effect 36
2.7.3 Radiation Effects on the human body 37
2.8 Units of Radioactivity 42
2.9 Radiation Dosimetry 43
2.10 Exposure Limits 45

CHAPTER III Methodology 47-79

3.1 Study Area 47
3.2 Sampling Locations 47
3.3 Sample Collection and Preparation 47
3.4 Experimental set-up 52
3.5 Apparatus Used 53
3.5.1 High Purity Germanium (HPGe) Detector 53
3.5.2 Standard Geometry Setup 63
3.5.3 Standard γ- Ray Sources 64
3.5.4 Calibration of Detector Parameters 64

3.5.5 Counting Efficiency of Gamma Spectrometry 66
3.5.6 Lower Limit of Detector of Radionuclides 68
3.5.7 Statistical Error in Counting 70
3.5.8 Prepared Standard Source efficiency results 72
3.6 Measurement set-up 73
3.7 Calculation of Activity concentration and Annual effective Dose of all samples 76
3.8 Radiometric Measurement 78

CHAPTER IV Results and Discussion 80-107

4.1 Introduction 80
4.2 Radioactivity in Paddy Samples 80
4.3 Radioactivity in Leafy vegetables Samples 85
4.4 Radioactivity in Arum Samples 90
4.5 Radioactivity in Papaya Samples 95
4.6 Annual intake of Radionuclides and Estimation Annual effective Dose 101
4.6.1 Annual effective Dose in Paddy Samples 101
4.6.2 Annual effective Dose in Leafy vegetables Samples 101
4.6.3 Annual effective Dose in Arum Samples 104
4.6.4 Annual effective Dose in Papaya Samples 104
4.7 Discussion 107

CHAPTER V Conclusion 108

References 109-113

LIST OF TABLES

Table no.	Description	Page
1.1	The Uranium Series	12
1.2	The Thorium Series	13
1.3	The Actinium Series	14
1.4	The Neptunium Series	15
1.5	Dose Limits for Individuals	24
2.1	Acute Radiation Syndromes	40
3.1	Detailed of the collected samples for study (with location- local name)	51
3.2	Characteristics of the shielding material used around the detector	62
3.3	Physical characteristics of ^{137}Cs and ^{60}Co radionuclide	64
3.4	Gamma ray energy calibration sources	66
3.5	Detection limits of the HPGe detector	70
3.6	Counting efficiencies of the HPGe detector used for activity calculation	72
3.7	Gamma lines used for γ-spectrometry determinations	79
4.1	Activity Concentrations of radioactive daughter elements of ^{226} Ra &^{232} Th radioactive series in Paddy samples under study	82
4.2	Activity Concentration of radio nuclei ^{226}Ra &^{232}Th and ^{40}K in Paddy samples	84
4.3	Activity Concentrations of radioactive daughter elements of ^{226} Ra &^{232} Th radioactive series in Leafy vegetables samples under study	87
4.4	Activity Concentration of radio nuclei ^{226}Ra &^{232}Th and ^{40}K in Leafy veg. samples	89
4.5	Activity Concentrations of radioactive daughter elements of ^{226} Ra &^{232}Th radioactive series in Arum	92

4.6	Activity Concentration of radio nuclei ^{226}Ra &^{232}Th and ^{40}K in Arum	94
4.7	Activity Concentrations of radioactive daughter elements of ^{226} Ra &^{232} Th radioactive series in papaya samples under study	97
4.8	Activity Concentration of radio nuclei ^{226}Ra &^{232}Th and ^{40}K in Papaya	99
4.9	Activity concentration (Bq/Kg) in Vegetables and Rice with different districts of Bangladesh**.**	100
4.10	Comparison of the present study with different parts of the world for radio nuclides in vegetables samples (Bq/Kg).	100
4.11	Annual intake of radionuclides in the Paddy samples and estimated annual effective Dose	102
4.12	Annual intake of radionuclides in the Leafy vegetables samples and estimated annual effective Dose	103
4.13	Annual intake of radionuclides in the Arum samples and estimated annual effective Dose	105
4.14	Annual intake of radionuclides in the Papaya samples and estimated annual effective Dose	106

Picture no. **LIST OF PICTURES** **Page**

3.1	Prepared samples	49
3.2	A complete setup of γ-counting system (HPGe Detector with 20% relative efficiency).	56
3.3	Digital Spectrum Analyzer (DSA) 1000	58
3.4	Shielding Arrangement of the Detector	61
4.1	Paddy sample grown on the Bank of Rupsha Rive	81
4.2	Paddy Sample dry in sun shine	81
4.3	Leafy vegetables sample grown on the Bank of Rupsha River	86

LIST OF PICTURES

Picture no.		Page
4.4	Leafy vegetables Sample dry in sun shine	86
4.5	Arum sample grown on the Bank of Rupsha River	91
4.6	Arum Sample dry in sun shine	91
4.7	Papaya sample grown on the Bank of Rupsha River	96
4.8	Papaya Sample dry in sun shine	96

LIST OF FIGURES

Figure no.	Description	Page
1.1	Radiation pathway	2
1.2	Alpha, Beta and Gamma radiation penetration	6
1.3	Types of Radiation in the Electromagnetic Spectrum	8
1.4	Elements of uranium, thorium and actinium series and their daughter products	9
2.1	Classifications of Biological Effects of Radiation	35
2.2	Stochastic Dose Response Curve	36
2.3	Deterministic Dose Response Curve	37
2.4	Radiation effect	42
3.1	Location map of sampling (using Google map) area Rupsha, Khulna, Bangladesh	48
3.2	Flow-chart illustrating the pretreatment of vegetable samples.	50
3.3	Block diagram of gamma spectroscopy system (HPGe detector) used in the present work.	55
3.4	Photograph of Cryostat	57

3.5	Block diagram of preamplifier	59
3.6	Efficiency curve of the HPGe detector of 20% relative efficiency for the solid matrix	74
3.7	CPS ratio Vs energy diagram	76
4.1	Graphical representation of the activity concentrations of daughters (^{214}Pb; ^{214}Bi) of ^{226}Ra in all Paddy samples	83
4.2	Graphical representation of the activity concentrations of daughters (^{212}Pb.^{208}Ti, ^{228}Ac) of ^{232}Th in all Paddy samples	83
4.3	Graphical representation of the activity concentrations of parents' nuclei ^{226}Ra, ^{232}Th and ^{40}K in all Paddy samples	84
4.4	Graphical representation of the activity concentrations of daughters (^{214}Pb; ^{214}Bi) of ^{226}Ra in all Leafy vegetables samples	88
4.5	Graphical representation of the activity concentrations of daughters (^{212}Pb.^{208}Ti, ^{228}Ac) of ^{232}Th in all Leafy vegetables sample	88
4.6	Graphical representation of the activity concentrations of parents' nuclei ^{226}Ra, ^{232}Th and ^{40}K in all Leafy veg. samples	89
4.7	Graphical representation of the activity concentrations of daughters (^{214}Pb; ^{214}Bi) of ^{226}Ra in all Arum samples	93
4.8	Graphical representation of the activity concentrations of daughters (^{212}Pb.^{208}Ti, ^{228}Ac) of ^{232}Th in all Arum samples	93
4.9	Graphical representation of the activity concentrations of parents' nuclei ^{226}Ra, ^{232}Th and ^{40}K in all Arum samples	94
4.10	Graphical representation of the activity concentrations of daughters (^{214}Pb; ^{214}Bi) of ^{226}Ra in all Papaya samples	98
4.11	Graphical representation of the activity concentrations of daughters (^{212}Pb.^{208}Ti, ^{228}Ac) of ^{232}Th in all Papaya samples	98
4.12	Graphical representation of the activity concentrations of parents' nuclei ^{226}Ra, ^{232}Th and ^{40}K in all Papaya samples	99
4.13	Variation of estimated Annual Effective Dose with all Paddy sampling locations	102

4.14	Variation of estimated annual effective Dose with all Leafy vegetables sampling locations	103
4.15	Variation of estimated annual effective Dose with all Arum sampling locations	105
4.16	Variation of estimated annual effective Dose with all Papaya sampling locations	106

ABBREVIATIONS

LLD	Lower Limit of Detection
BAEC	Bangladesh Atomic Energy Commission
ICRP	International Commission on Radiological Protection
IAEA	International Atomic Energy Agency
WHO	World Health Organization
HPGe	High Purity Germanium Detector
ICRU	International Commission on Radiological Units
INST	Institute of Nuclear Science and Technology
HPS	Health Physics Society
HPRWMU	Health Physics and Radioactive Waste management Unit
NaI	Sodium iodide crystal detectors
DSP	Digital signal processing techniques
HPGe	High purity germanium detectors
LN_2	Liquid nitrogen
DSA	Digital Spectrum Analyzer
MCA	Multi channel analyzer
TRP	Transistor reset preamplifier
ADC	Analog-to-digital converter
NCRP	National Committee on radiation Protection.
NAC	National Academy of Sciences

CHAPTER I

Introduction

1.1 General Introduction

Radiation is a part and parcel of our environment. There is no place or element in the universe without radiation. At the very beginning when there were no sign of lives in the universe, still was full of radiation (Kannan et al., 2002). Radiation and radioactivity are presence all the constituents of our environment such as soil, water, air, plants, wood, vegetables, food, fruits etc. all living and non living components. Radiation is everywhere, but high level of radiation definitely harmful to human being. Studies on radiation levels and radionuclide distribution in the environment provide vital radiological baseline information. Such information is essential in understanding human exposure from different sources of radiation.

Human and animal kingdom, however, make adjustment to the natural radiation sources. The main sources of radiation are the following:

1. Cosmogenic radionuclides produced by cosmic ray interactions
2. Radioactive substance in the earth crust
3. Trace amounts of radioactivity in the body
4. Human produced radionuclides
5. Cosmic rays from outer space which bombard the earth

The distribution of these radionuclides in nature, contribution and movements can seriously be affected by the activity population. Sometimes this can result in deleterious effect such as harmful consequence on environment and health hazards to human being, entering into the body through different metabolic pathway. For the assessment of effective dose equivalent to the population of Bangladesh, It is necessary to estimate the concentration of various radionuclides in the environment, entering the various organs of the body as a function of time. Fig 1.1 shows the radiation pathway.

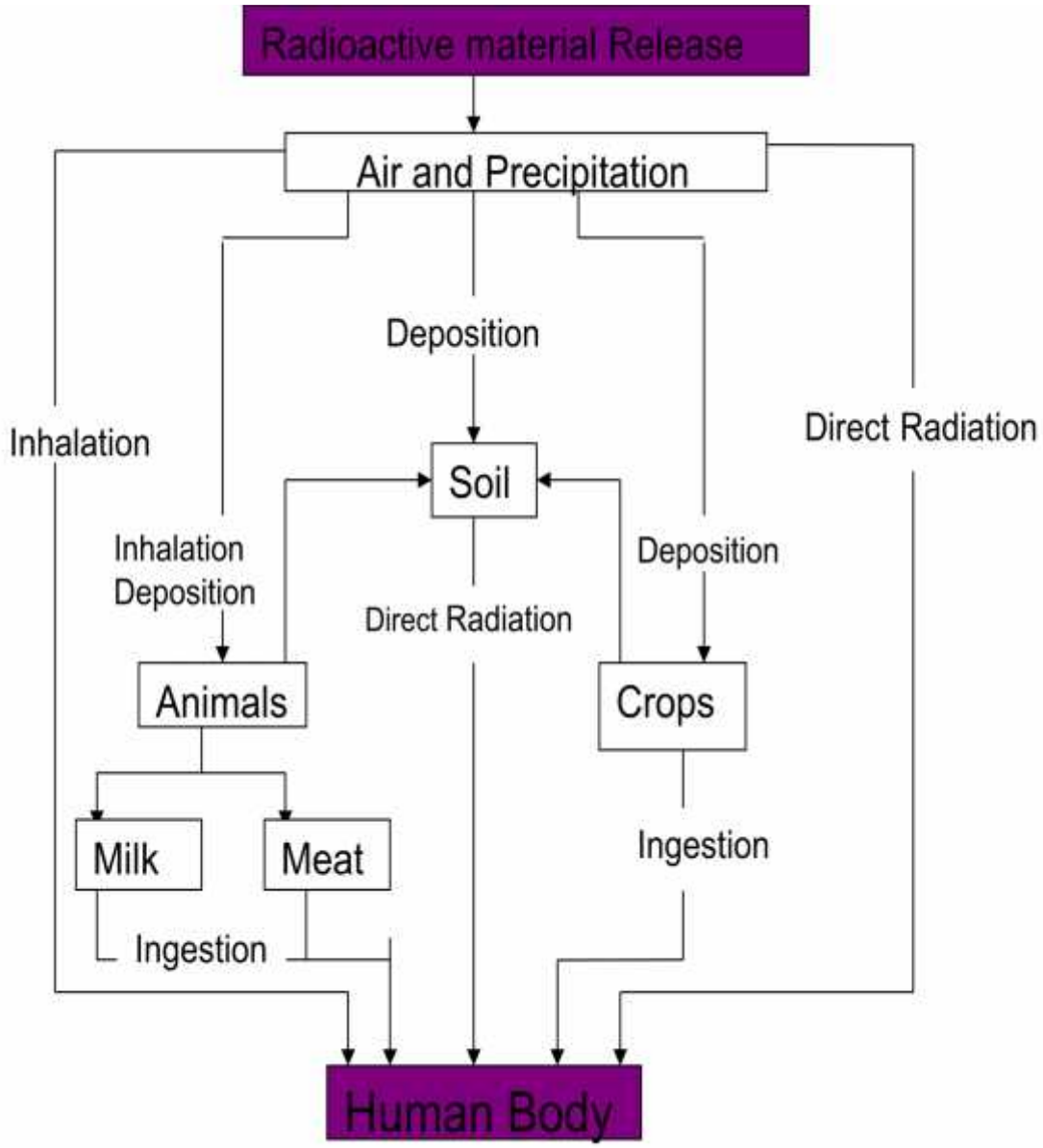

Fig. 1.1: Radiation pathway

The present study has been designed to determine the level of natural K-40, U-238 & Th-232 radioactivity in the food (crops and vegetables) samples. Radioactivity are not uniformly distributed and vary from region to region (Yeasmin and Begum, 2012). Therefore, the knowledge of their distribution in crops and vegetables (Paddy, Leafy vegetables, Arum and Papaya) play an important role in radiation protection activities. The radioactivity concentration of these nuclides above permissible level is very harmful to the human body. Therefore, measurement of natural radioactivity in these elements and the radiation doses arising from these radionuclides are of great interest to the researchers which have led the nationwide surveys throughout the world (Asimov and Isaac, 1976) (Zhang, 2012). Since natural radiation is the largest contributor of external dose to the world population, assessment of gamma radiation dose from natural sources is of particular importance.

Rupsha is one of the agricultural zones located at the bank of Rupsha river near the Khulna city. Large number of populations, some brick field, various shops and ship-industries in Khulna near the agricultural zones. Industrial activities discharge untreated or poorly treated industrial wastewater, effluent and even sludge into the surrounding environment which may contain elevated level of radioactivity. Besides, the farmers in that area are randomly using fertilizers and pesticides in agricultural lands out of their ignorance. A very little work has been done and almost no significant data are available on the radioactivity contents in the crops of the agricultural zones in Khulna, Bangladesh. Moreover, probable radiological impact on the people and environment due to the radioactivity content in these environmental elements needs to be determined for the radiation protection purpose.

The present study is to determine the probable radionuclides, radioactivity concentration and annual effective dose in the agricultural crops and vegetables such as Paddy, Leafy vegetables, Arum and Papaya etc. The present work helps the determination of radiation dose received by the people from these crops and vegetables to human food-chain.

1. 2 Radioactivity and radiation

Unstable atomic nuclei will spontaneously decompose to form nuclei with a higher stability. The decomposition process is called radioactivity. The energy and particles which are released during the decomposition process are called radiation. When unstable nuclei decompose in nature, the process is referred to as natural radioactivity. When the unstable nuclei are prepared in the laboratory, the decomposition is called induced radioactivity. Radioactivity, discovered by A. H. Becquerel is a phenomenon of spontaneous nuclear transformation resulting in the formation of new elements (Cember, 1989). Radioactivity is the term used to describe those spontaneous, energy-emitting, atomic transitions that involve changes in state of the nuclei of atoms. The energy released in such transformations is emitted in the form of electromagnetic or corpuscular radiations. In more specific words, it is found that a few naturally occurring substances consist of atoms which are unstable that is, they undergo spontaneous transformation into more stable product atoms (Martin and Samuel, 1979). Such substances are said to be radioactive, the transformation is called radioactivity and the transformation process is termed as radioactive decay. Radioactive decay is usually accomplished by the emission of charged particles and gamma rays.

All chemical elements may be rendered as radioactive by adding or subtracting (except for hydrogen and helium) neutrons from the nucleus of the stable ones (Bhuiyan, 2009). Studies of the radioactive decays of new isotopes far from the stable ones in nature continue as a major frontier in nuclear research. The availability of this variety of radioactive isotopes has stimulated their use in a wide range of fields including chemistry, biology, medicine, industry, artifact dating, agriculture and space exploration.

1. 3 Discovery of Radioactivity

In 1896, A. H. Becquerel, the father of radioactivity, was investigating the fluorescence of sulphate, uranium and potassium using a photographic plate. He found that the plate was affected by certain radiations, irrespective of whether or not the salt was caused to fluorescence. And thus, Becquerel gave the concept of radioactivity. After that, Marie

Curie investigated this property in a number of minerals containing which she found more active than uranium itself, and first coined the word radioactivity. In 1898, she and Pierre Curie discovered Polonium, and Radium in collaboration with G. Belmont. Later E. Rutherford showed that two types of radiation were emitted by uranium, namely the alpha rays that were completely stopped by a thin sheet of paper and the beta rays that were much more penetrating than alpha rays. In 1990, P. Villard discovered gamma rays, even more penetrating radiations. Subsequently, the alpha and beta rays were shown to be ionized helium-4 atoms and electrons respectively, and the gamma rays to be electromagnetic in nature i.e. energetic photon (NCR, 1994). Several decades later at 1934, Irene and Frederic Joliot Curie discovered man-made radioactivity.

1. 4 Classification of radiation

Radiation is broadly classified into two groups. They are,

(a) Ionizing Radiation.

(b) Non-ionizing Radiation.

1. 4. 1 Ionizing Radiation

Radiation with sufficiently high energy can ionize atoms; that is to say it can knock electrons off of atoms and create ions, as well as lower-energy damage such as breaking chemical bonds within molecules. Ionization occurs when an electron is stripped (or "knocked out") from an electron shell of the atom, which leaves the atom with a net positive charge. Because living cells and, more importantly, the DNA in those cells can be damaged by this ionization, exposure to ionizing radiation is considered to result in an increased chance of cancer. Thus "ionizing radiation" is somewhat artificially separated from particle radiation and electromagnetic radiation, simply due to its great potential for biological damage.

Classification of Ionizing Radiation:

When a radiation possesses sufficient energy to ionize a neutral atom, the radiation is said to be ionizing radiation. The ionization energy of an atom and the threshold energy for ionization are different atoms and the threshold energy depends on the nature of the atom. Clearly the radiation with energy less than the threshold energy is known to be non-

ionizing radiation. Ionizing radiation is very harmful for biological cells. In radioactive phenomenon, nuclear radiation occurs as a result of spontaneous disintegration of atomic nuclei. These nuclear changes can give rise to several types of radiation such as-

(a) α- radiation ,

(b) β- radiation and

(c) γ- radiation

γ-rays either from isomeric transitions or more commonly an excess energy following particle emission and interaction conversion of electrons, resulting from electromagnetic interaction between the nucleus and orbital electrons. Figure 1.2 shows Alpha, Beta and Gamma radiation penetration.

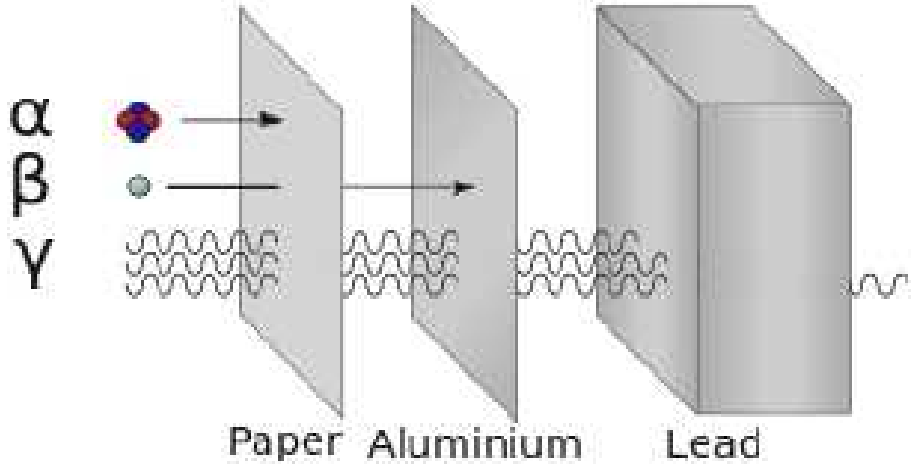

Fig. 1.2 Alpha, Beta and Gamma radiation penetration

A. Alpha Radiation

Alpha radiation is a coulomb repulsion effect and also a nuclear phenomenon. Alpha radiation consists of a stream of positively charged particles, called alpha particles, which have an atomic mass of 4 and a charge of +2 (a helium nucleus). When an alpha particle is ejected from a nucleus, the mass number of the nucleus decreases by four units and the atomic number decreases by two units.

For example $^{238}U_{92} \rightarrow {}^{4}He_{2} + {}^{234}Th_{90}$

Thus an alpha particle is a highly energetic helium nucleus that emitted from the nucleus of the radioactive isotope when the neutron- to-proton ratio is too low. The nuclei, which contain 210 or more nucleons are so large that the short-range nuclear forces that forces that hold then together are barely able to counter balance the mutual repulsion of their protons. Alpha decay occurs in such nuclei as a means of increasing their stability by reducing their size. Alpha particles are mono-energetic and energy lies between 4 - 9 MeV (Hendry et al., 2009).

B. Beta Radiation

Beta radiation is a stream of electrons, called beta particles. When a beta particle is ejected, a neutron in the nucleus is converted to a proton, so the mass number of the nucleus is unchanged, but the atomic number increases by one unit.

For example (Hendry, 2009):

$$^{234}Sr_{90} \rightarrow {}^{0}e_{-1} + {}^{234}Pa_{91}$$

They are emitted in radioactive decay with various energies ranging from nearly zero to a maximum energy characteristic of the decaying radioactive isotope. The beta rays can travel a few feet in air but cannot penetrate much beyond the depth of the skin of a person. Hence, like the α-rays, they are harmful only when they are inside the body. From outside they can cause only skin burns. Because of the lower mass of β- particles, than α-particles, β-particles (β^- & β^+) are more penetrating than α-particles.

C. Gamma Radiation

Gamma radiation is only type of electromagnetic radiations, similar to light but of much higher energy. The wavelength of gamma rays is much shorter than that of visible light. the energy of electromagnetic radiation or photon is given by $E=h\nu$, where h is the Planks' constant (6.63×10^{-34} J-sec), ν is the frequency equal to C/λ, C being the velocity of light (3×10^{8} m/sec) and λ is the wavelength of the radiation. Gamma rays are emitted in radioactive decay along with alpha or beta radiations. Gamma rays have discrete energies like alpha rays.

1.4.2 Non-ionizing Radiation

The kinetic energy of particles of non-ionizing radiation is too small to produce charged ions when passing through matter. For non-ionizing electromagnetic radiation, the associated particles (photons) have only sufficient energy to change the rotational, vibrational or electronic valence configurations of molecules and atoms. The effect of non-ionizing forms of radiation on living tissue has only recently been studied. Nevertheless, different biological effects are observed for different types of non-ionizing radiation even "non-ionizing" radiation is capable of causing thermal-ionization if it deposits enough heat to raise temperatures to ionization energies. These reactions occur at far higher energies than with ionization radiation, which requires only single particles to cause ionization. Figure 1.3 shows types of radiation in the electromagnetic spectrum.

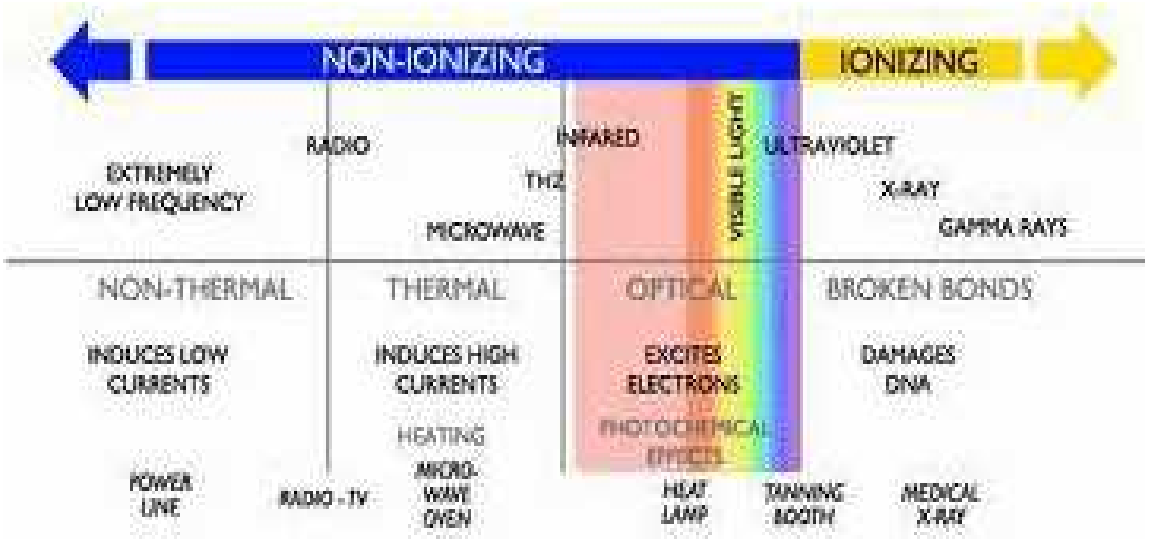

Fig. 1.3: Types of Radiation in the Electromagnetic Spectrum

1.5 Radioactive Decay

Radioactive decay is a stochastic (i.e. random) process at the level of single atoms, in that, according to quantum theory, it is impossible to predict when a particular atom will decay. However, the chance that a given atom will decay is constant over time. For a large number of atoms, the decay rate for the collection is computable from the measured decay constants of the nuclides (or equivalently from the half -lives). Fig.1.4 shows Elements of uranium, thorium and actinium series and their daughter products.

1.5.1 Natural Decay Series

A number of radionuclides occurring naturally are primordial, that is, associated with the formation of earth. Some elements having atomic number of or below that of, lead have one or more radioactive isotopes and all of these may be placed in one or the other radioactive series.

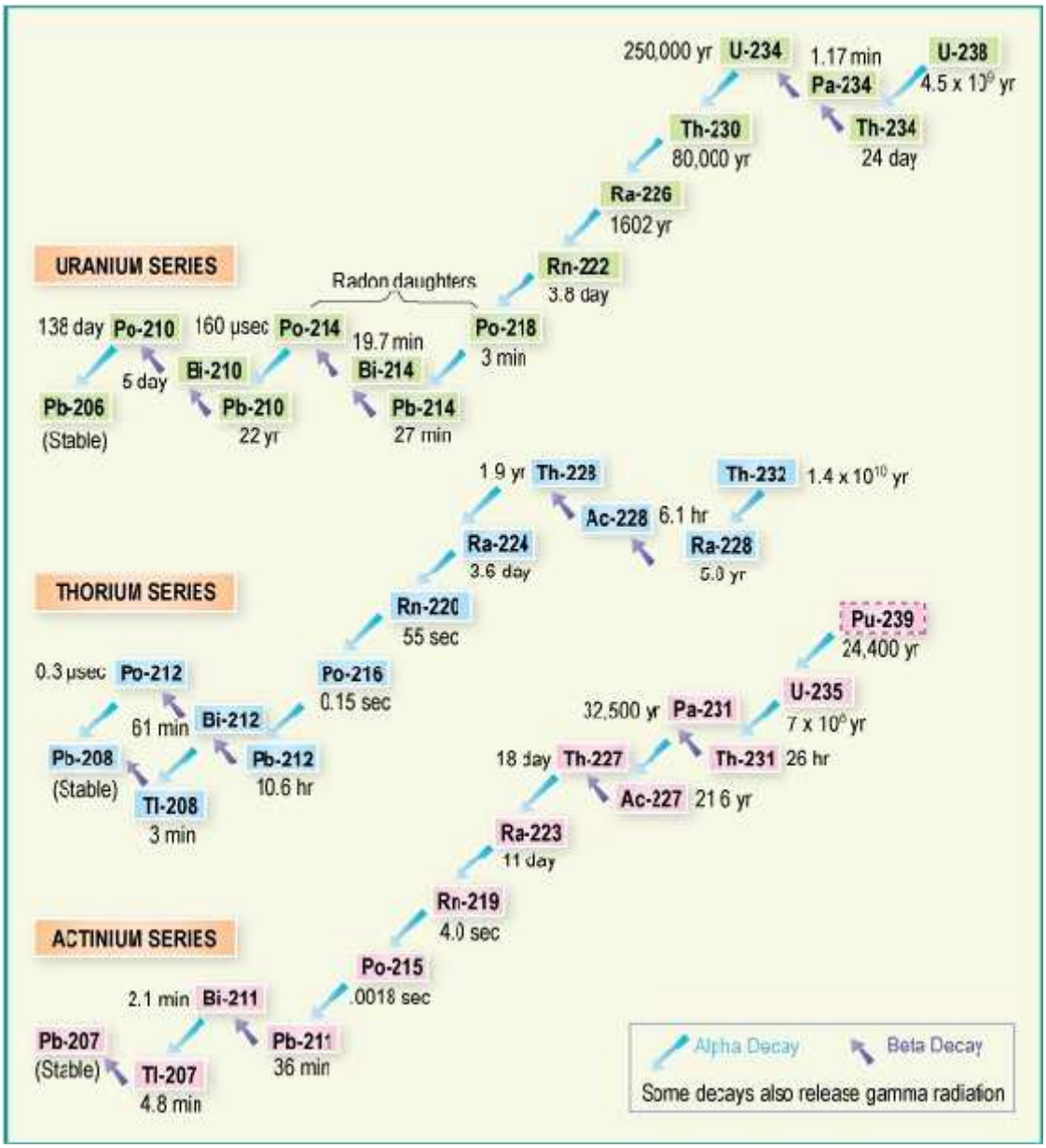

Fig.1.4: Elements of uranium, thorium and actinium series and their daughter products.

Natural radioactivity includes radiations from naturally occurring radioactive elements which arises from the sources external to the body and from the internal radiation materials contained in the human body itself. The external sources of radiation are cosmic rays, the ground and normal materials whilst the internal source of potassium and radium. Soils, rocks contain Uranium and Thorium with their decay products. Elements of uranium, thorium, and actinium series and their daughter products contribute major portion of the natural radioactivity (Clark, et al., 1966).

1. 6 Classification of Radioactivity

Generally there are two basic classes of radioactivity according to origin. They are,

- Natural Radioactivity
- Artificial or Induced Radioactivity

1.6.1 Natural Radioactivity

Natural radioactivity is the result of the spontaneous disintegration of naturally occurring radioisotopes (Cember, 1989). It originates from extraterrestrial sources as well as from radioactive elements in the earth's crust. It contributes about 90% of the total radiation (Quindos et al., 1992). Besides, natural radioactivity includes radiations from naturally occurring radioactive elements which arises from the sources external to the body and from the internal radioactive materials contained in the human body itself. A number of radionuclides occurring naturally are primordial that is, associated with the formation of the earth. A much large number of radioactive isotopes that now exist were produced when the universe was first formed around seven billion years ago. But most of them have decayed out of existence. The radionuclides which now exist are those that have half-life at least comparable to the age of the universe. Radioisotopes with half-life less than about 10^8 years have become undetectable whereas radionuclides with half-lives greater than 10^{10} years have decayed very little to the present time (Bhuiyan, 2009). In most cases, the natural radioactivity on earth varies only within relatively narrow limits. But in some localities, there are wide deviations from normal levels owing to the presence of abnormally high concentrations of radioactive minerals in the local soil and water. The external sources of radiation are cosmic rays, ground and the normal building materials while the internal sources are potassium and radium.

1.6.1.1 Origin of natural radionuclide

Most of the naturally occurring radionuclides are components of three chains of radioactive elements.

(1) The uranium series originating with ^{238}U.
(2) The thorium series originating with ^{232}Th.
(3) The actinium series originating with ^{235}U.

Elements of uranium, thorium and actinium series and their daughter products contribute major portion of the natural radioactivity (Eric, 1965). In addition, there are singly occurring radionuclides of both cosmic (^{14}C, ^{22}Na etc.) and terrestrial (^{40}K, ^{87}Rb etc.) origin which are also radioactive and do not belong to any series.

(1) The Uranium Series

The ^{238}U and ^{234}U belong to the uranium series. About 99.3% of naturally occurring uranium is ^{238}U, about 0.7% is ^{235}U and a trace quantity about 0.005% is ^{234}U. The Uranium series whose first member is ^{238}U consists of isotopes whose mass numbers are exactly divisible by 4 and leave a remainder of 2. This series, therefore, is called the 4n+2 series (Cember, 1989). Table 1.1 represents the Uranium Series.

(2) The Thorium Series

^{232}Th is the first member of another long chain of successive radioisotopes, called the thorium series. It is very commonly found in the earth's crust. The thorium content in the earth's crust is approximately three times than that of uranium (Mazibur, 1991). The mass numbers of all members of the thorium series are exactly divisible by 4. This series, therefore, is called the 4n series (Cember,1989). Table 1.2 represents the Thorium Series.

(3) The Actinium Series

The ^{235}U isotope of uranium is the first member of another series called the Actinium series. Here, the mass numbers of the isotopes are exactly divisible by 4 and leave a remainder of 3.

This series, therefore, is called the 4n+3 series (Cember, 1989) Table 1.3 represents the Actinium Series.

Table 1.1: The Uranium Series (Kaplan, 1964)

Radioactive species	Nuclides	Type of disintegration	Half life	Disintegration Constant, sce^{-1}	Particle energy, MeV
Uranium I (UI)	$_{92}U^{238}$	α	4.5×10^{9} y	4.88×10^{-18}	4.20
Uranium X_1 (UX_1)	$_{90}Th^{234}$	β	24.1 d	3.33×10^{-7}	0.19
Uranium X_2 (UX_2)	$_{91}Pa^{234}$	β	1.18m	9.77×10^{-3}	2.32
Uranium Z (UZ)	$_{91}Pa^{234}$	β	6.7 h	2.88×10^{-5}	1.13
Uranium II (UII)	$_{92}U^{234}$	α	2.5×10^{5} y	8.80×10^{-14}	4.768
Ionium (Io)	$_{90}Th^{230}$	α	8.0×10^{4} y	2.75×10^{-13}	4.68 m
Radium (Ra)	$_{88}Ra^{226}$	α	1620 y	1.36×10^{-11}	4.777 m
Ra emission (Rn)	$_{86}Em^{222}$	α	3.82 d	2.10×10^{-6}	5.486
Radium A (RaA)	$_{84}Po^{218}$	α, β	3.05 m	3.78×10^{-3}	α: 5.998 β:Energy not known
Radium B (RaB)	$_{82}Pb^{214}$	β	26.8 m	4.31×10^{-4}	0.7
Astatine-218 (At^{218})	$_{85}At^{218}$	α	1.5-2.0 s	0.4	6.63
Radium C (RaC)	$_{83}Bi^{214}$	α, β	19.7 m	5.86×10^{-4}	α: 5.51 m β: 3.17
Radium C' (RaC')	$_{84}Po^{214}$	α	1.64×10^{-4} s	4.23×10^{3}	7.683
Radium C" (RaC")	$_{81}Tl^{210}$	β	1.32 m	8.75×10^{-4}	1.9
Radium D (RaD)	$_{82}Pb^{210}$	β	19.4 y	1.13×10^{-9}	0.017
Radium E (RaE)	$_{83}Bi^{210}$	β	5.0 d	1.60×10^{-6}	1.155
Radium F (RaF)	$_{84}Po^{210}$	α	138.3 d	5.80×10^{-8}	5.300
Thallium-206 (Tl^{206})	$_{81}Tl^{206}$	β	4.2 m	2.75×10^{-3}	1.51
Radium G (RaG)	$_{82}Pb^{206}$	stable			

Table 1.2: The Thorium Series (Cember, 1989)

Radioactive species	Nuclides	Type of disintegration	Half life	Disintegration Constant, sec^{-1}	Particle energy, MeV
Thorium (Th)	$_{90}Th^{232}$	α	1.39×10^{10} y	1.58×10^{-18}	4.007
Mesothorium 1 (MsTh1)	$_{88}Ra^{228}$	β	6.7 y	3.28×10^{-9}	0.04
Mesothorium 2 (MsTh2)	$_{89}Ac^{228}$	β	6.13 h	3.14×10^{-5}	2.18
Radiothorium (RdTh)	$_{90}Th^{228}$	α	1.91 y	1.15×10^{-8}	5.423 m
Thorium X (ThX)	$_{88}Ra^{224}$	α	3.64 d	2.20×10^{-6}	5.681 m
Th Emanation (Tn)	$_{86}Em^{220}$	α	51.5 s	1.34×10^{-2}	6.280
Thorium A (ThA)	$_{84}Po^{216}$	α, β	0.16 s	4.33	6.774
Thorium B (ThB)	$_{82}Pb^{212}$	β	10.6 h	1.82×10^{-5}	0.58
Astatine-216 (At^{216})	$_{85}At^{216}$	α	3×10^{-4} s	2.3×10^{3}	7.79
Thorium C (ThC)	$_{83}Bi^{212}$	α, β	60.5 m	1.91×10^{-4}	α: 6.086 m β: 2.25
Thorium C' (ThC')	$_{84}Po^{212}$	α	3.0×10^{-7} s	2.31×10^{6}	8.780
Thorium C' (ThC'')	$_{81}Tl^{208}$	β	3.10 m	3.73×10^{-3}	1.79
Thorium D (ThD)	$_{82}Pb^{208}$	Stable			

Table 1.3: The Actinium Series (Kaplan, 1964)

Radioactive species	Nuclides	Type of disintegration	Half life	Disintegration Constant, sec^{-1}	Particle energy, MeV
Actinouranium (AcU)	$_{92}U^{235}$	α	7.10×10^{8} y	3.09×10^{-17}	4.559 m
Uranium Y (UY)	$_{90}Th^{231}$	β	25.6 h	7.51×10^{-6}	0.30
Protoactinium (Pa)	$_{91}Pa^{231}$	α	3.43×10^{4} y	6.40×10^{-13}	5.046 m
Actinium (Ac)	$_{89}Ac^{227}$	α, β	21.6 y	1.02×10^{-9}	α: 4.94
Radioactinium (RdAc)	$_{90}Th^{227}$	α	18.17 d	4.41×10^{-7}	6.03 m
Actinium K (AcK)	$_{87}Fr^{223}$	α, β	22 m	5.25×10^{-4}	α: 5.34, β: 1.2
Actinium X (AcX)	$_{88}Ra^{223}$	α	11.68 d	6.87×10^{-7}	5.864
Astatine-219	$_{85}At^{219}$	α, β	0.9 m	1.26×10^{-2}	α: 6.27
Ac Emanation (An)	$_{86}Em^{219}$	α	3.92 s	0.177	6.810 m
Bismuth-215	$_{83}Bi^{215}$	α, β	8 m	1.44×10^{-3}	energy not known
Actinium A (AcA)	$_{84}Po^{215}$	α, β	1.83×10^{-3} s	3.79×10^{2}	α: 7.37
Actinium B (AcB)	$_{82}Pb^{211}$	β	36.1 m	3.20×10^{-4}	1.39
Astatine-215	$_{85}At^{215}$	α	10^{-4} s	7×10^{3}	8.00
Actinium C (AcC)	$_{83}Bi^{211}$	α, β	2.15 m	5.28×10^{-3}	α: 6.617 m
Actinium C' (AcC')	$_{84}Po^{211}$	α	0.52 s	1.33	7.442 m
Actinium C'' (AcC'')	$_{81}Tl^{207}$	β	4.79 m	2.41×10^{-3}	1.44
Actinium D (AcD)	$_{82}Pb^{207}$	Stable			

Table 1.4: The Neptunium Series (Cember, 1989).

Radioactive species	Nuclides	Type of disintegration	Half life	Disintegration Constant,sce^{-1}	Particle energy, MeV
Plutonium	$_{92}Pu^{241}$	B	13.2 y	1.69×10^{-9}	0.021
Americium	$_{95}Am^{241}$	α, γ	462 y	4.80×10^{-11}	α: 5.546 γ: 0.062
Neptunium	$_{93}Np^{237}$	A	2.2×10^{6} y	9.99×10^{-15}	4.77
Protoactinium	$_{91}Pa^{233}$	β, γ	27.4 d	2.97×10^{-7}	β: 0.53, γ: 0.31
Uranium	$_{92}U^{233}$	α, γ	1.62×10^{5} y	1.36×10^{-13}	α: 4.823, γ: 0.08
Thorium	$_{90}Th^{229}$	A	7340 y	3.0×10^{-12}	5.02
Radium	$_{88}Ra^{225}$	B	14.8 d	5.42×10-^{7}	0.30
Actinium	$_{89}Ac^{225}$	A	10 d	8.02×10^{-7}	5.80
Francium	$_{87}Fr^{221}$	A	4.8 m	2.41×10^{-3}	6.30
Astatine	$_{85}At^{217}$	A	0.018 s	3.85×10^{1}	7.02
Bismuth	$_{83}Bi^{213}$	α, β	47m	2.46×10^{-4}	α: 5.86, β: 1.39
Polonium	$_{84}Po^{213}$	A	4.2×10^{-6}	1.65×10^{5}	8.336
Thallium	$_{81}Ti^{209}$	B	2.2 m	5.25×10^{-3}	1.99
Lead	$_{82}Pb^{209}$	B	3.32 h	5.84×10^{-5}	0.635
Bismuth	$_{83}Bi^{209}$	Stable			

1.6.1.2 Origin of Potassium

Potassium has a very simple form of radioactive decay. Only one of the several natural isotopes of potassium e.g. ^{40}K is radioactive and it has a relative isotopic abundance of only 0.0118% (Cember, 1989). Hence, among the low atomic numbered naturally occurring radioisotopes (^{40}K, ^{87}Rb, ^{138}La etc.), ^{40}K is the most important one from the health physics point of view because of its widespread distribution in the environment. No significant fraction of the potassium isotopes takes place in nature and so the radioactivity of potassium is almost constant under all conditions. It is characterized by a single gamma ray of energy 1.46 MeV. Potassium undergoes 3.3 gamma emissions per second per gram (Clark et al., 1966).

1.6.2 Artificial or Induced Radioactivity

The term artificial or induced radioactivity refers to the way in which the new radionuclides are produced rather than to their decay (Kaplan, 1964). Induced radioactivity occurs when a previously stable material has been made radioactive by exposure to specific radiation. Most radioactivity does not induce other material to become radioactive. The phenomenon by which even light elements are made radioactive by artificial or induced methods is called artificial radioactivity.

This artificial radioactivity was discovered by Irene Curie and F. Joliot in 1934. They observed that when lighter elements such as boron, magnesium and aluminium were bombarded with α-particles, there was a continuous emission of radioactive radiations, even after the α−source had been removed. Their study showed that the radiation was due to the emission of a particle carrying one unit positive charge with mass equal to that of an electron.

However, in this type of radioactivity, radioisotopes are produced by bombarding nuclei with nucleon particles in an accelerator or nuclear reactor. A nucleus becomes radioactive when it changes from a stable, unexcited state to an unstable excited condition. By bombarding atoms with charged particles of sufficient energy it is possible to raise the nucleus to a state of instability from which it will decay back to its stable state at a characteristic rate measured by the half-life. There are a few radioisotopes which emit neutrons. Beryllium has the lowest

neutron binding energy of all the nuclides and is used as a target with both alpha and gamma radioisotopes.

The exposure for an average person is about 3.6 $mSvyr^{-1}$, 80 percent of which comes from natural sources of radiation, the remaining 20 percent results from exposure to artificial radiation sources . Accelerators, reactors, atomic explosion and man-made radioactive sources are the most important sources of artificial radioactivity. The existing main types of man-made radiation sources are light sources, radio, TV, power supply lines, cellular phone network, nuclear medicine, nuclear power plants, nuclear weapon test, commercial products (e.g. tobacco), fertilizer, luminous watch dials and industrial activities. Most of the man-made sources belong to the medical sector. For average persons who have had no medical x-rays, only 3% of their annual radiation dose comes from artificial sources (UNSCEAR, 2000). Exposures to natural sources of radiation may vary little form year to year and involves the whole population of the world to about the same extent. On the contrary, man-made sources may vary significantly with time and the resulting exposures may differ substantially from one population group to another. Artificial radioactivity is also known as man-made radioactivity.

Some induced radioactivity is produced by background radiation, which is mostly natural. However, since natural radiation is not very intense in most places on Earth, the amount of induced radioactivity in a single location is usually very small. Nevertheless, in nuclear explosions, more than 200 radionuclides are produced with half-lives ranging from less than a second to many years (Balles and Sallow, 1951). In addition, a number of activation products arise from neutron activation of weapon materials and the surrounding atmospheric environment (Strom,1958), as mentioned earlier. A large number of these radioactive isotopes are used for purposes in different fields such as physical science, agriculture, industry, hydrology and medicine. But nonetheless its far-reaching effect can be and is very dangerous to the population and also to the individual one.

The only series containing artificial radioactive nuclides is known as the neptunium series. This fourth family of radioactivity is started with the nuclei ^{214}Pu which has a half-life of only 13.2 years and briefly existed only after its formation (Cember, 1989). The only surviving and also the terminal member of the neptunium family is the stable bismuth, ^{209}Bi. This series has

derived its name from the longest lived member of the group, neptunium ^{237}Np with half- life 2.2×10^{6} years. Here, the mass numbers of the isotopes are exactly divisible by 4 and leave a remainder of 1. This series, therefore, is called the 4n+1 series (Cember, 1989).

The 4n+1 series is also called the missing series. It is generally considered that the earth is about 5×10^{9} years old. According to the scientists, if it is assumed, as is probable, that neptunium was formed at the same time as the earth, then many half-lives have elapsed for this nuclide and the amounts still present would be too minute as to be beyond the possibility of detection (Kaplan, 1964). The absence of a naturally occurring 4n+1 series can therefore be discussed. Even if such a series did exist at one time, its members would long since have decayed to ^{209}Bi. Disposal of wastes from reprocessing power plantsonment are stated below (Chang Kyu Kim, 1990).

- Global fallout due to atmospheric weapon tests and satellite accidents.
- Local contamination from close-in-fallout from nuclear weapon tests.
- Accidents involving military aircraft and nuclear power plants.
- Disposal of wastes from reprocessing power plants

1.7 Sources of Radiation

Background radiations from random sources can be conveniently grouped into six categories:

- The natural radioactivity of the constituent materials of the detector itself.
- The natural radioactivity of the ancillary equipments, supports and shielding placed in the immediate vicinity of the detector.
- Radiations from the activity of the earth's surface (terrestrial radiation), construction materials of the laboratory, or other far-away structures.
- Radioactivity in the air surrounding the detector.
- The primary and secondary components of cosmic radiation.
- Radioactivity in the human body.

In addition to the natural sources of background radiation many artificial sources of radiation have been introduced in the past 80 years. These artificial sources now add a significant contribution to the total radiation exposure of the population (Martin and Samuel, 1979).

Different types of sources of radioactivity can be found in the nature. More than 80% of the all exposed ionizing radiation to human body comes from the natural environment. But the radioactivity found in nature is negligible compared to their fruitful uses in the field of agriculture, industry, and medical research and development. So, to meet the increasing demand of radioactivity it is being produced artificially can be divided into three classes.

Such as-

1) Natural sources

2) Manmade sources

3) Radiation exposure from background Radiation

1. Natural sources

Throughout the history of life on earth, organisms continuously have been exposed to cosmic rays, radio nuclides produced by cosmic ray interactions in the atmosphere, and radiation from naturally occurring substances which are ubiquitously distributed in all living and nonliving components of the environment. It is clear that contemporary life have adjusted or are doing so to all features and limitations of the environment, including the natural radiation background.

(a) Cosmic Radiation

A significant component of detector background arises from the secondary radiations produced by cosmic ray interactions in the earth's atmosphere. Cosmic radiation reaches the earth from interstellar space and from the sun. It is composed of a very wide range of penetrating radiations which undergo many types of reactions with the elements they encounter in the atmosphere. The atmosphere acts as a shield and reduces considerably the amount of cosmic radiation reaching the earth's surface. This filtering action means that the dose rate at sea-level is less than at high altitudes. The average dose rate in the British Isles from cosmic radiation is about 0·5 $mSvyr^{-1}$. However, the primary cosmic radiation, which can be either galactic or solar origin, is made up mainly protons, might also be a small number of electrons based upon recent studies, plus some helium nuclei and heavy ions, with extremely high kinetic energies. In their interaction with atmosphere, a large amount of secondary

particles is produced with energies that extend into hundreds of MeV range. Some of these radiations reach the earth's surface and can create background pulses in many types of detectors. Besides, these radiations expose to population and environment as well. On the earth itself, the effect of cosmic rays has been mainly detected in interactions with the atmosphere. ^{14}C perhaps is the first such observed nuclei (Nazrul, 2009). Subsequently, ^{3}H, ^{7}Be, ^{10}Be, ^{22}Na and other nuclides have also been observed.

(b) Terrestrial sources

Terrestrial radiation only includes sources that remain external to the body. The major radionuclides of concern are potassium, uranium and thorium and their decay products, some of which, like radium and radon are intensely radioactive but occur in low concentrations. Most of these sources have been decreasing, due to radioactive decay since the formation of the Earth, because there is no significant amount currently transported to the Earth. Thus, the present activity on earth from uranium-238 is only half as much as it originally was because of its 4.5 billion year half-life, and potassium-40 (half-life 1.25 billion years) is only at about 8% of original activity. The effects on humans of the actual diminishment (due to decay) of these isotopes is minimal however. This is because humans evolved too recently for the difference in activity over a fraction of a half-life to be significant. Put another way, human history is so short in comparison to a half-life of a billion years, that the activity of these long-lived isotopes has been effectively constant throughout our time on this planet. In addition, many shorter half-life and thus more intensely radioactive isotopes have not decayed out of the terrestrial environment, however, because of natural on-going production of them. Examples of these are radium-226 (decay product of uranium-238) and radon-222 (a decay product of radium-226).

(C) Food and water

Some of the essential elements that make up the human body, mainly potassium and carbon, have radioactive isotopes that add significantly to our background radiation dose. An average human contains about 30 milligrams of potassium-40 (^{40}K) and about 10 nanograms (10^{-8} g) of carbon-14 (^{14}C) which has a decay half-life of 5,730 years. Excluding internal contamination by external radioactive material, the largest component of internalradiation exposure from biologically functional components of the human body is from potassium-40.

The decay of about 4,000 nuclei of 40K per second makes potassium the largest source of radiation in terms of number of decaying atoms. The energy of beta particles produced by 40K is also about 10 times more powerful than the beta particles from ^{14}C decay. ^{14}C is present in the human body at a level of 3700 Bq with a biological half-life of 40 days (http//www.ead/carbon 14.). There are about 1,200 beta particles per second produced by the decay of ^{14}C. However, a ^{14}C atom is in the genetic information of about half the cells, while potassium is not a component of DNA. The decay of a ^{14}C atom inside DNA in one person happens about 50 times per second, changing a carbon atom to one of nitrogen (Asimov, 1976). The global average internal dose from radionuclides other than radon and its decay products is 0.29 mSv/a, of which 0.17 mSv/a comes from 40K, 0.12 mSv/a comes from the uranium and thorium series, and 12 μSv/a comes from ^{14}C. (Quindos et al., 1992)

2. Man–Made Sources

Individual effects from man-made sources of radiation vary greatly. Most people receive a relatively small amount of artificial radiation, but a few get many thousand times the amount they receive from natural sources. This variability is generally greater for man-made sources than for natural ones. Most man-made sources can be controlled more readily than most natural ones. Though exposure to external radiation due to fallout from past nuclear explosions, for example, is almost as inescapable and uncontrollable as that due to cosmic rays from beyond the atmosphere or to radiation from out of the earth itself.

(a) Medical Sources

In industrial and medical applications, typically only single radio nuclides is involved, thus simplifying identification of leakage pathways from encapsulation, from radioactive tracer tests and for disposal process.

The use of radioisotopes in medicine is widespread and may potentially have significant radiological impact. These applications can be classified as (1) diagnostic uses, (2) therapy, (3) analytical procedures and (4) and similar portable sources.

Most often radio nuclides used in medicine are: ^{99m}Tc, ^{131}I and ^{57}Co.

^{99m}Tc--Bone marrow scan, brain scan, cerebral blood scan, hears scan, lung scan, thyroid scan, placental localization;

^{131}I--Blood volume, liver scan, placental localization, thyroid scan, and thyroid therapy;

^{57} Co--Schilling test; ^{32} P-Bone metastases

(b) Nuclear Explosions

For the last 50 years, everyone has been exposed due to radiation from fall-out from nuclear weapons. Almost all is the result of atmospheric nuclear explosions carried out to test nuclear weapon. This testing reached two peaks: first between 1954 and 1958 and second, greater, in 1961 and 1962. In 1963 the three countries (USSR, United States, and United Kingdom) signed the Partial Test Ban Treaty, undertaking not to test nuclear weapon in the atmosphere, oceans and outer space. Over next two decades France and China conducted series of much smaller tests, but they stopped, too, after 1980. Underground tests are still being carried out, but they generally give rise to virtually no fall-out. Some of the radioactive debris from atmospheric tests lands relatively close to the site of explosion. Some stays in the troposphere, the lowest layer of the atmosphere, and carried by wind around the world at much the same latitude. As it travels it gradually falls to earth, remaining about month in the air. But most is pushed into the stratosphere, the next layer of the atmosphere (10 to 50 km up) where it stays for many months, and whence it slowly descent all over the earth. These various types of fall-out contain several hundred different radio nuclides, but only few contribute much to human exposure, as most are produced in very small amounts or decay quickly. Those few, in declining order of importance, are carbon-14, caesium-137, zirconium-95 and stronium-90. Zirconium-95, which has half-life of 64 days, is already completely decayed. Caesium-137 and stronium-90, half-lives of about 30 years, are still present, but amounts of them less than half from initial amounts. Only carbon-14, with half-life of 5730 year, will stay active into far future.

(c) Industrial Source

Radioisotopes are much more widely used in industry than is generally recognized and represent a significant component in the man-made radiation environment. The principal applications include industrial radiography, radiation gauging, smoke detectors and self-luminous materials. Hence the average annual dose rate equivalent from artificial radiation comes mainly from industrial source. Insoluble contamination passes through the digestive tract and is excreted in the feces. During its passage through the body it will irradiate the tract and the large intestine. In this way man can be affected by the radioactive elements.

(d) Nuclear power production

A fission reactor produces enormous amount of radioactivity as waste. This radioactivity is generated in the core of the reaction that houses the fissionable fuel. But the average population dose resulting from fission products is comparatively much less than the maximum permissible dose limit. United Kingdom is generating 12% of its electricity by nuclear energy; the average annual dose to population is about 0.01% of the total dose equivalent from all background radiation. Therefore, it is clear that the nuclear power industry under normal operating condition contributes a minor part to the total radiation dose .

Radiation Protection Standards

As the use of radiation became more widespread and its deleterious effects better recognized, the need arose to establish permissible levels of exposure to radiation for workers. First in 1925, the International Commission on Radiological Units (ICRU) recommended that the annual permissible dose of radiation be one-tenth of the erythematic dose - the acute dose that just produce visible reddening of skin. In the mid - 1930's the permissible exposure for whole body X-radiation was set at 1 R/week by the ICRP and 0.5 R/week by the NCRP. After World War II, routine operations in the atomic energy industry exposed workers to neutrons as well as radiation from radioactive materials. So one is to work within certain limits of radiation hazard. The basic dose equivalent limits for all occupational workers are given in Table 1.5.

Table 1.5 Dose Limits for Individuals (ICRP, 1996)

Organ to tissue	Maximum permissible doses for occupationally exposed adults	Dose limits for members of the public
Total body	50 mSv in a year	5 mSv or 1 mSv in a year
gonads', red bone marrow	50 mSv in a year	5 mSv in a year
Skin, bone thyroid	300 mSv in a year	30 mSv in a year
Hands and forearms feet And ankles	750 mSv in a year	75 mSv in a year
Other single organs	150 mSv in a year	15 mSv in a year

1. 9 Objective of the Present Study

Both natural and artificial radioactive substances are existing in the atmosphere which in various ways spread into the soil, water, air, foodstuff etc. As a results soil, water, air, foodstuff are contaminated and the level of contamination varies place to place.

In the present study Paddy and three types vegetables samples such as papaya, Arum and Leafy vegetables have been collected from eight locations from the bank of Rupshs river, Khulna, Bangladesh. These locations are Deara, Khan Mohammadpur, Aichgati, Joypur, Jabusa, Elahipur, Noeihati and Kharabad in Khulna.

The aim of the present work is to determine the concentration of the natural and artificial radionuclides and annual effective dose in the collected vegetable samples. The concentration of the radionuclide's present in the vegetables samples are expected to be greatly influenced by large number of populations, some brick fields, various shops and ship-industries in Khulna near the agricultural zones of these locations. The present results will be useful for comparing

with other previous radioactivity measurements for subsequent measurement establishment of a relation about its impact on the man and the environment of the selected location.

As such this work would be useful as base line data for the planning and for the future work of this area. This work is extremely important to carry out approximately designed for environmental radioactivity and radiation monitoring aimed at minimizing radiation exposure to population.

CHAPTER II

Literature Review

2. 1 Introduction

We have been living in a radioactive environment since the beginning of our lives. Human and animal kingdom, however, make adjustment to the natural radiation sources. Environment raises many problems concerning the safety of biotic life, food chain and ultimately human. Due to the fact that radionuclides can have harmful effects on the habitat and can also pose health hazard problems for human, the assessment of gamma radiation dose from natural sources is of particular importance as natural radiation is the largest contributor to the external dose of the world population**.** The measurement of radionuclides in various environmental elements is very importance for living in world. For this reason, Scientists feels the necessity for the assessment of the radioactive sources in the environment.

The interaction of ionizing radiation with the human body arising either from external sources outside the body or from internal contamination of the body by radioactive substance, leads to biological effects which may later shown up as clinical symptoms. The nature and severity of these symptoms and the time at which they appear depend on the amount of radiation absorbed and the rate at which it is received.

The measurement of radionuclides in crops and vegetables samples has been done widely, especially abroad, in several countries, and the results on it have been reported in many journals. A review work on it has been carried out by searching the recent editions of some journals. Some of the important works are summarized below.

2. 2 Review of the previous work

2.2.1 A review on natural background radiation

Shahbazi-Gahrouei et al., (2013): The world is naturally radioactive and approximately 82% of human-absorbed radiation doses, which are out of control, arise from natural sources such as cosmic, terrestrial, and exposure from inhalation or intake radiation sources. Gamma

radiation emitted from natural sources (background radiation) is largely due to primordial radionuclides, mainly ^{232}Th and ^{238}U series, and their decay products, as well as ^{40}K, which exist at trace levels in the earth's crust. Their concentrations in soil, sands, and rocks depend on the local geology of each region in the world. Naturally occurring radioactive materials generally contain terrestrial-origin radionuclides, left over since the creation of the earth. In addition, the existence of some springs and quarries increases the dose rate of background radiation in some regions that are known as high level background radiation regions. The type of building materials used in houses can also affect the dose rate of background radiations.

Islam et al., (2014): The south-eastern part of Bangladesh at Cox's Bazar district area radio-nuclides from ingested vegetables (Papaya) were The activity concentrations of ^{226}Ra in papaya samples ranged from 41.82 to 120.08 Bq/ kg with an average of 80.95±13.61 Bq/ kg. The concentrations of ^{238}U ranged from 18.57 to 110.98 Bq/ kg with an average of 64.77±38.47 Bq/ kg. The concentrations of ^{232}Th ranged from 39.58 to 127.48 Bq/ kg with an average of 83.53±20.50 Bq/ kg and the concentrations ^{40}K ranged from 1030.88 to 2352.02 Bq/ kg with an average of 1691.45±244.98 Bq/ kg the concentration of ^{40}K was found very high. Annual intake of ^{226}Ra, ^{238}U, ^{232}Th and ^{40}K from papaya was 1.1 mSv y^{-1} of which 0.21 mSv was from ^{40}K and 0.89 mSv was from ^{226} Ra, ^{238} U and ^{232}Th

Hariandra and Amin, (2008): The uptake of naturally occurring thorium, radium and potassium by sawi from Kuala Lumpur, Malaysia, The highest values of radionuclides in the sawi were ^{40}K which is 446 Bq/kg and the lowest was ^{226}Ra which is 17.5 Bq/kg. The activity of ^{232}Th is 65.2 Bq/kg. The highest values of radionuclides in the soil were ^{40}K which is 52.8 Bq/ kg and the lowest was ^{226}Ra which is 6.51 Bq/kg. The activity of Th-232 is 18.5 Bq/kg. The soil to plant transfer factors (TF) were calculated and observed to be 2.68 for ^{226}Ra 3.52 for ^{232}Th and the highest which is 3.97 for ^{40}K.

Jibiri et al., (2007): The activity concentrations of ^{226}Ra, ^{228}Th, and ^{40}K were determined in cereals, tubers and vegetables in Bitsichi area of the Jos Plateau, Nigeria. The corresponding activity concentrations in the food crops ranged from below detection limit BDL to 684.5 Bq/kg for ^{40}K, from BDL to 83.5 Bq/kg for ^{226}Ra, and from BDL to 89.8 Bq/ kg for ^{228}Th. Activity concentrations of these radionuclides were found to be lower in cereals than in tubers

and vegetables. As for the soil samples, activity concentrations of these radionuclides varied from BDL to 166.4 Bq/kg, from 10.9 to 470.6 Bq/kg, and from 122.7 to 2,189.5 Bq/kg for ^{40}K, ^{226}Ra, and ^{228}Th, respectively. Average external gamma dose rates were found to vary across the farms from 0.50 ± 0.01 μSv h^{-1} to 1.47 ± 0.04 μSv h^{-1}.

Vahid et al., (2013): Natural radioactivity levels in wheat and corns of Eilam province, Iran. In wheat and corn samples, the average activity concentrations of ^{226} Ra, ^{232} Th, and ^{40} K were found to be 1.67 Bq/kg, 0.5 Bq/kg, 91.73 Bq/kg, and 0.81 Bq/kg, 0.85 Bq/kg, 101.52 Bq/kg (dry weight), respectively. The obtained values of AGDE are 30.49 $mSvy^{-1}$for wheat samples and 37.89 mSv y^{-1} for corn samples; the AEDE rate values are 5.28 mSv y^{-1} in wheat samples and this average value was found to be 6.13 mSv y^{-1} in corn samples in Eilam.

Ele Abiama et al., (2012): Concentrations of naturally occurring radionuclides ^{226}Ra, ^{228}Ra and ^{40}K were determined in five most consumed vegetables in a high-level background radiation area (HLBRA) in the southwest region of Cameroon. A total of 25 foodstuff samples collected from Akongo, Ngombas, Awanda, Bikoué and Lolodorf rural districts. The average activity concentration values of ^{226}Ra, ^{228}Ra and ^{40}K were respectively 2.30, 1.50 and 140.40 Bq/ kg fresh-weights. The estimated total daily effective doses from the ingestion of the investigated foodstuffs for each natural radionuclide were respectively 0.41 μSv for ^{226}Ra, 0.84 μSv for ^{228}Ra and 0.71 μSv for ^{40}K. The total annual effective dose was estimated at 0.70 mSv y^{-1}. ^{228}Ra (44%) and ^{40}K (36%) were found to be the main sources for radiation.

Tuo et al., (2016): The activities of ^{238}U, ^{228}Ra, ^{226}Ra, ^{40}K and ^{137}Cs were determined in samples of vegetables, tea, cereal (rice, wheat and corn), meat, poultry, freshwater product, seafood and seaweed that collected from the 30km safety zone of the Nuclear Power Plants (NPPs) areas of China. The geometric mean concentrations Bq/kg wet weight) for 238U, 228Ra, 226Ra, 40K, and 137Cs in all investigated foodstuffs samples, are 0.13 Bq/kg, 0.16 Bq/kg, 0.11 Bq/kg, 68 Bq/kg and 0.02 Bq/kg, respectively. The arithmetic mean concentrations wet weight) for ^{238}U, ^{228}Ra, ^{226}Ra, ^{40}K, and ^{137}Cs in all investigated foodstuffs samples, are 0.34 Bq/kg, 0.65 Bq/kg, 0.32 Bq/kg, 111 Bq/kg and 0.09 Bq/kg, respectively. Radiation doses due to the consumption of these foodstuffs to humans are estimated to comprise around 37-46% of the annual Dose.

2.3 Information on the Effects of Radiation

Biological effects of radiation are very harmful to population. The National Committee on radiation Protection (NCRP) introduced the first significant concept of permissible radiation exposure for radiation workers in 1949. The development of a better understanding of the genetic effects of radiation comes from the British Medical Research council (MRC) and the National Academy of Sciences (NAC) which described a lower maximum permissible dose equivalent (Sullivan, 1957). The ICRP introduced the term lower maximum permissible dose equivalent distinguish between the effects for which the probability of occurrence does not depend on the dose received and those for which the severity is related to dose.

2. 4 Energy, Activity, Intensity and Exposure of radiation

Different radioactive materials and X-ray generators produce radiation at different energy levels and at different rates. It is important to understand the terms used to describe the energy and intensity of the radiation. The four terms used most for this purpose are: energy, activity, intensity and exposure.

Radiation Energy: As mentioned previously, the energy of the radiation is responsible for its ability to penetrate matter. Higher energy radiation can penetrate more and higher density matter than low energy radiation. The energy of ionizing radiation is measured in electronvolts (eV). One electronvolt is an extremely small amount of energy so it is common to use kiloelectronvolts (keV) and megaelectronvolt (MeV). An electronvolt is a measure of energy, which is different from a volt which is a measure of the electrical potential between two positions. Specifically, an electronvolt is the kinetic energy gained by an electron passing through a potential difference of one volt. X-ray generators have a control to adjust the keV or the kV.

Activity: The strength of a radioactive source is called its activity, which is defined as the rate at which the isotope decays. Specifically, it is the number of atoms that decay and emit radiation in one second. Radioactivity may be thought of as the volume of radiation produced in a given amount of time. It is similar to the current control on a X-ray generator. The

International System (SI) unit for activity is the becquerel (Bq), which is that quantity of radioactive material in which one atom transforms per second. The becquerel is a small unit. In practical situations, radioactivity is often quantified in kilobecqerels (kBq) or megabecquerels (MBq). The curie (Ci) is also commonly used as the unit for activity of a particular source material. The curie is a quantity of radioactive material in which 3.7×10^{10} atoms disintegrate per second. Once a radioactive nucleus decays, it is no longer possible for it to emit the same radiation again. Therefore, the activity of radioactive sources decrease with time and the activity of a given amount of radioactive material does not depend upon the mass of material present.

Intensity: Radiation intensity is the amount of energy passing through a given area that is perpendicular to the direction of radiation travel in a given unit of time. The intensity of an X-ray or gamma-ray source can easily be measured with the right detector. Since it is difficult to measure the strength of a radioactive source based on its *activity*, which is the number of atoms that decay and emit radiation in one second, the strength of a source is often referred to in terms of its intensity. Measuring the intensity of a source is sampling the number of photons emitted from the source in some particular time period, which is directly related to the number of disintegrations in the same time period (the activity).

Exposure: One way to measure the intensity of x-rays or gamma rays is to measure the amount of ionization they cause in air. The amount of ionization in air produced by the radiation is called the exposure. Exposure is expressed in terms of a scientific unit called a roentgen (R or r). The unit roentgen is equal to the amount of radiation that produces in one cubic centimeter of dry air at 0°C and standard atmospheric pressure ionization of either sign equal to one electrostatic unit of charge. Most portable radiation detection safety devices used by a radiographer measure exposure and present the reading in terms of roentgens or roentgens/hour, which is known as thedose rat**e.**

2. 5 Biological effect of radiation

Radiation is one of the best-investigated hazardous agents. Because of the vast accumulation of quantitative dose-response data, specialists are able to set environmental radiation levels so

that applications of nuclear technologies may continue at a level of risk that is much less than with many other technologies.

2.5.1 External and Internal Radiation Exposures

External:

External exposure is exposure which occurs when the radioactive source (or other radiation source) is outside (and remains outside) the organism which is exposed. Examples of external exposure include:

- A person who places a sealed radioactive source in his pocket
- A space traveler who is irradiated by cosmic rays
- A person who is treated for cancer by either teletherapy or brachytherapy. While in brachytherapy the source is inside the person it is still considered external exposure because it does not result in a committed dose.
- A nuclear worker whose hands have been dirtied with radioactive dust. Assuming that his hands are cleaned before any radioactive material can be absorbed, inhaled or ingested, skin contamination is considered external exposure.

Internal:

Internal exposure occurs when the radioactive material enters the organism, and the radioactive atoms become incorporated into the organism. This can occur through inhalation, ingestion, or injection and skin contact. These exposures can occur when radioactive material is airborne; is inhaled and absorbed by the lungs and deposited in the body; is present in contaminated food, drink or other consumable items and is ingested; or is spilled or aerosolizes onto the skin and absorbed or enters through cuts or scratches. Internal deposition may also result from contaminated hands, with subsequent eating or rubbing of eyes. Internal exposures arise when radiation is emitted from radioactive materials present within the body. Although external hazards are primarily caused by x-rays, gamma rays, high energy betas and

neutrons, all forms of radiation (including low energy betas, gammas and alphas) can cause internal radiation exposures. Alpha particles create a high concentration of ions along their path, and can cause severe damage to internal organs and tissues when they are inhaled, ingested or are present on the skin. Once these particles get into the body, damage can occur since there is no protective dead skin layer to shield the organs and tissues. Internal exposures are not limited to the intake of large amounts at one time (acute exposure). Chronic exposure may arise from an accumulation of small amounts of radioactive materials over a long period of time.

2.6 Cell Radiosensitivity

Radiosensitivity is the relative susceptibility of cells, tissues, organs, organisms, or other substances to the injurious action of radiation. In general, it has been found that cell radiosensitivity is directly proportional to the rate of cell division and inversely proportional to the degree of cell differentiation. In short, this means that actively dividing cells or those not fully mature are most at risk from radiation. The most radio-sensitive cells are those which:

- have a high division rate
- have a high metabolic rate
- are of a non-specialized type
- are well nourished

Examples of various tissues and their relative radiosensitivities are listed below (Rubin, 1968).

High Radiosensitivity

Lymphoid organs, bone marrow, blood, testes, ovaries, intestines.

Fairly High Radiosensitivity:

Skin and other organs with epithelial cell lining (cornea, oral cavity, esophagus, rectum, bladder, vagina, uterine cervix, urethras).

Moderate Radiosensitivity:

Optic lens, stomach, growing cartilage, fine vasculature, growing bone.

Fairly Low Radiosensitivity:

Mature cartilage or bones, salivary glands, respiratory organs, kidneys, liver, pancreas, thyroid, adrenal and pituitary glands.

Low Radiosensitivity:

Muscle, brain, spinal cord.

2.6.1 The Interaction of Radiation with Cells

The processes leading to radiation damage are often considered in four stages:

The initial physical stage, lasting about 10^{-16} seconds in which energy is deposited in the cell and causes ionization**.** In water the process may be written as:

$$H_2O \longrightarrow H_2O^+ + e^-$$

The physico-chemical stage, lasting about 10^{-6} seconds in which the ions interact with other water molecule resulting in a number of new products, i.e., the positive ion ($H_2O^{+)}$ dissociates:

$$H_2O^+ \longrightarrow H^+ + OH$$

The negative ion (e^-) attaches to a neutral water molecule which undergo further dissociation:

$$H_2O + e^- \longrightarrow H_2O^-$$

$$H_2O^- \longrightarrow H + OH^-$$

Thus the products of the reactions are H^+, OH^-, H and OH. The ions H^+ and OH^- do not take part in subsequent reactions, since all body fluids already contain significant concentrations of both these ions.

But the free radicals H and OH are chemically highly reactive and may combine with like radicals. The free OH radicals are formed close enough together to enable them to combine with each other before they can recombine with free H radicals. Therefore, another reaction product is hydrogen peroxide (H_2O_2) which is a strong oxidizing agent:

$$OH + OH \longrightarrow H_2O_2$$

The chemical stage, lasting a few seconds in which the reaction products interact with the important organic molecules of the cell. The free radicals and the powerful oxidizing agents (H_2O_2) can affect molecules or cells.

The biological stage, in which the time scale varies from tens of minutes to tens of years depending on the particular symptoms. The chemical changes can affect individual cell in a number of ways, i.e.

- the early death of the cell
- the prevention or delay of cell division, or
- a permanent modification which is passed on to daughter cells

The effects of radiation on the human body are the result of damage to the individual cells.

2.7 Health Effects from Exposure of Radiation

Production of ion pairs and excited atoms in biological cells leads to cell damage. As the amount of radiation dose received increases, so does the damage to tissue and organs. Living tissue is constructed of cells and cells themselves consist of a nucleus surrounded by cytoplasm and a membrane. The nucleus contains the chromosome, stands of DNA that contain the coded information for the behavior of the cell and are responsible for the functioning and replication of the cell. As radiation passes through living tissue, energy is deposited and ionization of atoms occurs. It is this ionization process that is responsible for radiation damage; it causes breaks in the DNA stands and also produces chemical toxins with the cells. As with all living tissue, a recovery process operates within cells and damaged DNA may be repaired. However, the effectiveness of this repair process depends on the degree of damage and incorrect repair may occur. This can result in chromosomes that contain incorrect information for the behavior of the cell, which in turn might lead to the development of cancerous tissue. High doses of ionizing radiation can lead to various effects, such as skin burns, hair loss, birth defects, illness, cancer, and death. The basic principle of toxicology, “the dose determines poison,” applies to the toxicology of ionizing radiation as well as to all other branches of toxicology. In the case of threshold effects (“deterministic effects” in the language of radiation toxicology), such as skin burns, hair loss, sterility, nausea, and cataracts, a certain

minimum dose (the threshold dose), usually on the order of hundreds or thousands of rad, must be exceeded in order for the effect to be expressed. An increase in the size of the dose above the threshold dose will increase the severity of the effect. The resulting health effects are of two types. Figure 2.1 shows classifications of Biological Effects of Radiation

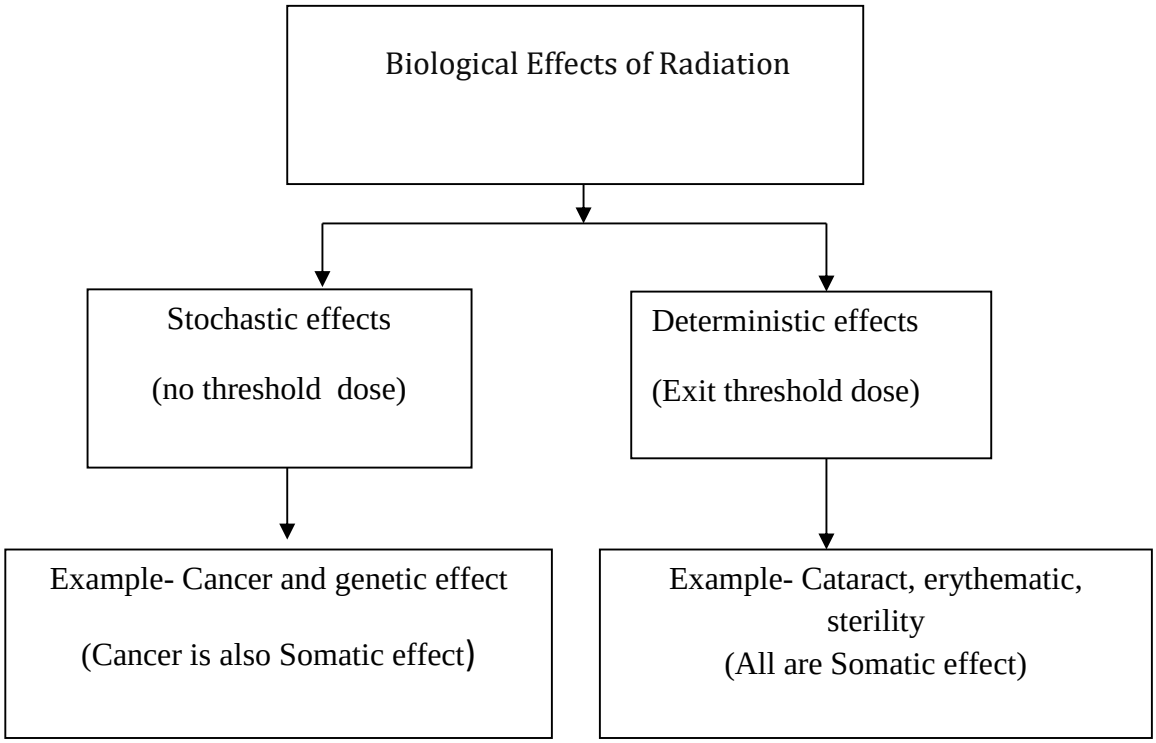

Fig. 2.1: Classifications of Biological Effects of Radiation.

2.7.1 Stochastic Effect

Stochastic effects occur with increasing probability as dose increases with any dose resulting in some probability of the effect occurring. Radiation effects, generally occurring without a threshold level of dose, whose probability is proportional to the dose and whose severity is independent of the dose (Figure 2.2).Such effects include cancer induction and heredity effects.

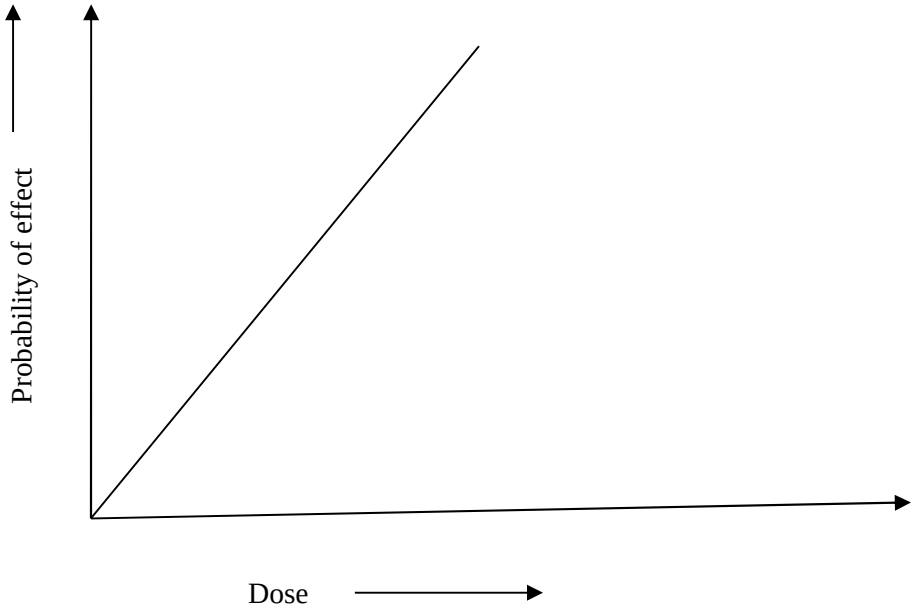

Fig. 2.2: Stochastic Dose Response Curve

2.7.2 Non-Stochastic Effect or Deterministic Effect

Those effect which are through not to occur below a dose threshold are called non-stochastic effects shown in Figure 2.3, and the severity of these effects increases with increasing dose. Non-stochastic effects are also called threshold effects. Formation of eye cataracts is an example of a non-stochastic effect. Most biological effects fall into the category of deterministic effects. These effects are characterized three quantities:
1) A certain minimum dose must be exceeded before the particular effect is observed.
2) The magnitude of the effect increases with the size if the dose.

3) There is a casual relationship between exposure to the noxious agent and the observed effect.

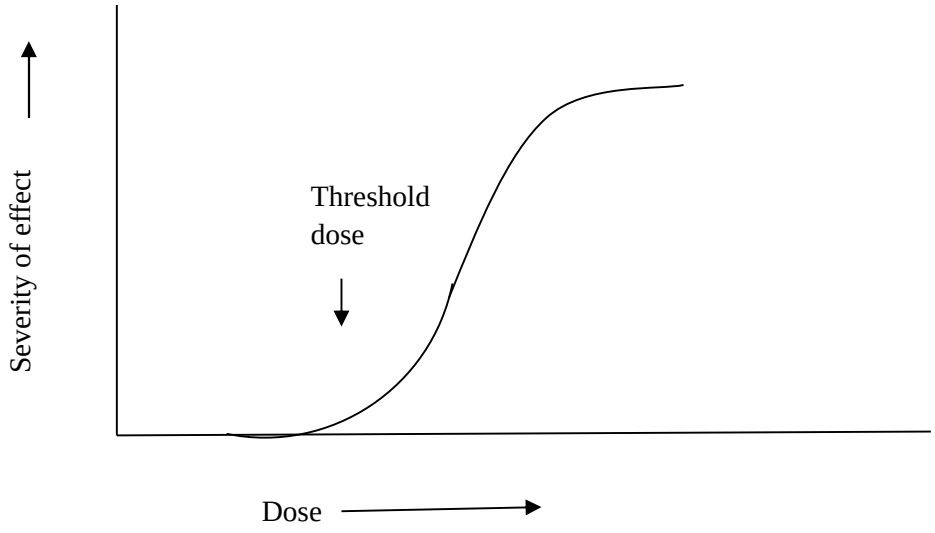

Fig. 2.3: Deterministic Dose Response Curve

2.7.3. Radiation Effects on the human body

The effect of radiation on the human body is the result of damage to the individual cells. These effects may be divided into two classes:

I. Somatic effect, and

II. Hereditary

I. **The Somatic Effect of Radiation**

The somatic effects arise from damage to the ordinary cells of the body and affect only the irradiated person. Various Forms of the Somatic Effects of Radiation are:

a. Early radiation effects or acute effects:

The early radiation effects are those which occur in the period from a few hours up to a few weeks after an acute whole body radiation overexposure. Since not all organs and organ systems are equally sensitive to radiation, the pattern of response, or disease syndrome, in an overexposed individual depends on the magnitude of the dose. In order of increasing severity, the acute radiation syndrome is subdivided into three categories:

(i) the haemopoietic syndrome

(ii) the gastrointestinal syndrome

(iii) the central nervous system syndrome

Certain effects are common to all categories and these include;

- nausea and vomiting
- malaise and fatigue
- increased temperature
- blood changes

(i) Haemopoietic syndrome

- © appears after a gamma dose of 2 Gy (200 rads)
- © depression or ablation of the bone marrow and the physiological consequences are seen the platelet count falls steadily until a minimum is reached about a month after exposure
- © the degree of change in the blood, as well as the rate of change, is a function of radiation dose
- © nausea, vomiting begin within several hour of exposure
- © hair loss (epilation), which is almost always seen in the 2^{nd} or 3^{rd} week after exposure
- © death may occur between 1 to 2 months after the exposure if medical treatment is not sought or successful

(ii) Gastrointestinal syndrome

- © Appears following a total body dose of about 10 Gy or greater

- © bone marrow is completely destroyed
- © severe nausea, vomiting and diarrhea begin very soon or immediately after exposure
- © death within 1 to 2 weeks after exposure is the most likely outcome of the exposure

(iii) Central nervous system syndrome

- © appears after a total body dose in excess of about 20 Gy
- © damages the central nervous system as well as all the other organ systems in the body
- © unconsciousness follows within minutes after exposure
- © the rapidity of onset of unconsciousness is directly related to dose death in a matter of hours to several days

Other acute effects

Skin, because of its physical location, is subject to more radiation exposure, particularly in the cases of low energy X-rays and ℘rays than other tissues. An exposure of about 3 Gy of low energy (in the diagnostic range) X-rays will result in erythema, that is reddening of the skin. Gonads are also particularly radiosensitive. A single dose of only 300 mGy (30 rads) to male gonads results in temporary sterility and a 3 Gy (300 rads) dose to female gonads produces temporary sterility. Higher doses increase the period of temporary sterility.

Table 2.1: Acute Radiation Syndromes (Liton, 2012)

Gamma-ray whole-body dose (rad)	Effects	Remarks
0-25	Not detectable	
25-100	Blood changes; person fells little or no effect	Lymph nodes and spleen damaged; lymphocyte count drops, Bone marrow damaged, deceased in white blood cell, platelet and red blood cell count
100-300	Blood changes, vomiting malaise, fatigue, loss of appetite	Antibiotic treatment may be necessary. Recovery can be expected.
300-600	Above effects plus hemorrhaging, infection, diarrohea, epilation and temporary sterility	Antibiotics and blood transfusions administered. Expect recovery in about 50% of cases at 500 rad possible bone marrow transplant.

(b) Delayed Effects or Delayed Somatic Effects

Radiogenic effects that can develop many years after either acute or protracted radiation exposure, even without apparent symptoms at the time of exposure are called delayed effects or delayed (late) somatic effects. These may occur in persons who have been exposed to very high doses of radiation but may also arise from chronic exposure to lower doses of radiation as experienced, for example, by radiation workers. The delayed effects of radiation are various forms of cancer, cataract and sterility.

(i) Cancer:

Cancers induced by radiation often develop many years after the radiation was received. There is evidence to show that radiation can produce cancer in the blood-forming tissue, skin, bone, lung, thyroid and connective tissue of a man. The minimum latent period for most cancers induced by radiation is 10 years or more.

(ii) Cataracts:

The word cataract is used to describe a loss of transparency of the lens of the eye. Radiation is known to produce lens opacities with a latent period of several years. It appears that there is a threshold dose, below which cataract cannot be induced. While a few hundred rad of low-LET radiation will produce some changes in the lens, significant cataracts probably require 500-1000 rad. High-LET radiation is considerably more effective

(iii) Sterility:

Permanent histological sterility, the complete absence of gametes, requires absorbed doses of photons to the gonads of 3.5 to 6 Gy for men and 2.5 to 6 Gy for women. Sterility can appear as an acute symptom.

II. Hereditary effects of radiation

The hereditary effects of radiation result from damage to the reproductive cells. The damage takes places which know as genetic mutation, in the hereditary material of the cell. It has already been mention that reproduction occurs when the ovum is fertilized by sperm. As, a result, the offspring receives a complete set of genetic material from each parent. Thus the child receives two complementary sets of genes, one from each of its parents. In general, it is found that one gene is dominant and the other recessive. The dominant gene determines the particular characteristic with which it is associated.

Recessive genes are only recognized when by chance two of the recessive type. Genes come together. A considerable number of diseases are associated with , with recessive genes and will therefore only manifest themselves when both parents have the same recessive genes. Spontaneous mutation accounts have the same recessive genes. An appreciable fraction of the

world‘s population suffers from one of the 500 more defects or diseases attributable to hereditary effects. Radiation can induce gene mutations which are indistinguishable from naturally occurring mutation. It should be noted in passing that heat and chemicals can also cause mutations. Mutated genes are generally received and so it is generally assumed that all mutation is harmful (Nusrat, 2013). Fig 2.4 shows the radiation effect.

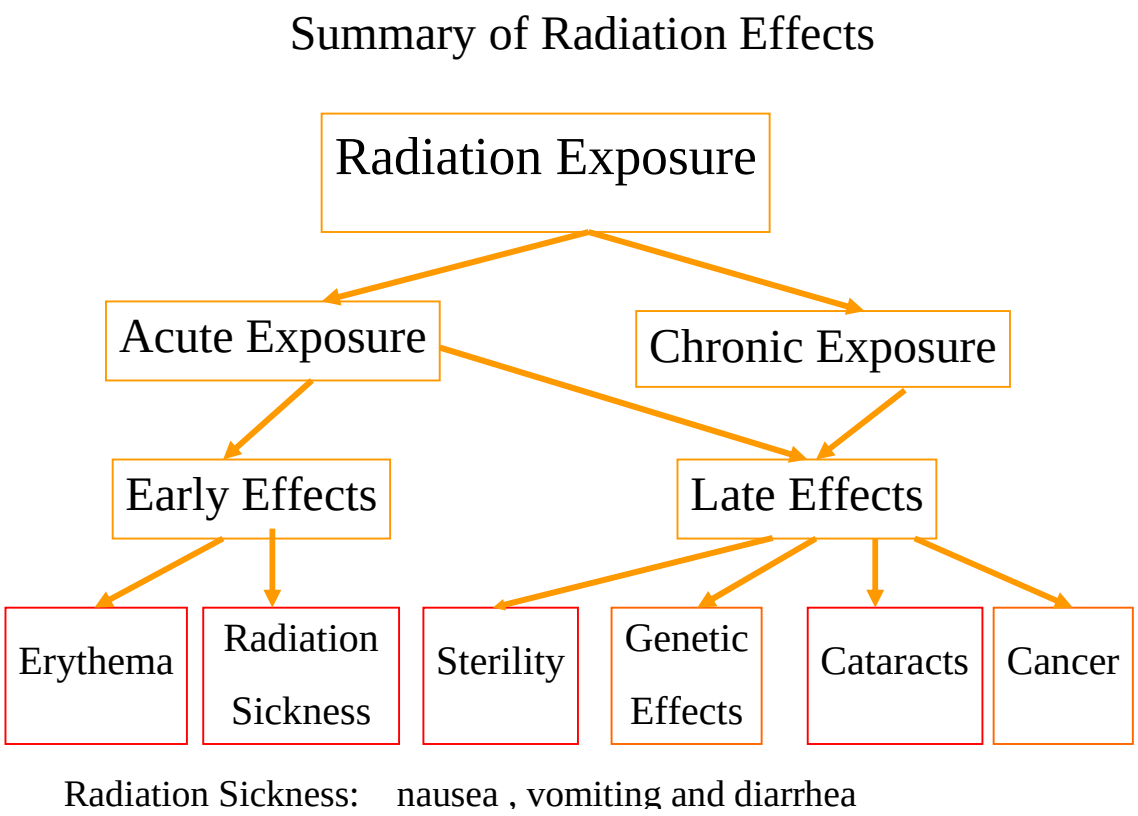

Fig. 2.4: Radiation effect

2. 8 Units of Radioactivity

The radioactivity of a source is defined in terms of the number of disintegration it undergoes in one second. The associated units of the radioactivity are discussed below.

- **The Becquerel**

The S.I. unit of radioactivity is called Becquerel. The Becquerel (Bq) is that quantity of radioactive material in which one atom is transformed per second.

1 Bq =1 transformation per second = 1 tps.

It must be emphasized that, although the Becquerel is defined in terms of a number of atoms transformed per second, it is not a measure of rate of transformation. The Becquerel is a measure only of quantity of radioactive material (Cember,1989), For many purposes, the Becquerel is a very small quantity of activity, and multiples of the Becquerel are commonly used.

- **The Curie**

The curie, symbolized by Ci, is the unit for quantity of radioactivity that was used before the adoption of the SI units and the Becquerel. The curie, which originally was defined as the activity of 1 gram ^{226}Ra, is more explicitly defined as:

The curie is the activity of that quantity of radioactive material in which 3.7×10^{10} atoms are transformed per second. The curie is related to the Becquerel by

$$1 \text{ Ci} = 3.7\times10^{10} \text{ Bq}.$$

For health physics, as well as for many other purposes, the curie is a very large amount of activity. Sub-multiples of the curie, as listed below, are therefore used.

2.9 Radiation Dosimetry

Radiation dosimetry tells us about precise unit of radiation dose that is suitable either for radiation protection or radiation therapy. For radiation protection purposes, the mostly common used ‘dosimeter’ is a piece of dental film with a paper clip attached. However, radiation absorbed by the body is energy dependent and it is thus necessary to talk and distinguish about radiation absorbed dose and radiation exposure. In terms of human biological tissue damage, the factors that must be considered are the type of radiation encountered, the amount of energy transferred by that radiation and the radio-sensitivity of the particular tissue or organ in which that energy is deposited.

Absorbed Dose

When living cells are exposed to ionizing radiation, they may absorb some or all of the energy carried by the ionizing radiation. The amount of energy actually deposited by radiation in cells is known as absorbed dose (or absorbed energy).

a.Gray *:* The International System of Units (SI unit) of absorbed dose is called the gray (Gy) which is defined as one joule (J) of energy absorbed from any ionizing radiation in one kilogram (kg) of any material. 1 Gy = 1 J/kg**.**

b. Rad*:* The former unit of absorbed dose is rad (radiation absorbed dose).

1 rad = 100 ergs/gm

Equivalent Dose

The tissue or organ absorbed dose (Gy or J/kg) multiplied by the radiation weighting factor. The SI unit of equivalent dose is sievert (Sv).

Effective Dose

The sum of the products of the organ or tissue equivalent doses and the appropriate organ or tissue weighting factors is known as Effective Dose. The SI unit of effective dose is sievert (Sv). [1 Sv = 100 rem]

Exposure Unit (X- unit*)*

One X-unit is defined as that quantity of X-ray or gamma radiation that produces ions (in air) carrying 1coulomb of charge (either sign) per kilogram of air.

1 X-unit = 1 C/kg (in air).

X-unit is limited to x-rays or gamma rays whose quantum energies do not exceed 3Mev.

Roentgen

Before the SI unit of exposure was adopted, the unit of x-ray exposure was called roentgen (R). One roentgen was defined as that quantity of x-ray or gamma radiation that produces ions carrying one statcoulomb of charge (either sign) per cubic centimeter of air at 0^0C and 760mm Hg. 1 R = 1 SC/cm^3.

The relationship between the exposure unit and the roentgen can be written as,

1 X-unit = 3881 R.

KERMA (Kinetic Energy Released in the Medium*)*

For practical convenience, the concept of air Kerma is used to specify the radiation quantity instead of exposure. Air Kerma gives an idea about the energy transferred per unit mass of air – a unit introduced by ICRU to describe the initial interaction between radiation and an electron in certain medium.

The initial kinetic energy of the primary ionizing particles (e.g. photoelectrons, Compton electrons) produced by the interaction of the incident indirectly ionizing radiation (e.g. x-rays, gamma rays, fast neutrons) per unit mass of the interacting medium is called the Kerma. Kerma in SI system is measured in JKg^{-1} or Gy.

The usefulness of air Kerma can be extended to the determination of the radiation output at a specified distance from a radiation source in terms of mGy per hour. The air Kerma rate at 1 meter and the activity of gamma source can be correlated using exposure rate constant applicable for that source. For example, 1 GBq of Cobalt-60 gives an Air-Kerma output of $0.31mGy\ h^{-1}$. (Johns and Cunningham,1964)

2. 10 Exposure Limits

As discussed in the introduction, concern over the biological effect of ionizing radiation began shortly after the discovery of X-rays in 1895. The guidelines for radiation exposure have had two principle objectives: 1) to prevent acute exposure; and 2) to limit chronic exposure to "acceptable" levels. It means that every reasonable effort must be made to keep the dose to workers and the public as far below the required limits as possible (ICRU, 1925).

Regulatory Limits for Occupational Exposure

For industrial radiographers who generally are not concerned with an intake of radioactive material, the Code sets the annual limit of exposure at the following:

1) The more limiting of:

- A total effective dose equivalent of 5 rems (0.05 Sv) or
- The sum of the deep-dose equivalent to any individual organ or tissue other than the lens of the eye being equal to 50 rems (0.5 Sv).

2) The annual limits to the lens of the eye, to the skin, and to the extremities, which are:

- A lens dose equivalent of 15 rems (0.15 Sv)
- A shallow-dose equivalent of 50 rems (0.50 Sv) to the skin or to any extremity.

The shallow-dose equivalent is the external dose to the skin of the whole-body or extremities from an external source of ionizing radiation. This value is the dose equivalent at a tissue depth of 0.007 cm averaged over and area of 10 cm^2.The lens dose equivalent is the dose equivalent to the lens of the eye from an external source of ionizing radiation. This value is the dose equivalent at a tissue depth of 0.3 cm.The deep-dose equivalent is the whole-body dose from an external source of ionizing radiation. This value is the dose equivalent at a tissue depth of 1 cm. The total effective dose equivalent is the dose equivalent to the whole-body.

Declared Pregnant Workers and Minors

Because of the increased health risks to the rapidly developing embryo and fetus, pregnant women can receive no more than 0.5 rem during the entire gestation period. This is 10% of the dose limit that normally applies to radiation workers. Persons under the age of 18 years are also limited to 0.5rem/year.

Non-radiation Workers and the Public

Dose limit to non-radiation workers and members of the public are two percent of the annual occupational dose limit. Therefore, a non-radiation worker can receive a whole body dose of no more that 0.1 rem/year from industrial ionizing radiation. This exposure would be in addition to the 0.3 rem/year from natural background radiation and the 0.05 rem/year from man-made sources such as medical x-rays.

CHAPTER III

Methodology

3.1 Study Area

The present study area is the bank of Rupsha River, which is located Rupsha Upazilla, Khulna district, Bangladesh. The coordinates of the sampling area of Rupsha upzilla is in between 22°45′27.09″N to 22°50′12.47″N and 089°34′12.49″E to 089°36′29.62″E. The locations of sample collection under current study are shown in Figure 3.1.

3.2. Sampling Locations

Samples are collected from 8 locations, which is Deara, Khan Mohammadpur; Aichgati, Joypur, Jabusa, Elahipur, Noeihati and Karabad in the bank of Rupsha River. Total of 28 samples namely; 6 Paddy, 7 Leafy vegetables, 8 Arum and 7 Papaya samples; were collected from around the Rupsha River located at Rupsha upazilla, Khulna. The samples were collected during the whole day on 1 May to 5 May, 2015.

3.3: Sample Collection and Preparation

I have done study on Paddy and three vegetables sample such as- Leafy vegetables, Arum and Papaya. A total number of 28 samples were collected from in and about 10 kilometers in eight direction on the Bank of Rupsha River at Rupsha upazilla, Khulna. In the present work the samples were collected at different home (papaya) and different field (Paddy, Leafy vegetables and Arum) of the selected location. About 2.1-4.75 Kg of samples were collected from each location and each of the samples was placed in hand bag and transported to the laboratory of the Health Physics and Radioactive Waste management Unit (HPRWMU), Bangladesh Atomic Energy Commission (BAEC), Savar, Dhaka for processing and characterization.

Each of the collected vegetables samples was first weighed(at green),then cut the vegetables into small pieces, then dried by the Sun shine and then about 100^0C in an Oven for 24 to 72 hours and there after grind into a fine powder with a Grinder and collected after passing through a 20-mesh screen. Thus homogenized sample was transferred to sealable cylindrical plastic container of 7 cm height and 5.5 cm in diameter, marked individually with

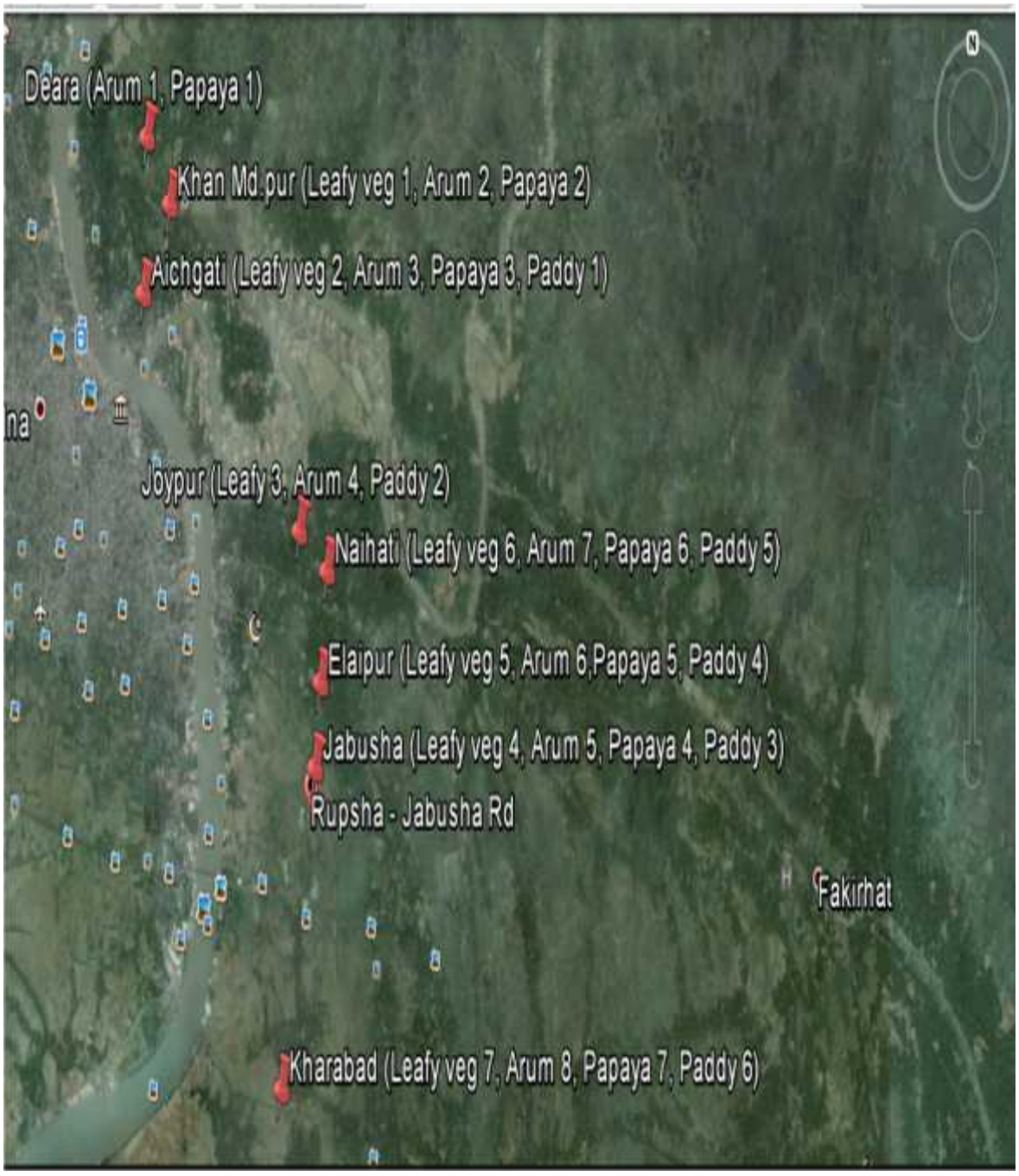

Fig. 3.1: Location map of sampling (using Google map) area Rupsha, Khulna, Bangladesh.

Identification parameters i.e., name and location of the sample date of preparation and net weight. All the samples containers were sealed tightly with cap and Teflon and thick Vinyl tapes around their screw necks and finally air tightened and stored for minimum four weeks prior to counting, allowing establishment of Secular equilibrium between the long lived ^{214}Pb, ^{232}Th, ^{228}Ac, and their daughter products. Detailed of the sample were described in Flow-chart 3.2 and Table-3.1. The prepared samples are shown in Picture 3.1

Picture 3.1: Prepared samples

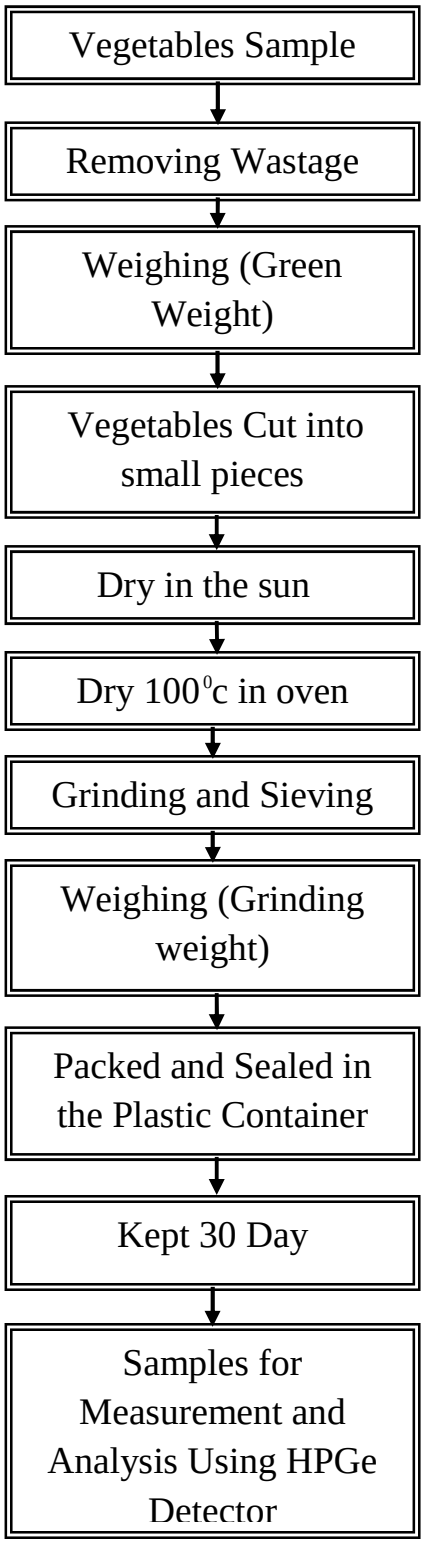

Fig. 3.2: Flow-chart illustrating the pretreatment of vegetable samples.

Table 3.1**:** Detailed of the collected samples for study (with location- local name)

Collection Area	Sample ID	Date of Collection	Date of Preparation	Quantity of Vegetables Samples Net weight in(gm)
Deara	Papaya 1	01/05/2015	20/05/2015	61.47
	Arum 1		19/05/2015	132.83
Khan Mohammadpur	Papaya 2	02/05/2015	20/05/2015	43.27
	Arum 2		19/05/2015	138.57
	Leafy veg.1		18/05/2015	78.31
Aichgati	Papaya 3	02/05/2015	20/05/2015	67.79
	Arum 3		19/05/2015	138.1
	Leafy veg.2		18/05/2015	79.85
	Paddy 1		21/05/2015	101.34
Joypur	Arum 4	03/05/2015	19/05/2015	141.57
	Leafy veg. 3		18/05/2015	67.48
	Paddy 2		21/05/2015	105.16
Jabusa	Papaya 4	03/05/2015	20/05/2015	76.46
	Arum 5		19/05/2015	143.8
	Leafy veg. 4		18/05/2015	70.74
	Paddy 3		21/05/2015	91.42
Elahipur	Papaya 5	04/05/2015	20/05/2015	71.79
	Arum 6		19/05/2015	132.22
	Leafy veg.5		18/05/2015	64.91
	Paddy 4		21/05/2015	104.96
Noeihati	Papaya 6	05/05/2015	20/05/2015	68.04
	Arum 7		19/05/2015	133.13
	Leafy veg. 6		18/05/2015	66.99
	Paddy 5		21/05/2015	105.17
Kharabad	Papaya 7	05/05/2015	20/05/2015	88.06
	Arum 8		19/05/2015	152.64
	Leafy veg. 7		18/05/2015	70.58
	Paddy 6		21/05/2015	100.17

3.4 Experimental Set Up

A general description of the radionuclide detection technique for Paddy, Leafy vegetables, Arum and Papaya samples are given below, including the description of detector and the calibration process of the gamma spectrometry system. The experimental layout and treatments used are then outlined and finally the analytical methods used for the analysis of all samples are described.

3.4.1 Radionuclide Detection Technique of Radioactive Samples

A number of analysis systems exists which are able to determine the activity and radionuclide content of various types of samples and geometry. For all types of samples, gamma spectrometry is generally the most effective technique to analyze the gamma emitting radionuclides in these samples. The method is highly suited for accurate multi-nuclide analysis without any chemical separation for environmental materials. The system is now widely used by laboratories, which are dealing with the analysis of gamma emitting radionuclides in environmental samples. The detection of radionuclides and its activity can be done using chemical separation methods, however, the method is costly and time consuming. On the other hand, gamma spectrometry is not expensive but some preliminary work (such, an energy calibration and self absorption and efficiency calibration) must be undertaken before using the system for the analysis of multi-nuclides in contaminated.

First, an energy calibration has to be performed. The sample for this must contain various radionuclides, which have a good spread of ¥ -energies i.e., the energies must range from the detectable minimum up to the detectable maximum. This produces a much more accurate calibration. Secondly, in order to measure the activity of a sample, it is necessary to know the system's detection efficiency, which is obtained by employing known standard sources. The calibration standard source must have physical dimensions, chemical composition and density similar to the samples that will be analyzed, so that the deviation in the measured activity is normalized. However, it is necessary to subtract background counts from the standard source counts to measure the accurate count rates of standard samples (Debertin and Helmer, 1988), (Koddis et al., 1992).The two most important gamma analysis detectors that are available presently are sodium iodide crystal detectors (NaI) and liquid nitrogen cooled high purity

germanium detectors (HPGe). HPGe detectors, due to their excellent resolution have become an important tool for the analysis of radioactive samples using gamma-ray spectrometric techniques. The absolute efficiency response of these detectors is an important parameter for almost all work based on absolute method. A high purity germanium detector is widely used to determine quantitatively the concentrations of radionuclides in the radioactive waste samples. A brief description of an HPGe detector is given in the following section.

3.5 Apparatus Used

3. 5. 1 High Purity Germanium (HPGe) Detector

Now-a-days HPGe detector is extensively used for gamma ray spectrometry. The world-wide popularity of germanium as semiconductor radiation detector is attributable to the excellent charge transport properties, which allows the use of large crystals without excessive carrier losses due to trapping or recombination. The greater efficiency, large photo fraction and lower cost of sodium iodide may well tip the balance in its favor when only a few gamma ray energies are involved. Germanium detectors are clearly preferred for the analysis of complex gamma ray spectra involving many energies and peaks, it also aids in the detection of weak sources of discrete energies when superimposed on a broad continuum.

Germanium detectors are semiconductor diodes having a p-I-n structure in which the intrinsic region is sensitive to ionizing radiation, particularly X-rays and gamma rays. Under reverse bias, an electric field extends across the intrinsic or depleted region. When photons interact with the material within the depleted volume of a detector, charge carriers (holes and electrons) are produced and are swept over by the electric field to the p and n electrodes.

This charge, which is in proportion to the energy deposited in the detector by the incoming photon, is converted into the voltage pulse by an integral charge sensitive preamplifier (Canbera, pro.831. asp). (Roy, 1991).

HPGe detectors are available in two relatively simple geometries:

a. The planer detector in which the electric field is fairly uniform and

b. The co-axial configuration in which the electric field varies inversely with the radial distance from the detector axis.

The gamma ray detection efficiency and response function for the HPGe detector are identical to those observed in a Ge (Li) detector of the same size and shape.

A p-type co-axial HPGe detector of volume 93 cm^3 supplied by CANBERRA Model No. GC-2018 and serial No. 04089411 has been used in the present experiment at the Health Physics and Radioactive Waste Management Unit (HPRWMU) Laboratory, Institute of Nuclear Science and Technology (INST), Atomic Energy Research Establishment (AERE), Savar, Dhaka. The HPGe detector used is co-axial geometry type with electrical contacts in the form of concentric cylinders closed at the end. This geometry makes it possible to produce very large volume detector elements with excellent efficiencies for high-energy photons. Thus the HPGe detector is basically a cylinder of germanium with an n+-type contact on the outer surface and a p+-type contact on the surface of the axial wall. The n+-type contact is formed by evaporation of lithium into a lapped surface of germanium and p+-type contact consists of a metal to semiconductor surface barrier junction. These results are an n+-p-p+ configuration of the detector in which the depletion region formed by reverse biasing requires that a positive voltage is to be applied to the n+ contact with respect to p +surface. The depletion effectively begins at the n+ edge of the central region and extends further into the p region as the voltage is raised. Since there is a significant dead layer on the n+ face, the p+ face is normally used as the entrance window. Ion implantation techniques are also used to form the p+ contact especially when very thin entrance window is needed.

The main characteristics of the HPGe detector are high atomic number, low impurity concentration, i.e., large deletion depth, lowest ionizing energy required to produce an electron hole pair, higher conductivity, compact size, fast time response, high resolution and relative simplicity of operation at room temperature.

The main parts of this detector coupled with other accessories are:

(1) Liquid nitrogen (LN_2),
(2) Cryostat,
(3) Digital Spectrum Analyzer (DSA) 1000
    i. A preamplifier,
    ii. Spectroscopy amplifier,

iii. High voltage detector power supply,

iv. Multi channel analyzer (MCA),

(4) Shielding arrangement of the detector and

(5) Computer

The block diagram of HPGe detector with its accessories and a photograph of this set-up are shown in Fig 3.3and Picture 3.2 respectively. Brief descriptions of these parts are given below

(1) Liquid Nitrogen (LN_2) Dewar

Germanium has relatively low band gap, these detectors must be cooled in order to reduce the thermal generation of charge carriers (thus reverse leakage current) to an acceptable level. Otherwise, leakage current introduced noise destroys the energy resolution of the detector. Liquid nitrogen (LN_2), which has temperature of $77\ ^0$ K is the common cooling medium for such detectors. The detector is mounted in a vacuum chamber, which is attached to or inserted into an LN_2 Dewar. The sensitive detector surfaces are thus protected from moisture and condensable contaminants. The liquid nitrogen Dewar serves as reservoir of liquid nitrogen, while the cryostat provides a path via the cooper steam for heat transfer from the detector to nitrogen reservoir.

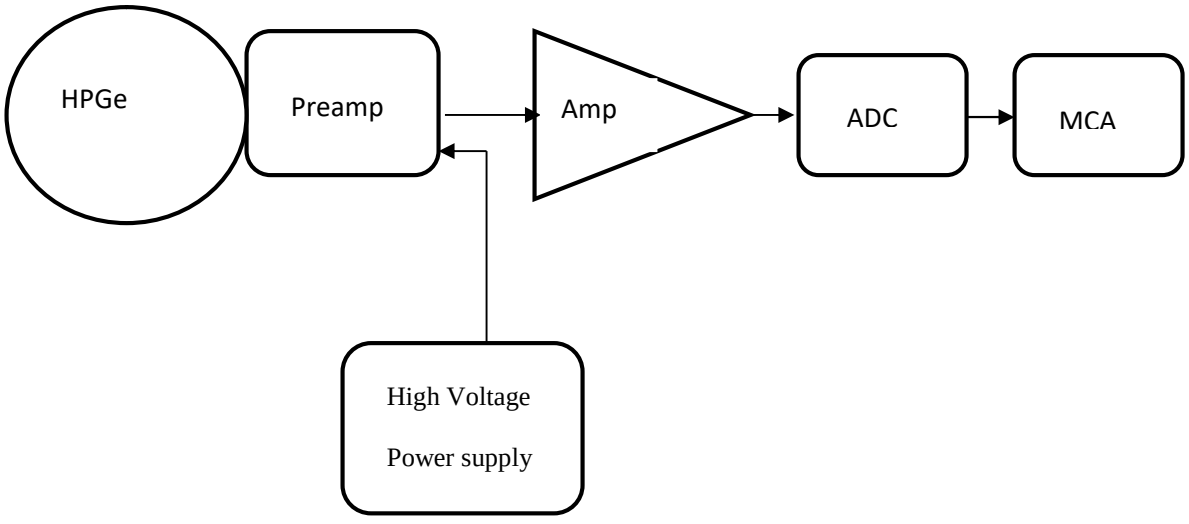

Fig. 3.3: Block diagram of gamma spectroscopy system (HPGe detector) used in the present work.

Picture 3.2: A complete setup of γ-counting system (HPGe Detector with 20% relative efficiency).

(2) Cryostat

A cryostat consists of a vacuum chamber which houses the detector element plus a Dewar (double wall vacuum-insulated vessel) for the liquid nitrogen cryogen. Integral cryostats have a common vacuum chamber for the Dewar and detector. Unlike the dipstick type, the detector chamber and Dewar cannot be separated without breaking vacuum. A basic integral cryostat is shown in Fig 3.4. The cryostat is a sealed vacuum chamber and usually the vacuum is maintained by a passive system, a molecular sieve and placed in the bottom of the cold finger

assembly. This molecular sieve absorbs any gaseous molecules, which can loose inside the cryostat and prevents them from depositing on the surface of the cryostat. Otherwise, the increasing surface contamination on the crystal would result in increased surface currents, which, in turn, elevates the noise and broadens the resolution (Roy, 1991).

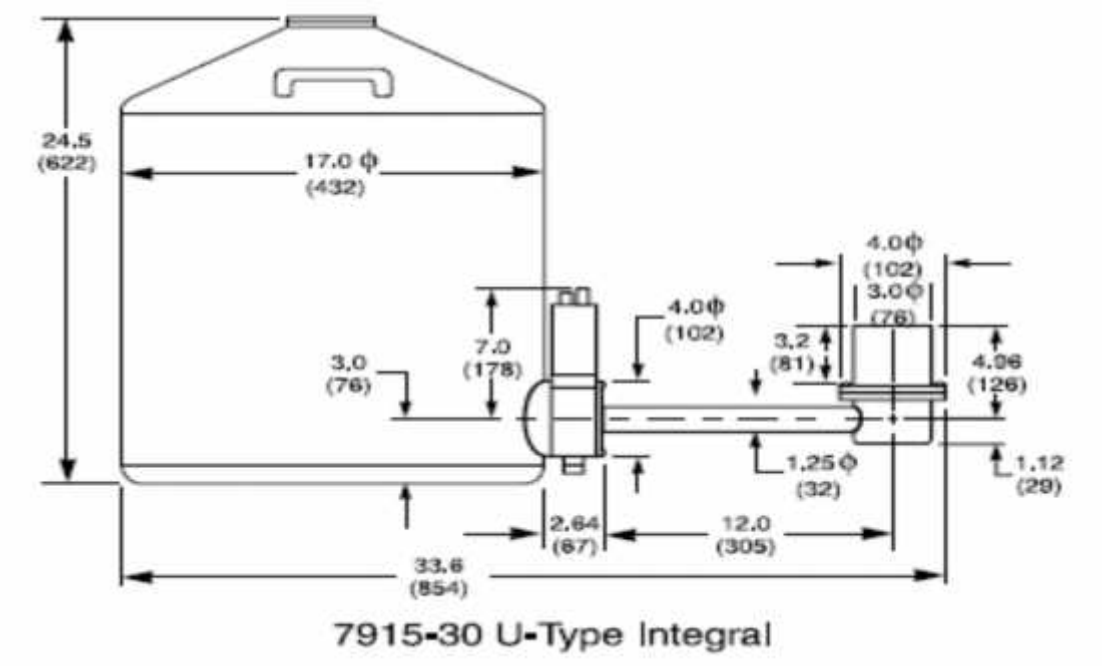

Fig. 3.4: Photograph of Cryostat

(3) Digital Spectrum Analyzer (DSA) 1000

The DSA-1000 is a full featured 16K channel integrated Multichannel Analyzer based on advanced digital signal processing techniques (DSP). When paired with the computer of choice, the DSA-1000 becomes a complete spectroscopy workstation, capable of highest quality acquisition and analysis. Picture 3.3 shows the Digital Spectrum Analyzer.

Picture 3.3: Digital Spectrum Analyzer (DSA) 1000

The main components are given below:

i. Preamplifier (Model 2002 CSL)

The preamplifier associated with radiation detectors performs three essential functions:

a. Conversion of charge to voltage pulse
b. Signal amplification
c. Pulse shaping.

Most preamplifiers in use today are charge sensitive and provide an output pulse with amplitude proportional to the integrated charge output from the detector. General-purpose preamplifiers have a RC feedback network (Fig 3.5) which results in a quasi-step function output. For extremely low noise, the feedback resistor is eliminated and the output signal becomes a true step function, which builds in random staircase fashion and is reset by so called pulsed-optical feedback circuitry. For many high count rate and high resolution applications with HPGe detectors, the transistor reset preamplifier (TRP) offers the best performance (Koddis et. al, 1992).

There are two basic types of preamplifiers used in germanium detectors:

(a) Charge sensitive that employs either dynamic charge restoration (RC feedback),

(b) Pulse charge restores type (pulse optical or transistor reset) for discharging the integrator.

Absorption of photon by detector produces a current pulse at the preamplifier input. These pulses are too small to measure without amplification into a measurable electric signal. Therefore, the first element in a signal processing chain is a preamplifier that provides

interference between the detector and pulse processing and analyzing electronics. The preamplifier has been located as close as possible to the detector to minimize the signal from noise and captive loading. It also serves as an impedance matcher, presenting high impedance to the detector to minimize loading, while providing a low impedance output to drive succeeding components. Canberra Model 2002 CSL used in the present work has the following characteristics.

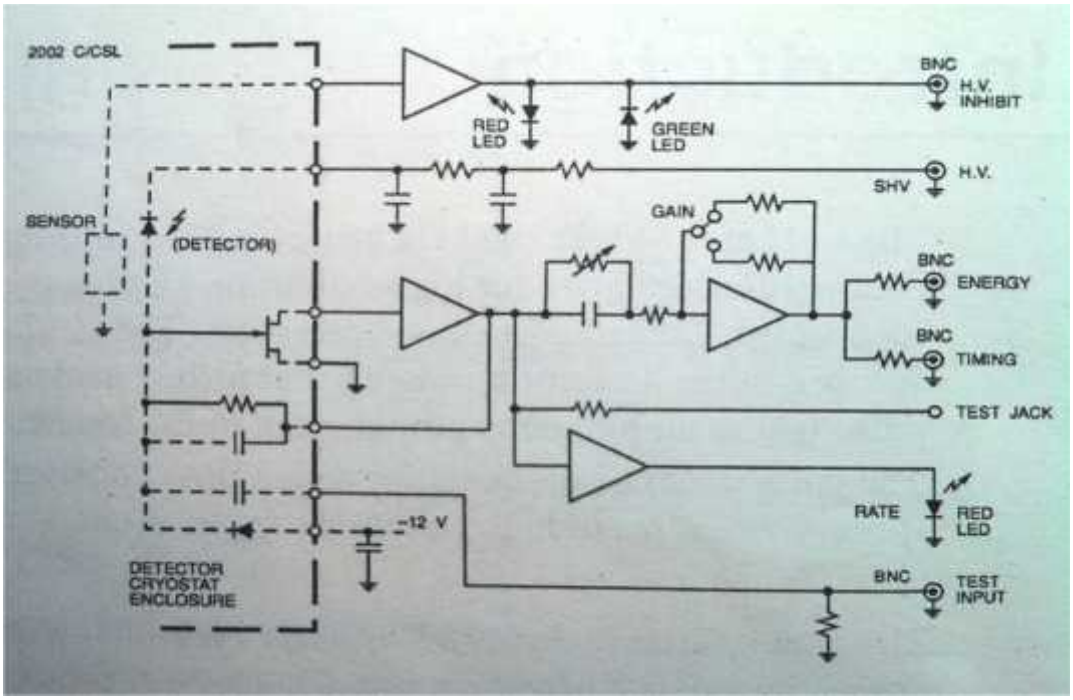

Fig. 3.5: Block diagram of preamplifier

Characteristics of Model 2002C Preamplifier:

Noise	: < 500 eV.
Charge or energy sensitivity	: 100 or 500 mV/MeV (Ge).
Charge or energy rate capability	: 2 $\times 10^5$ MeV/sec.
Rise time	: < 50 ns.
Bias rating	: 5000

ii. Amplifier

Accepts positive or negative signals from an associated detector preamplifier; amplitude for full scale conversion ±10 V divided by selected gain; maximum input (signal +dc) for linear operation is dependent on the Input Attenuator setting; Attenuator OFF (x1): ± 4 V, Attenuator ON (x 0.25): ±12 V, dc coupled and protected to ±24 V maximum; rise time: less than the selected Rise Time + Flat Top settings; acceptable preamplifier decay time constant: 45 μs to infinity; Zin is 1.3 kΩ; rear panel BNC connector.

iii. High Voltage Power Supply

Dual range and polarity high voltage power supply; voltage range and polarity selected by programming modules: ±10 to ±1300 V dc or ±1300 to ±5000 V dc; rear panel SHV connector. Low end of the 5000 V range is limited to 1300 V by software.

iv. Multi Channel Analyzer (MCA)

MCA is capable of analyzing pulses simultaneously with many different intervals or channels. In fact, MCA's are heart of most modern experimental measurements. It's essential functions are collection of data providing a visual monitor and producing output either in the form of final results or as raw data for later analysis. The MCA consists of an analog-to-digital converter (ADC), MCA buffer and a display. The main component of the MCA is an analog-to-digital converter (ADC), which converts the incoming analog amplifier signal to a group of standard shaped pulses. The pulses are digitized by a Wilkinson type analog-to-digital converter (ADC) and the output pulses are stored in a computer type memory (Wilkinson, 1950).The channel number is the memory address and is proportional to the input signal voltage. Therefore, pulses of constant amplitude will always be stored in a signal channel. Each pulse is digitized and a count is added to the appropriate memory location. So the ADC is the key element in determining the performance characteristics of the analyzer.

(4) Shielding Arrangement

The shielding of the detector from the environmental radiation is an absolute necessity for low-level measurement of activity. The shielding arrangement surrounding the detector has been designed and fabricated by using lead and steel material, available in local market. Because of high density (11.4 gm/cc) and large atomic number (Z = 82) of lead, it is widely

used for the construction of radiation shielding. Hard gamma rays from external background source (such as 1.46 MeV from ^{40}K) can be absorbed efficiently by lead. Moreover, it is reasonably effective for removing many of the cosmic ray components of the background radiation. The photoelectric absorption of gamma rays in the lead shielding around the detector can lead to the generation of characteristic X-ray, which is covered by steel. Steel has much lower atomic number (34) compared to that of lead. A photograph of the shielding arrangement of the Detector is shown in Picture 3.4.

Picture 3.4: Shielding Arrangement of the Detector

The Shielding expression is

$$I = I_0 e^{-\alpha t} \qquad (3.1)$$

Where I is the beam intensity after penetrating a thickness t of the material, α is the linear attenuation coefficient of absorbing material and I_0 is the intensity when thickness t = 0. Theoretically, the shielding arrangement was found to attenuate 95%-99.99% of unwanted gamma flux of energy ranging from 303 KeV to 1332 KeV, where most of the gamma lines from background radiation (Thorium, Uranium, and Actinium series) were found to decrease

by 74% to 96% (Roy, 1991) The shielding material around the detector (lead rings) has the characteristics given below: Table 3.2: shows the characteristics of the shielding material used around the detector

Table 3.2: Characteristics of the shielding material used around the detector

Shielding Lead Ring:

a. Internal diameter	: 305 mm
b. External diameter	: 406 mm
c. Wall thickness	: 51mm
d. Shielding height	: 559 mm

Double Part, Top Opening & Sliding Load Door:

a. External Diameter	: 406 mm
b. Thickness	: 51 mm

Base Plate (Lead & MS)

a. External Diameter	: 406 mm
b. Thickness	: 51 mm
c. Thickness of the Bottom of Base Plate (MS Plate)	: 10 mm

Table /platform:

a. Height	: 3048 mm
b. Size	: 1219.2x 609.6mm^2

(Made of 51x 51 mm^2 Ms box , 3mm MS plat, 457x 457 mm^2 support box)

Replacement Arrangement:

a. Height	: 3048 mm
b. Size	: 1219.2 x 609.6mm^2

(Materials 51x51 mm^2 MS box, 3mm MS plat)

(5) Computer

The energy spectrum of the radiation was observed in computer. The configuration of the computer is shown below:

Processor : Intel(R) Pentium(R) 4

RAM	: 504 MB
Monitor	: CRT (cathode ray tube)
Operating System used	: Microsoft window XP professional
Software used	: version 2002 service pack 2

As a whole, the following are the specifications of the HPGe detector (Model GC 2018):

Detector	: HPGe
Detector model	: GC 2018
Serial number	: 04089411
Crystal geometry	: closed-end coaxial
Crystal diameter	: 6.2 cm
Crystal length	: 3.1 cm
Crystal active volume	: 93 cm^3
Crystal / Window distance	: 0.5 cm
Dewar capacity	: 30 litre
Cooling temperature of the Ge Crystal	: 77^0 K (i.e., LN_2 temperature)
Energy resolution of the detector (FWHM at 1332 KeV of ^{60}C gamma rays)	: 2 KeV (specified by manufacturer)
Relative Efficiency	: 20 %
Peak to Compton ratio	: 50: 1

3.5.2 Standard Geometry Setup

For the measurement of radionuclide in investigated sample such as Paddy, Leafy vegetables, Arum and Papaya samples, a standard geometry is needed which is similar to the geometry of calibration standard..3.75cm × 8.5cm plastic container was used to measure the radionuclides activity. To measure the radionuclide of the sample, the samples were transferred to the plastic container and then placed on the top of the detector.

3.5.3 Standard ¥- Ray Sources

Gamma ray reference point sources are essential in any laboratory to calibrate the γ-spectrometer for the measurement purposes. The calibration sources available in the Health Physics and Radioactive Waste Management Unite (HP&RWMU), Institute of Nuclear Science & Technology (INST), AERE, Savar, Dhaka, were all supplied by Amershem International, USA. Their physical characteristics are listed in Table- 3.3.

The activity of a source at any time from the day of its initial activity A_o can be calculated by using the radioactive decay equation as

$$A_t = A_o e^{\frac{-0.693 \times t}{t_{1/2}}} \qquad (3.2)$$

Where, A_o is the initial activity of the standard source at $t = 0$, A_t is the activity of the source after time t and $t_{1/2}$ is the half- life of source.

Table 3.3: Physical characteristics of ^{137}Cs and ^{60}Co radionuclide

Radio nuclides	Half time (Year)	Energy E in KeV	Intensity (Iγ)
^{137}Cs	30	661.62	0.8521
^{60}Co	5.27	1173.2	0.9990
		1332.5	0.9998

3.5.4 Calibration of the Detector Parameters

In the gamma spectrometry the spectra accumulated on the computer based Multi Channel analyzer (MCA) provides data on both count rate and the location of each peak depending on gamma energy. In order to convert these data onto either emission rate or energy, the spectrometer should be calibrated with gamma sources of known energy. For this purpose details information on the following parameters are necessary.

a. Energy calibration of MCA
b. Counting Efficiency Calibration

c. Lower limits of detection
d. Background spectrum

(a) Energy Calibration

In gamma spectrometry, radiation pulses are recorded by a multi-channel analyzer (MCA) and the location of the peak depends on the gamma ray energy. For identifying a particular radionuclide of unknown sample, it is necessary to calibrate the MCA by observed γ-ray energy spectrum against the channel number. The displayed spectrum from a HPGe detector is usually a series of photo peaks superimposed on a more or less varying background. The peak location indicates gamma ray energy. The value of the baseline, i.e., channel number has no real significance until it can be calibrated proportionally to read in terms of energy.

For HPGe detector the relation between gamma energy and output pulse height is nearly linear. Therefore, two or more known peaks of sufficiently different energy will serve to establish the energy calibration, Let E_1 and E_2 are the known energies of peaks and let X_1 and X_2 are the peak locations measured in the pulse height spectrum. Thus, energy per channel can be calculated as:

$$E = mX + b \qquad (3.3)$$

Where X is any channel number, energy per channel (m) = $(E_2-E_1)/(X_2-X_1)$,
Constant (b) = E_1-mX_1Thus X = (E-b)/m
In the present study calibration of the MCA was carried out by using good geometry point sources placed close to the detector inside the shield. The gamma spectra obtained on the MCA monitor after the equipment set up of live time, high voltage power supply (4500 Volts), adjustment of spectroscopy amplifier such as course gain (50), fine gain (0.8), shaping time (2μsec). The energies of the calibration source in keV were entered in the MCA to convert all 16384 channels to respective energies. The following Table 3.4 gives a list of calibration source and their energies.

Table 3.4: Gamma ray energy calibration sources

Source	Energy in keV	Emission Probability	Half Life In years
^{137}Cs	661.66	85.20	30.17
^{60}Co	1173.2	99.89	5.272
	1332.5	99.98	5.272

(b) Counting Efficiency Calibration

The most import parameters characterizing a radiation detector are efficiency and energy resolution. The efficiency calibration should be performed with great care because the accuracy of the experimental result depends on it.

3.5.5 Counting Efficiency of Gamma Spectrometry

The efficiency of a detector is a measure of the number of gamma rays detected out of a total number of gamma-rays that are actually emitted by the source. The full energy peak efficiency is defined as

$$£_{(E)} = \frac{n(E)}{R(E)} \qquad (3.4)$$

Where n(E) = count rate (number of counts in the peak divided by the measuring time) in the peak corresponding to the energy,

R(E) = Rate at which photon of energy E are emitted from the source i.e. activity of the source.

$$£_{(E)} = \frac{n(E)}{A} \qquad (3.5)$$

Where A = activity.

This efficiency is related to a specific source-detector geometry and particular peak analysis procedure; it varies with the detector size and type of counting geometry, height and weight of the standard sample (Eric, 1965) and the environment surrounding the detector system. The counting efficiencies are measured with standard or reference samples in which the activities or concentrations of radio-nuclides are exactly known. Sometimes it may not be possible to obtain all the desired reference samples. In such a situation the best way is to plot an efficiency calibration curve from the available standard sources and extrapolate the curve.

Three types of efficiencies are described below:

(a) Intrinsic Photo-peak Efficiency: The intrinsic photo peak efficiency is defined as the fraction of mono energetic gamma-rays which on striking the detector will produce counts in the corresponding photo peak, efficiency can be obtained by using the following expression,

$$£_p = 1 - e^{-\mu t} \qquad (3.6)$$

Where, $£_p$ = Photo-peak efficiency

μ = Linear attenuation coefficient of the detector at energy of interest

t = Thickness of detector.

(b) Absolute Efficiency: The absolute (or total) efficiency $£_T$ of a counting system is the probability that a gamma ray emitted from a point source at a particular source to detector distance will produce a count in the corresponding photo-peak.

$$£_T = \frac{\text{Photopeak count rate}}{\text{Gamma ray emission rate}} \qquad (3.7)$$

The absolute efficiency is the product of the probability that a gamma ray will strike the detector and the probability that it will interact and will produce an event in the photo peak. In general it depends on the source to detector distance. Equation (3.7) can be restated as

$$£_T = £_g £_p \qquad (3.8)$$

Where is the probability of gamma ray striking detector, sometimes called the geometric efficiency. Thus in case of detector of area A positioned a distance r from a point gamma source, the absolute counting efficiency can be expressed a:

$$£_T = \frac{A.£_p}{4®r^2} \qquad (3.9)$$

(c) Relative Efficiency: Relative efficiency is the ratio (the percent) of the absolute efficiency of the HPGe detector for counting the 1332 keV gamma ray from the ^{60}Co at 25 cm distance to the absolute efficiency of a 3"× 3" thick NaI (Tl) crystal at the same source to detector distance. Absolute efficiency of a standard 3"× 3" NaI crystal positioned at 25 cm away is 1.2 $\times 10^{-3}$. The relative photo peak efficiency =

$$\frac{R_1}{R_2} \times 100 \qquad (3.10)$$

Where, R_1 = $\frac{\text{No. of counts in the 1.33 MeV photopeak for HPGe}}{\text{Counting time in second}}$

And R_2 = Gamma activity of the source in counts per second × Efficiency of the NaI detector (i.e. 1.2 × 10^{-3}).

In the present work, the value of relative efficiency of the detector was found to be 20% measured for 93 cc HPGe detector.

3. 5.6 Lower Limit of Detection of Radionuclides

The detection limit, as it is known as minimum detectable emission rate or lower limit of detection (LLD) is a term used to express the detection capability of a measurement system under certain conditions. The limit depends on the sample geometry, the energy of the radiation, the source-detector distance, the detector efficiency, the background, the available time for measurement and the quantity of samples (mass and volume). In a measurement if the measured number of counts, N in the time T is large, then number of background counts N_b , in the same interval T must be known from a measurement without the sample. The statistical fluctuation of N_b can be described by the standard deviation S (N_b) = $\sqrt{N_b}$ provided N_b was taken in the same interval T as N. If the number of additional counts due to photons from the

sample, N_s = N- N_b is of the order of background fluctuations, i.e. of $S(N_b)$ then there is no clear evidence of the existence of a sample effect. On the other hand, if N_s is, say larger than 3 $S(N_b)$, the probability of the presence of a sample effect is rather high. Therefore, the detector limit can be given as $L = 3\sqrt{N_b}$. The lower limit of detection (LLD) at the 95% confidence level has been defined by Pasternak (Koddis et al., 1992) as: $LLD = 1.645 (2\sqrt{2})S_b$, where S_b is the standard deviation of the background. The standard deviation of the distribution is the square root of the mean value for a particular sampling interval, the S.D. is the observed number of counts $n\sqrt{n}$. The standard deviation associated with a count rate is $S= \sqrt{n} / t$. The S. D. of the sum or difference of two measurements is the square root of the sum of the squares of the standard deviations associated with the measurements. The standard deviations of the net count rate obtained is

$$S_n = \sqrt{(S_g + S_b)}$$

$$= [n_g / t_g^{\,2} + n_b / t_b^2]^{1/2} \qquad (3.11)$$

The lower limit of detection for the counting portion of the analysis is:

$$LLD = 1.65(2\sqrt{2})\, S_b$$

$$= 4.653\, [n_b / t_b^2]^{1/2} \qquad (3.12)$$

For the calculation of the lower limit of detection of food and environmental samples the following equation was used:

$$LLD = \frac{4.653 \times S_b}{E \times I \times V} \qquad (3.13)$$

Where S_b is the standard deviation in the region of interest, E is the counting efficiency, I is the intensity of gamma energy and V is the sample in litre. Counting efficiency E is different for different gamma energies and counting geometries.

When S_b is $3\pm$ then,

$$LLD = \frac{4.653 \times 3\pm}{E \times I \times V}$$

$$\frac{4.653 \times 3}{E \times I \times V}$$

$$= [n_b / t_b^2]^{1/2} \qquad (3.14)$$

Where n_b is the background count and t_b is the background time.

$$S.D (\pm) = [n_g / t_g^{\,2} + n_b / t_b^2]^{1/2} = X \text{ cps}$$

For activity calculation,

$$S.D (\pm) = \frac{X \text{ cps} \times 100}{\% E \times I \times W \text{ (in Kg)}} \quad Bq.Kg^{-1} \qquad (3.15)$$

Where n_g is the gross count and t_g is the counting time with sample. The LLD of different gamma energy regions for 150gm samples of geometry size rad.4.9× ht.7.0 was used in the present work; the counting times were 20000 seconds. The results have been given in Table 3.5.

Table 3.5**:** Detection limits of the HPGe detector

Radionuclides	Detection limits of HPGe detector
^{214}Pb	0.0466
^{214}Pb	0.0308
^{208}Tl	0.0393
^{208}Tl	0.0067
^{214}Bi	0.0137
^{228}Ac	0.0244
^{228}Ac	0.0390
^{214}Bi	0.0433
^{40}K	0.1311

3. 5.7. Statistical Error in Counting

In gamma ray spectrometry the quantity of interest, like the activity of a source or the energy of gamma ray are derived from other measured quantities by a mathematical relationship. The radioactive decay is random in time and so the number of particles of photons counted in a

given time will fluctuate about an average value. The standard deviation σ is a measure of the scatter of a set of observations about their average value. The most common method of analysis gamma-spectrum of samples containing a mixture of nuclides is to use the full energy peak counts of various isotopes for estimating activities because the full energy peak is a characteristic of the isotopes it is in this energy region that a better sample to background counts is obtained.

Sometimes the constituent nuclides emit gamma rays of closely spaced energies, from which a small portion of the full energy peak of each of them are selected. This reduces the region of mutual overlap of adjacent peaks, thereby improving source counts to background ratio for each of the radionuclides. To minimize the statistical error if an isotope emits more than one gamma ray, the most abundant gamma energy should be taken for analysis. If there are several gamma energies comparable abundance, the highest energy that is likely to have least Compton contribution from other nuclides should be selected.

Since the nuclei undergoing radioactive transformation in a sample is random event occurring in a few of atoms, the Poisson distribution may be applied and errors in the recorded counts are usually expressed as the standard deviation that is simply the square root of the number of counts. One standard deviation implies that 68.3% result lies within this range.

The counting error can be reduced by increasing

(1) counting efficiency, (2) Volume and (3) Counting time.

Additionally, the background of counts of the detector will also increase counting accuracy. For count of N in time 't' the standard deviation= $\sqrt{N}$

$$\frac{N}{t} = [RT]^{1/2}/t = [RT]^{1/2} = \left[\frac{N}{t^2}\right]^{1/2} \qquad (3.16)$$

The standard deviation of the net counting rate is

$$\sigma_s = \left(\sigma_g + \sigma_{bg}\right)^{\frac{1}{2}} = \left[\frac{r_g}{t_g} + \frac{r_{bg}}{t_{bg}}\right]^{1/2} \qquad (3.17)$$

Where, σ_g =standard deviation of gross counting rate

σ_b =standard deviation of background counting rate,

r_g=gross counting rate,

r_b =Background counting rate,

t_g=time during which gross counting was made,

t_b =time during which background count was made.

Percent of error= $\frac{\sigma}{A} \times 100$ (3.18)

Where A = the activity of the sample. In present work, 2σ counting error has been taken for the calculation of activity measurement.

3. 5.8. Prepared Standard Source efficiency results

An efficiency curve was obtained for standard using the 8 experimental points available. The results of measured peak efficiencies for the standard geometry of 400 ml are shown in Table-3.6. The HPGe detector efficiencies have been measured with uncertainties between 5-7%. The values of the function parameters were determined by regression analysis. The experimentally measured data cover 80-3000 KeV range for this geometry. The chi-square results show the establishment of the satisfactory response curves in the 180 to 3000 KeV ranges. The intensities for the corresponding gamma ray energies were taken from IAEA guide book (IAEA, 1989).

Table 3.6: Counting efficiencies of the HPGe detector used for activity calculation.

Radionuclides	Peak energy (KeV)	Intensity, I	Efficiency (%)
^{212}Pb	238	0.435	0.041105157
^{214}Pb	295	0.1815	0.034304887
^{214}Pb	351	0.351	0.029632951
^{208}Tl	583	0.307	0.019327001
^{214}Bi	609	0.446	0.018629617
^{228}Ac	911	0.266	0.013270423
^{228}Ac	969	0.1623	0.012598144
^{214}Bi	1120	0.147	0.011151435
^{40}K	1460	0.107	0.00891975
^{214}Bi	1764	0.151	0.007606088
^{208}Tl	2613	0.356	0.005462992

3.6 Measurement Set-up

The detection and measurement of radionuclides in the samples were carried out by gamma spectrometry system using a vertical coaxial cylindrical high purity germanium (HPGe) detector of 93 cm^3 active volume and with 20% relative efficiency. The p-type HPGe detector supplied by CANBERRA (Model- GC-2018), had a resolution of 1.8 KeV at 1332 KeV of Cobalt-60 gamma-ray line. The detector was coupled to a 16 k-channel analyser. The samples was placed on the top of the detector inside the shielding arrangement and counted for 20,000 seconds after adjustment of the necessary parameters such as resolution, peak to Compton ratio etc. And after determination of minimum detectable activity of the detectors the spectra of all samples were perfectly analyzed using Genie-2000 spectra analysis software (which matched various gamma energy peaks to a library of all possible radionuclides) to calculate the concentrations of ^{238}U, ^{232}Th and ^{40}K. The detector was enclosed in a cylindrical shielding container made of lead and iron with 51 mm thickness, 559 mm height and 305 mm internal diameter and having a fixed bottom and moving cover to reduce the external gamma-ray background. All the samples were counted for 10 ks. Prior to the measurement of the samples, the environmental gamma background at laboratory site was determined with an identical empty plastic container used in the sample measurement. The energy regions selected for the corresponding radionuclides were 295 KeV and 352 KeV of ^{214}Pb and 609 KeV and 1120 KeV of ^{214}Bi for ^{226}Ra, 238 KeV of ^{212}Pb, 583 KeV of ^{208}Tl, 911 KeV and 969 KeV of ^{228}Ac for ^{232}Th and 1460 KeV for ^{40}K (Roessier et al., 1970).

3. 6.1. Calibration of samples by the HPGe Detector

The energy calibration of the detector by gamma-rays emitted from the radionuclides present in the samples and efficiency calibration of the detector was performed by standard sources of solid and liquid matrixes prepared using Ra-226 standard using identical containers used for the measurement of the samples, e.g., 180 ml plastic container. The preparation process of standard sources had been reported elsewhere (Harb et al., 2008).

a. Energy Calibration

Energy calibration of the detector is a basic requirement to distinguish gamma-rays emitted from the radionuclides present in the samples. After the energy calibration of the detector it is

possible to identify exactly the photo peaks present in the spectrum. The procedure for the exact identification of the radionuclides within a spectrum depends on the methods which match the energies of the principal gamma-rays by known radionuclides. The energy calibration of the HPGe detector is done by measuring mixed standard sources of known radionuclides with the well defined energies within the energy range of interest.

b. Efficiency Calibration

The efficiency of a detector is a measure of the number of gamma-rays that detected by it from the total number of gamma-rays emitted by the source. An accurate efficiency calibration of the system is required to connect on the counts obtained from the spectral analysis to the unit of activity of radionuclides present in a sample. It is essential that this calibration be performed with great care, because the accuracy of all quantitative results will depend on it. The efficiency changes with the physical changes of counting system and the environment surrounding it. For low level activity of the environmental samples, it is desirable to increase the efficiency as much as possible in order to increase the minimum level of detection. The detector efficiency calibration curves as function energy for solid matrixes are shown in Figure 3.6 the energy calibration of the detector was performed by ^{137}Cs and Cobalt-60 point sources

.

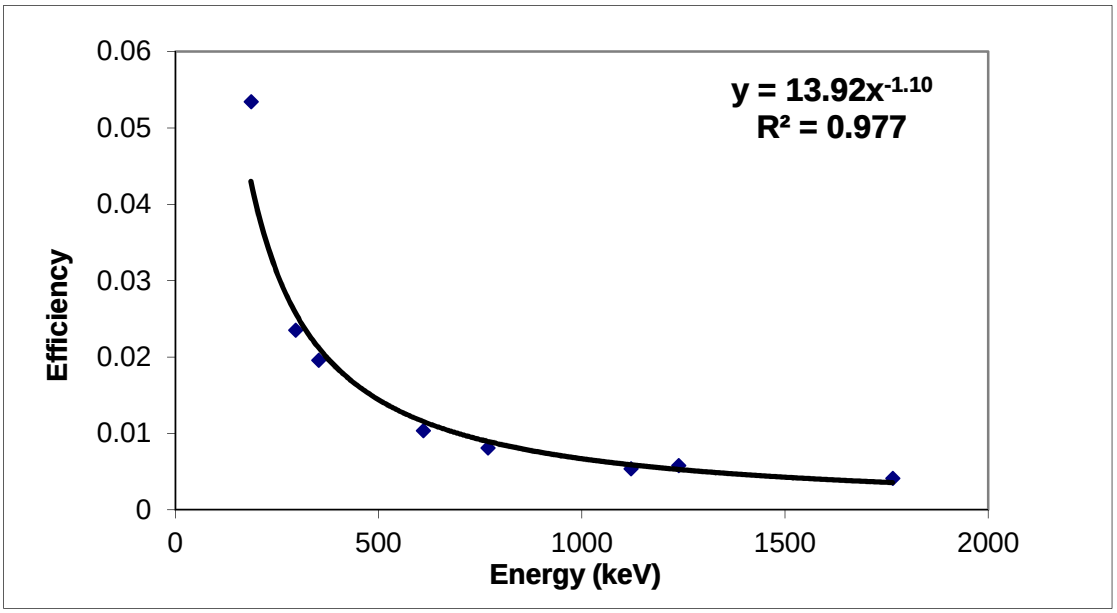

Fig. 3.6: Efficiency curve of the HPGe detector of 20% relative efficiency for the solid matrix

a) Homogeneity Test and Density Correction for Standard Source

The counting efficiency curve for HPGe detector, shown in Figure 3.7, was done using Al_2O_3 standard source. This Al_2O_3 standard was prepared by mixing Ra-226 of known activity with Al_2O_3 matrix. Therefore, the homogeneity test of Al_2O_3 standard and density effect for the collected samples was performed.

3.9.1 Homogeneity Testing

The homogeneity of the Al_2O_3 standard was tested using the HPGe detector. The peak areas for the corresponding nuclides were measured. The counting rates CPS (counts per second) were calculated. For particular gamma energy the CPS's were the same. This confirmed the homogeneity of the Al_2O_3 standard.

3.9.2 Density Correction

To determine how the gamma rays are affected by the density and composition of the sample an experiment was performed in the present work. For this, IAEA-Soil-6, Al_2O_3 standards and gamma emitting point sources of ^{60}Co, ^{133}Ba, ^{137}Cs and ^{152}Eu covering the low and high energies were used. All the point sources were counted individually in two different ways:

1) First the pot containing IAEA-Soil-7 was placed at 10 cm distance from the detector using the counting holder. Then each of the point sources was counted one by one for 2 hours by placing them on the top of the pot.

.

2) The Al_2O_3 standard was also placed in the same position on the detector and all the point sources were counted in the same way as mentioned above.

The cps (count per second) ratio of various gamma energies emitting from point sources and passing through both standards were determined and plotted as in Fig. 3.7 Detail study is mentioned elsewhere.

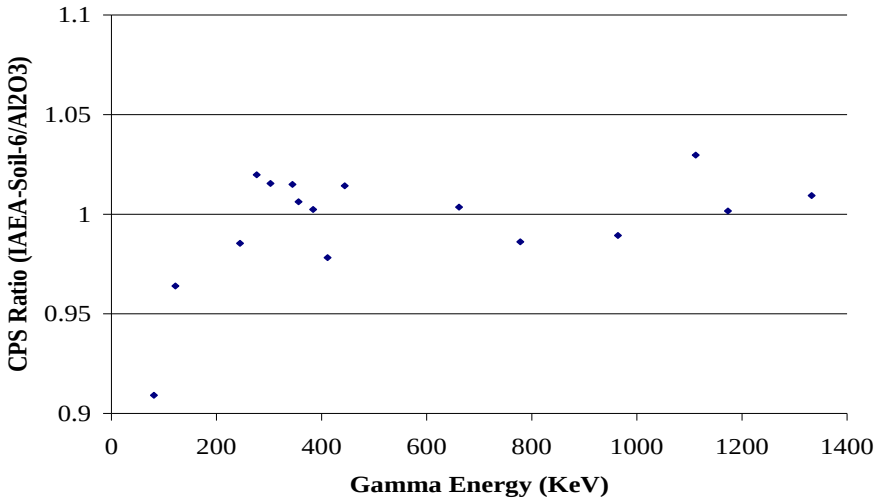

From the plot, the density effect was observed at low energies (below 200 keV) and for the present study, the activity levels were measured for radio-nuclides at energies much higher than 200 keV. As a result the density correction of the measured soil samples is negligible.

Fig. 3.7: CPS ratio Vs energy diagram

3. 7 Calculation activity Concentrations and annual effective Dose of all samples

The radionuclide contents and their activity levels of the each sample were measured using a calibrated HPGe detector of energy resolution of 2.0 KeV at 1.33 MeV of Cobalt-60 for a period of 20,000s. The activity concentrations (A) of each radionuclide in the sample was determined by using the count per second (cps) after subtracting the background counts from the gross counts for the same counting time under the selected photo peaks, weight of the sample, the photo-peak efficiency and the gamma intensity at a specific energy as (Usif and Taher, 2008) Using known standard radioactive source, the efficiency can be determined as:

Activity Concentrations:

$$\text{CPS} = \frac{\text{Net area under a photo peak}}{\text{counting time (in sec)}}$$

$$C = \frac{CPS}{E \times I \times w} \qquad (3.19)$$

Where, C = Activity concentrations of the sample in $Bqkg^{-1}$ or BqL^{-1}.

Cps = the net counts per second = cps for the sample - cps for the background value

E = the counting efficiency of the gamma energy

I = Absolute intensity of the gamma ray and

W = Net weight of the sample (in kilogram or litre).

The errors in the measurements were expressed in terms of standard deviation (±σ), where σ is expressed as (Knoll .G. F, 1989**)**

$$\pm = \left[\frac{N_s}{T_s^2} + \frac{N_b}{T_b^2} \right]^{1/2} \qquad (3.20)$$

Where, N_s is the sample counts measured in time T_s, and N_b is the background counts measured in time T_b. The standard deviation ±2σ in cps was converted into activity in $Bqkg^{-1}$ according to equation (3.19)

Annual Effective Dose (AED):

The annual effective dose due to the intake of radionuclides from food and vegetables samples were calculated using the following equation (Ajayi and Owolabi, 2008):

$$\text{AED } (\mu\text{Sv}) = C \times I \times E \times 10^6 \qquad (3.21)$$

Where, *C* is the activity concentration of radionuclides in the collected samples (Bq/kg), *I* is the annual intake of food and vegetables, *E* is the ingested dose conversion factor for radionuclides (Sv/Bq) (ICRP,1977).

3.8: Radiometric Measurement

In the present work the measurement of the concentration of natural radioactivity (Ra, Th and K) in paddy, Leafy vegetables, Arum and papaya samples were performed by γ-ray spectrometric system, using high purity germanium (HPGe) detector having a relative efficiency of 20% and resolution (FWHM) 1.8 KeV at 1332 KeV γ-energy of ^{60}Co. The detector was connected to a multi-channel analyzer (MCA). Spectral data from the detector was accumulated on an MCA and analyzed using Genie-2000 software from Canberra. The detector was maintained in a vertical position with a lead cylindrical shield to avoid background radiation. All the samples were placed coaxially 10 cm from the surface of the detector and the counting time was 20,000 seconds.

The main contributors to radiological significance are the members of ^{238}U & ^{232}Th decay series and ^{40}K. Therefore, the emphasis was on the determination of natural activity of ^{226}Ra, ^{232}Th and ^{40}K. The content of ^{40}K was determined by measuring its single peak, 1460.88 KeV (10.7). Assuming secular equilibrium in the uranium and thorium decay series, the ^{226}Ra and ^{232}Th activities were determined indirectly via the activities of their daughter products. The choice of the reference nuclides was made so that the related peaks were sufficiently discriminated and intense. Based on such criteria, the nuclides chosen are shown in Table 3.7 for ^{226}Ra and ^{232}Th (Bruzzi et al., 2000).

The content of ^{226}Ra was measured using γ-energy of 295.18 KeV (18.15) ^{214}Pb, 351.92 KeV (35.10) ^{214}Pb, 609.35 KeV (44.60) ^{214}Bi, 1120.5KeV (14.70) ^{214}Bi and 1764.5 KeV (15.10). The contents of ^{232}Th was determined using 238.76 KeV (43.50) ^{212}Pb, 583.24 KeV (30.70) ^{208}Tl, 911.32 KeV (26.60) ^{228}Ac, 969.19 KeV (16.23) ^{228}Ac and 2613.2 KeV (35.60) ^{208}Tl. The background level was subtracted from each recorded spectrum.

Table 3.7: Gamma lines used for γ-spectrometry determinations.

Principal radionuclide	Daughter product	Energy (KeV)	Intensity (yields)
^{226}Ra	^{214}Pb	295.18	0.1815
	^{214}Pb	351.92	0.351
	^{214}Bi	609.35	0.446
	^{214}Bi	1120.5	0.147
	^{214}Bi	1764.5	0.151
^{232}Th	^{214}Pb	238.76	0.435
	^{208}Tl	583.24	0.307
	^{228}Ac	911.32	0.266
	^{228}Ac	969.19	0.1623
	^{208}Tl	2613.2	0.356
^{40}K		1460.9	0.107

CHAPTER IV

Result & Discussion

4.1 Introduction

In order to determine the presence of natural and probable artificial radioactivity in the human food-chain, the radioactivity level in the Paddy, Arum, Papaya & Leafy Vegetables samples collected from different parts on the Bank of Rupsha River at Rupsha Upazilla in Khulna, Bangladesh, have been studied in the present study. An error analysis of the data has also been performed. Moreover, based on the activity level and the annual intake of radionuclides through the consumption of these samples, the annual effective doses due to these radionuclides has also been estimated with the help of gamma spectrometry system using High Purity Germanium (HPGe) detector at Savar Atomic Energy Commission. This chapter presents an account of the results of all the samples analyzed in the study.

4.2 Radioactivity in Paddy Samples

The radioactivity of natural radionuclides in the Paddy sample was measured by using High Purity Germanium Detector of 20% relative efficiency. In this study the daughter of ^{226} Ra, ^{232}Th series and ^{40}K radionuclides of the Paddy samples has been analyzed using gamma ray spectra and the activity level of ^{226}Ra, ^{232}Th, and ^{40}K radionuclides has been calculated. The activity concentrations of all the samples have also been reported in Bq.Kg^{-1} in wet weight basis with a counting error of ±2σ.

The activity concentration of all the daughter nuclides of ^{226}Ra & ^{232}Th series for Paddy samples are given in Table 4.1. It is seen that the concentration of ^{214}Pb, ^{214}Bi, ^{212}Pb, ^{208}Tl and ^{228}Ac are found to be varied between BDL to 35.1±4.76 Bqkg^{-1}, 11.39±12.93 Bqkg^{-1} to 49.53±17.01 Bqkg^{-1}, BDL to 3.64±1.67 Bqkg^{-1}, BDL to 6.38±4.63 Bqkg^{-1} and BDL to 2.19±12.24 respectively. Bar diagram in Fig: 4.1 and Fig: 4.2 shows the variation of activity concentrations all the daughter radionuclides present in the Paddy samples.

On the other hand, the activity concentration of ^{226}Ra, ^{232}Th and ^{40}K in Paddy samples has been found to be varied between 17.59±4.44 to 42.32±4.48 Bqkg^{-1}, BDL to 3.75±2.995 Bq/kg,

and 35.97±150 Bqkg^{-1} to 170.12±135.49 Bqkg^{-1} respectively, with an average of 24.43±5.16 Bqkg^{-1}, 2.048±2.798 Bqkg^{-1} and 93.96±133.75 Bqkg^{-1}. The highest activity concentration of 170.12±135.49 Bqkg^{-1} for ^{40}K has been found in Paddy samples collected from Kharabad. It is less than world average activity concentration. The values of activity concentration in Paddy samples are shown in Table 4.2 Bar diagram 4.3 shows activity concentration of ^{226}Ra, ^{232}Th, and ^{40}K in all Paddy samples collected from various locations in the bank of Rupsha River, Khulna.Picture 4.1 and 4.2 shows Paddy Sample and drying process in sun shine.

Picture 4.1: Paddy sample grown on the Bank of Rupsha River

Picture 4.2: Paddy Sample dry in sun shine

Table 4.1: Activity Concentrations of radioactive daughter elements of ^{226}Ra & ^{232}Th radioactive series in Paddy samples under study

Sl. no.	Sampling Location	Sample ID	Activity concentration (Bq/kg)				
			Pb-214	Bi-214	Pb-212	Tl-208	Ac-228
1	Aichgati	Paddy 1	21.11±3.76	14.06±5.11	1.11±1.36	6.38±4.63	BDL
2	Joypur	Paddy 2	24.84±3.81	19.91±5.15	0.7±1.29	BDL	BDL
3	Jabusa	Paddy 3	35.1±4.76	49.53±17.01	3.64±1.67	BDL	2.19±12.42
4	Elahipur	Paddy 4	33.37±4.13	11.39±12.93	2.41±1.38	BDL	BDL
5	Noeihati	Paddy 5	29.99±4.02	15.64±5	0.47±1.28	BDL	BDL
6	Kharabad	Paddy 6	BDL	12.22±5.09	BDL	BDL	BDL
Maximum			35.1±4.76	49.53±17.01	3.64±1.67	6.38±4.63	2.19±12.24
Minimum			BDL	11.39±12.93	BDL	BDL	BDL
Average			28.3±4.08	20.46±8.38	1.67±1.39	-	-

*BDL: Below Detection Level

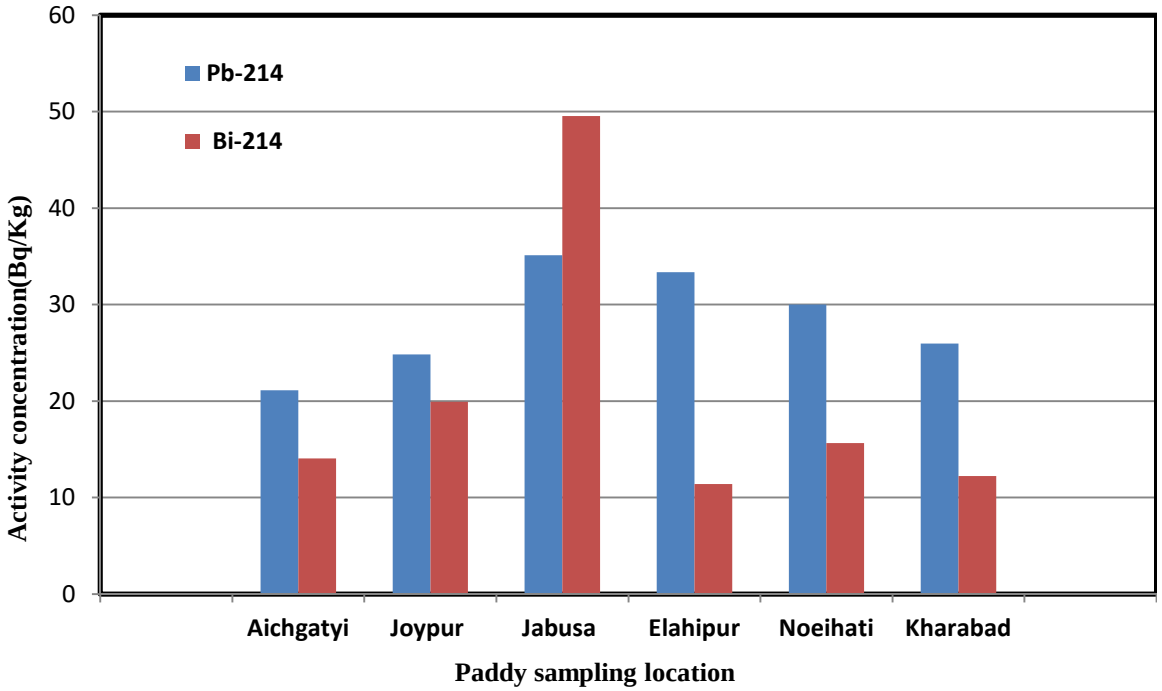

Fig. 4.1: Graphical representation of the activity concentrations of daughters (^{214}Pb; ^{214}Bi) of ^{226}Ra in all Paddy samples.

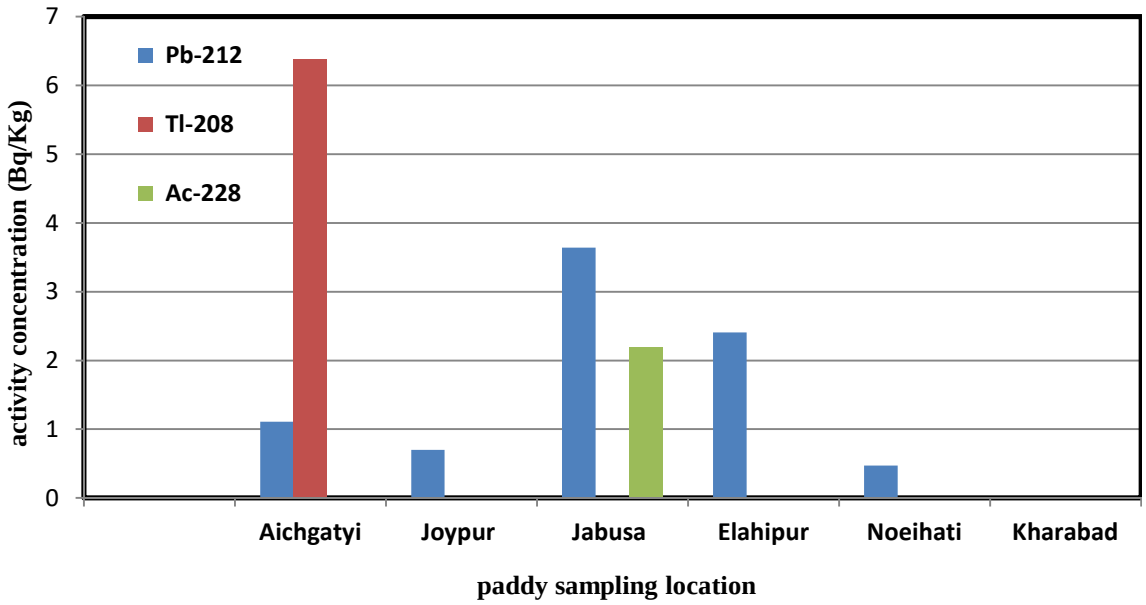

Fig. 4.2: Graphical representation of the activity concentrations of daughters (^{212}Pb.^{208}Ti, ^{228}Ac) of ^{232}Th in all Paddy samples.

Table 4.2: Activity Concentration of radio nuclei Ra-226 &Th-232 and K-40 in Paddy

Sl no.	Sampling Location	Sample ID	Activity concentration (Bq/kg		
			Ra-226	Th-232	K-40
1	Aichgati	Paddy 1	17.59±4.44	3.745±2.995	84.08±132.6
2	Joypur	Paddy 2	22.375±4.48	0.7±1.29	121.53±128.43
3	Jabusa	Paddy 3	42.32±4.48	2.915±7.045	35.97±150.34
4	Elahipur	Paddy 4	22.38±8.53	2.41±1.38	71.06±127.92
5	Noeihati	Paddy 5	22.815±4.51	0.47±1.28	81.01±127.77
6	Kharabad	Paddy 6	19.085±4.45	BDL	170.12±135.49
Maximum.			42.32±4.48	3.745±2.995	170.12±135.49
Minimum			17.59±4.44	BDL	35.97±150.34
Average			24.43±5.16	2.048±2.798	93.96±133.75
World Average UNSCEAR- 2000			67	82	310

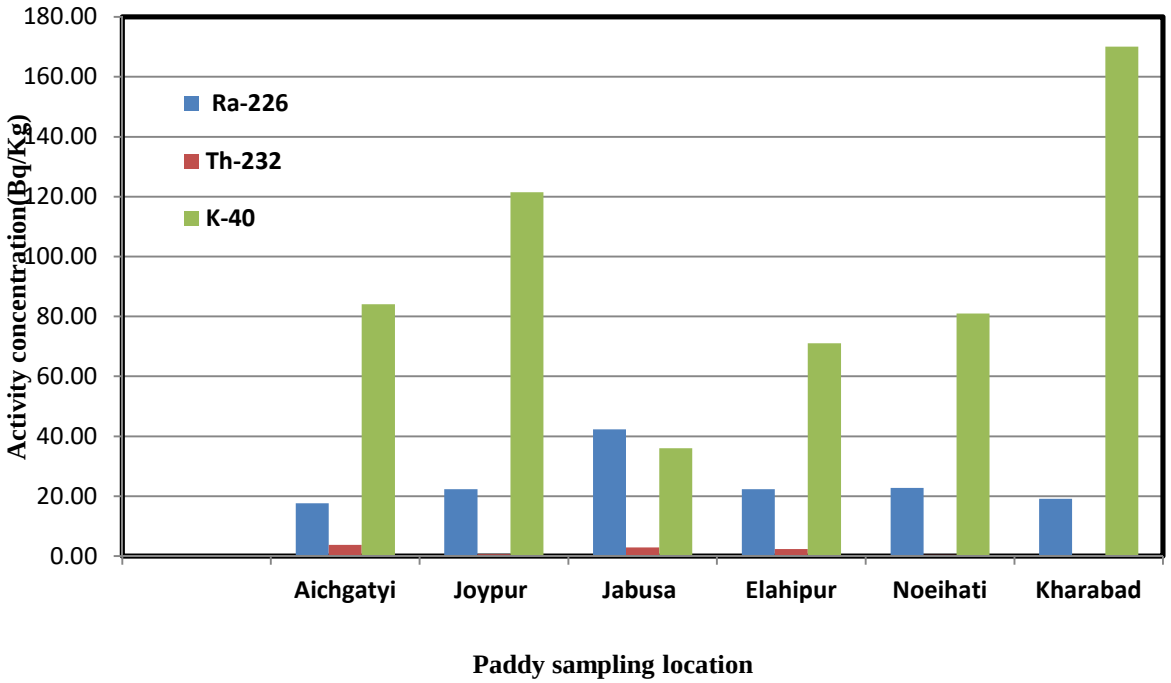

Fig. 4.3: Graphical representation of the activity concentrations of parents' nuclei ^{226}Ra, ^{232}Th and ^{40}K in all Paddy samples.

4.3 Radioactivity in Leafy vegetables Samples

The activity concentration of all the daughter nuclides of ^{226}Ra & ^{232}Th series in Leafy veg. samples are given in Table 4.3 It is seen that the concentration of ^{214}Pb, ^{214}Bi, ^{212}Pb, ^{208}Tl and ^{228}Ac are found to be varied between 27.55±4.79 Bqkg^{-1} to 47.71±6.34 Bqkg^{-1}, 13.86±17.25 Bqkg^{-1} to 58.2±21.17 Bqkg,$^{-1}$ BDL to 5.14±1.91 Bqkg^{-1}, BDL to 9.63±6.07 Bqkg^{-1} and BDL to 33.01±16.87 respectively. Bar diagram in Fig: 4.4 and Fig: 4.5 shows the variation of activity concentrations all the daughter radionuclides present in the Leafy vegetable samples

On the other hand, The activity concentration of ^{226}Ra, ^{232}Th and ^{40}K in Leafy vegetables samples has been found to be varied between 49.11±13.48 Bqkg^{-1} to 25.97±11.28 Bqkg^{-1}, BDL to 17.075±11.515 Bqkg^{-1}, and 626.88±176.34 Bqkg^{-1} to 1378.25±225.93 Bqkg^{-1} respectively, with an average of 34.22±12.55Bqkg^{-1}, 9.84±10.63 Bqkg^{-1} and 1110.50±200.24 Bqkg^{-1}. The highest activity concentration of 1378.25±225.93 Bqkg^{-1} for ^{40}K has been found in Leafy veg. sample (sample ID Leafy veg.5) collected from Elahipur. The values of activity concentration in Leafy veg. samples have been shown in Table 4.4. Bar diagram 4.6 shows activity concentration of ^{226}Ra, ^{232}Th, and ^{40}K in all Leafy veg. samples collected from various locations in the bank of Rupsha River, Khulna.

Picture 4.3 Leafy vegetables Samples grown on the Bank of Rupsha River and picture 4.4 shows drying process of Leafy vegetables Sample in sun shine

Picture 4.3: Leafy vegetables sample grown on the Bank of Rupsha River

Picture 4.4: Leafy vegetables Sample dry in sun shine

Table 4.3: Activity Concentrations of radioactive daughter elements of ^{226}Ra &^{232}Th radioactive series in Leafy vegetables samples under study

Sl no.	Sampling Location	Sample ID	Activity concentration (Bq/kg)				
			Pb-214	Bi-214	Pb-212	Tl-208	Ac-228
1	Khan md.pur	Leafy veg. 1	38.07±5.3	13.86±17.25	BDL	9.63±6.07	0.47±17.53
2	Aichgati	Leafy veg. 2	27.55±4.79	37.26±18.18	5.14±1.91	2.7±5.56	5.18±13.93
3	Joypur	Leafy veg. 3	47.71±6.34	34.7±20.87	BDL	BDL	15.5±16.89
4	Jabusa	Leafy veg. 4	40.01±5.79	58.2±21.17	BDL	1.14±6.16	33.01±16.87
5	Elahipur	Leafy veg. 5	37.8±6.07	22.38±21.12	BDL	BDL	BDL
6	Noeihati	Leafy veg. 6	40.28±5.9	15.7±17.27	BDL	5.43±5.79	BDL
7	Kharabad	Leafy veg. 7	34.41±5.58	31.13±20.02	BDL	BDL	BDL
Maximum			47.71±6.34	58.2±21.17	5.14±1.91	9.63±6.07	33.01±16.87
Minimum			27.55±4.79	13.86±17.25	BDL	BDL	BDL
Average			37.98±5.68	30.46±19.42	5.14±1.91	4.73±5.89	13.54±16.31

*BDL: Below Detection Level

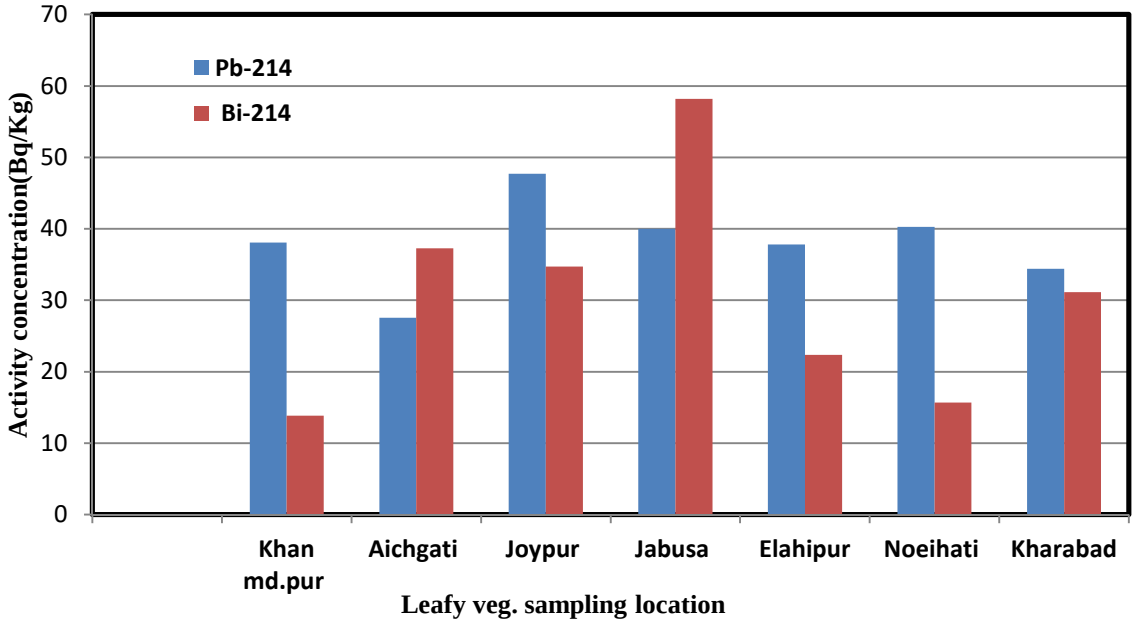

Fig. 4.4: Graphical representation of the activity concentrations of daughters (^{214}Pb; ^{214}Bi) of ^{226}Ra in all Leafy vegetables samples.

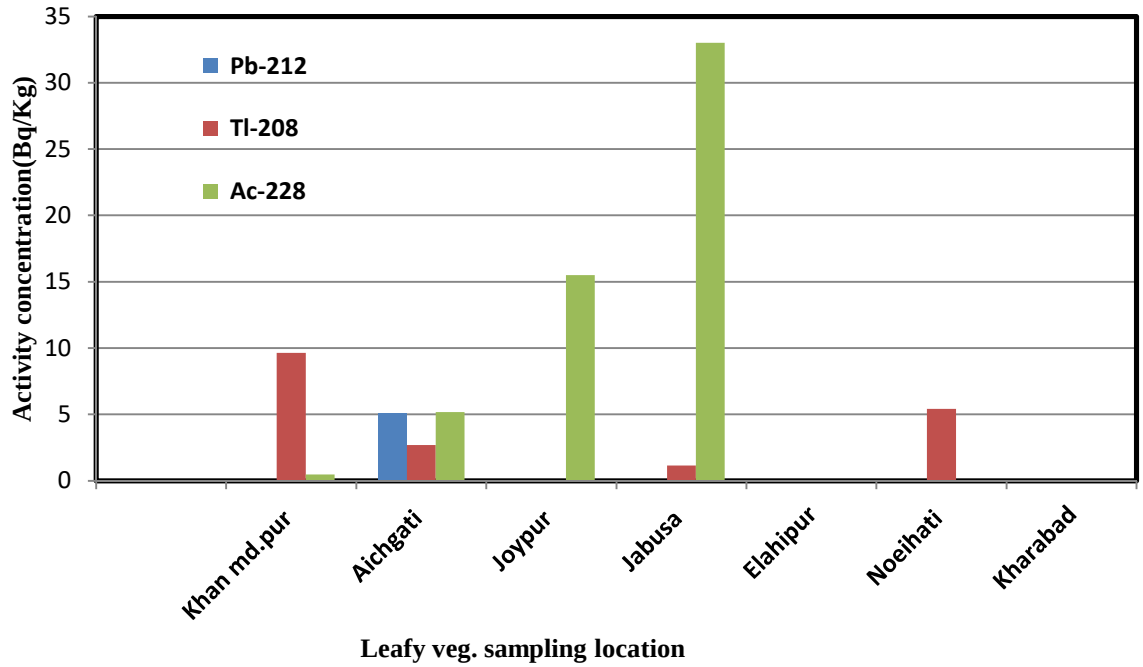

Fig 4.5: Graphical representation of the activity concentrations of daughters (^{212}Pb.^{208}Ti, ^{228}Ac) of ^{232}Th in all Leafy vegetables sample**.**

Table 4.4: Activity Concentration of radio nuclei Ra-226 &Th-232 and K-40 in Leafy veg. samples

Sl no.	Sampling Location	Sample ID	Activity concentration (Bq/kg)		
			Ra-226	Th-232	K-40
1	Khan md.pur	Leafy veg. 1	25.97±11.28	5.05±11.80	924.81±184.08
2	Aichgati	Leafy veg. 2	32.41±11.49	4.34±7.1333	626.88±176.34
3	Joypur	Leafy veg. 3	41.205±13.605	15.5±16.89	1373.11±218.01
4	Jabusa	Leafy veg. 4	49.11±13.48	17.075±11.515	1159.28±205.77
5	Elahipur	Leafy veg. 5	30.09±13.62	BDL	1378.25±225.93
6	Noeihati	Leafy veg. 6	27.99±11.59	5.43±5.79	938±182.26
7	Kharabad	Leafy veg. 7	32.77±12.8	BDL	1373.16±209.31
Maximum.			49.11±13.48	17.075±11.515	1378.25±225.93
Minimum			25.97±11.28	BDL	626.88±176.34
Average			34.22±12.55	9.84±10.63	1110.50±200.24

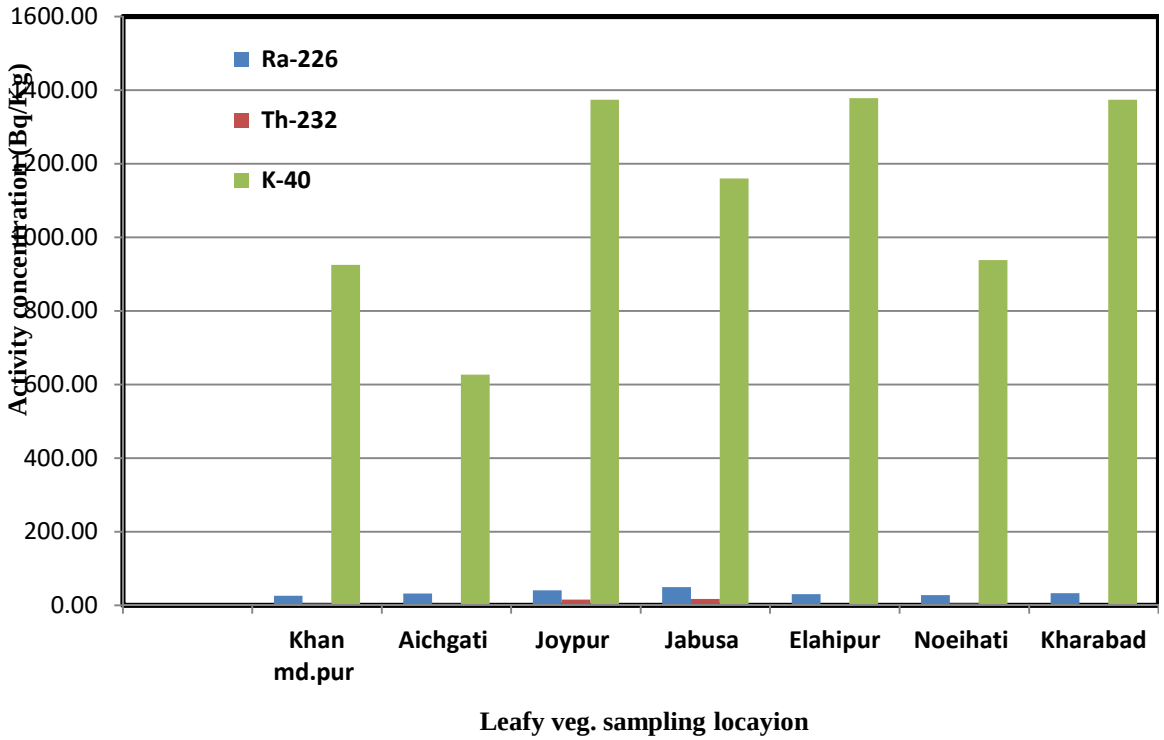

Fig 4.6: Graphical representation of the activity concentrations of parents' nuclei ^{226}Ra, ^{232}Th and ^{40}K in all Leafy veg. samples.

4.4 Radioactivity in Arum samples

The activity concentration of all the daughter nuclides of ^{226}Ra & ^{232}Th series in Arum samples has been given in Table 4.5 It is seen that the concentration of ^{214}Pb, ^{214}B, ^{212}Pb, ^{208}Tl and ^{228}Ac has been found to be varied between BDL to11.12±2.55 $Bqkg^{-1}$, BDL to 6.44±3.6 Bqkg,$^{-1}$ BDL to 4.53±1.21 $Bqkg^{-1}$, BDL to 5.19±3.57 $Bqkg^{-1}$ and BDL to 1.84±8.36 Bqkg,$^{-1}$ respectively. Bar diagram in Fig. 4.7 and Fig. 4.8 shows the variation of activity concentrations all the daughter radionuclides present in the Arum sample.

On the other hand, the activity concentration of ^{226}Ra, ^{232}Th and ^{40}K in Arum samples has been found to be varied between BDL. to 8.78±3.08 $Bqkg^{-1}$, BDL to 2.53±4.32 $Bqkg^{-1}$, and 426.91±107.23 $Bqkg^{-1}$ to 1280.71±133.89 $Bqkg^{-1}$ respectively, with an average of 5.77±2.97 $Bqkg^{-1}$ of ^{226}Ra, maximum Arum samples have been found BDL for ^{232}Th and 758.298±109.66 $Bqkg^{-1}$ of ^{40}K The highest activity concentration of 1280.71±133.89 $Bqkg^{-1}$ for ^{40}K was found in Arum sample (sample ID Arum 2) collected from Khan Mohammadpur. The values of activity concentration in Arum samples are shown in Table 4.6. Bar diagram in Fig. 4.9 represents activity concentration for all Arum samples.

Picture 4.5 Arum Samples grown on the Bank of Rupsha River and picture 4.6 shows drying process of Arum Sample in sun shine.

Picture 4.5: Arum sample grown on the Bank of Rupsha River

Picture 4.6: Arum Sample dry in sun shine

Table 4.5: Activity Concentrations of radioactive daughter elements of ^{226}Ra & ^{232}Th radioactive series in Arum samples under study

SI no.	Sampling Location	Sample ID	Activity concentration (Bq/kg)				
			Pb-214	Bi-214	Pb-212	Tl-208	Ac-228
1	Deara	Arum 1	2.88±2.95	BDL	0.79±1.04	BDL	BDL
2	Khan md.pur	Arum 2	2.47±2.38	BDL	1.79±1.2	BDL	BDL
3	Aichgati	Arum 3	11.12±2.55	6.44±3.6	0.69±.99	2.15±1.25	BDL
4	Joypur	Arum 4	5.662.21	BDL	BDL	BDL	BDL
5	Jabusa	Arum 5	BDL	BDL	0.66±.96	BDL	BDL
6	Elahipur	Arum 6	6.84±2.4	BDL	0.56±1.03	5.19±3.57	1.84±8.36
7	Noeihati	Arum 7	3.37±2.17	2.15±3.56	4.53±1.21	2.43±3.39	BDL
8	Kharabad	Arum 8	2.85±1.92	BDL	0.62±.9	4.85±3.11	BDL
Maximum			11.12±2.55	6.44±3.6	4.53±1.21	5.19±3.57	1.84±8.36
Minimum			BDL	BDL	BDL	BDL	BDL
Average			5.03±2.26	4.29±3.58	1.38±1.05	3.66±2.83	1.84±8.36

*BDL: Below Detection Level

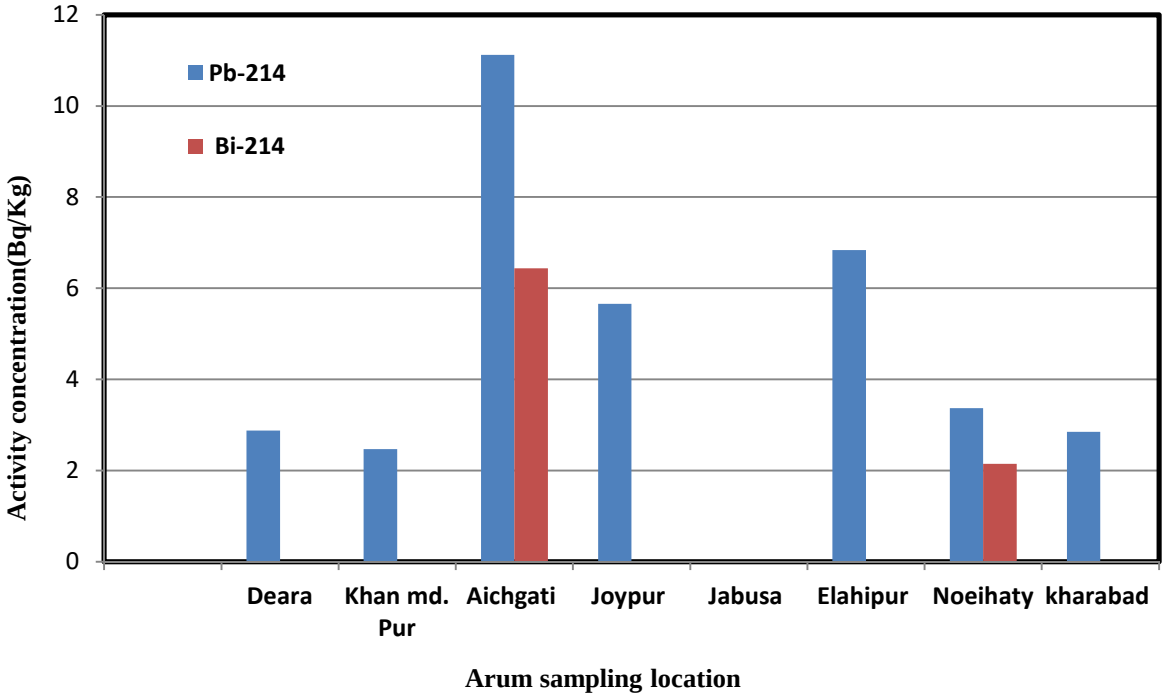

Fig 4.7: Graphical representation of the activity concentrations of daughters (^{214}Pb; ^{214}Bi) of ^{226}Ra in all Arum samples.

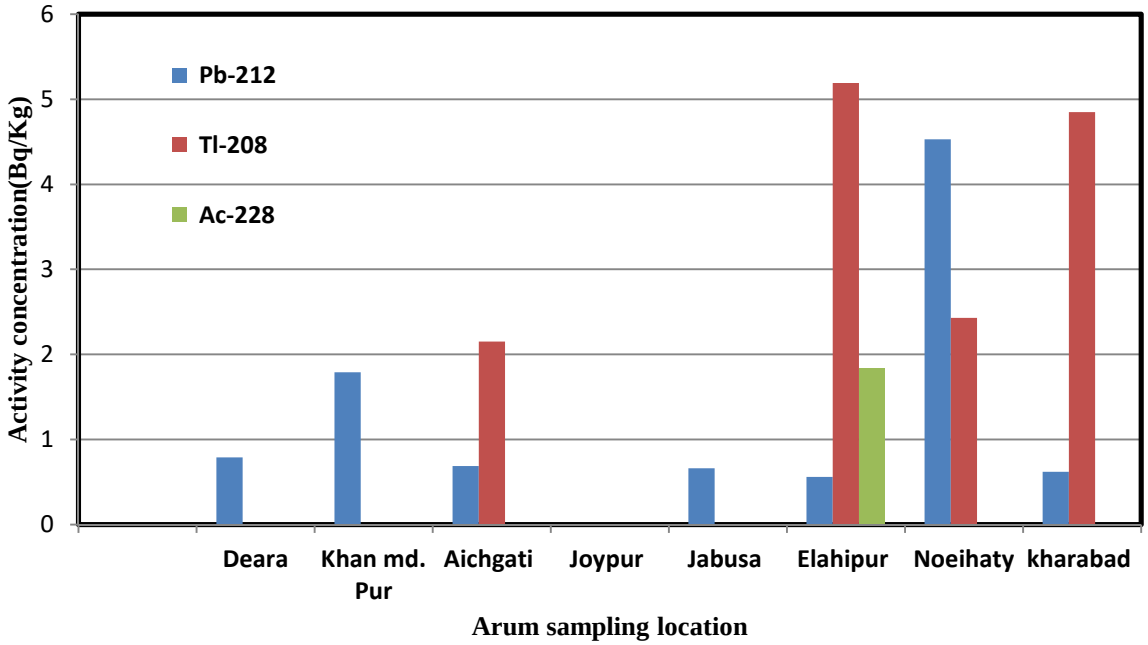

Fig. 4.8: Graphical representation of the activity concentrations of daughters (^{212}Pb.^{208}Ti, ^{228}Ac) of ^{232}Th in all Arum samples.

Table 4.6: Activity Concentration of radio nuclei Ra-226 &Th-232 and K-40 in Arum

SI no.	Sampling Location	Sample ID	Activity concentration (Bq/kg)		
			Ra-226	Th-232	K-40
1	Deara	Arum 1	BDL	BDL	1034.32±115.53
2	Khan md.pur	Arum 2	BDL	BDL	1280.71±133.89
3	Aichgati	Arum 3	8.78±3.08	BDL	701.79±106.97
4	Joypur	Arum 4	BDL	BDL	571.75±102.71
5	Jabusa	Arum 5	BDL	BDL	638.94±102.52
6	Elahipur	Arum 6	BDL	2.53±4.32	426.91±107.23
7	Noeihati	Arum 7	2.76±2.9	BDL	783.99±111.77
8	Kharabad	Arum 8	BDL	BDL	627.97±96.68
Maximum.			8.78±3.08	2.53±4.32	1280.71±133.89
Minimum			BDL	BDL	426.91±107.23
Average			5.77±2.97	-	758.298±109.66

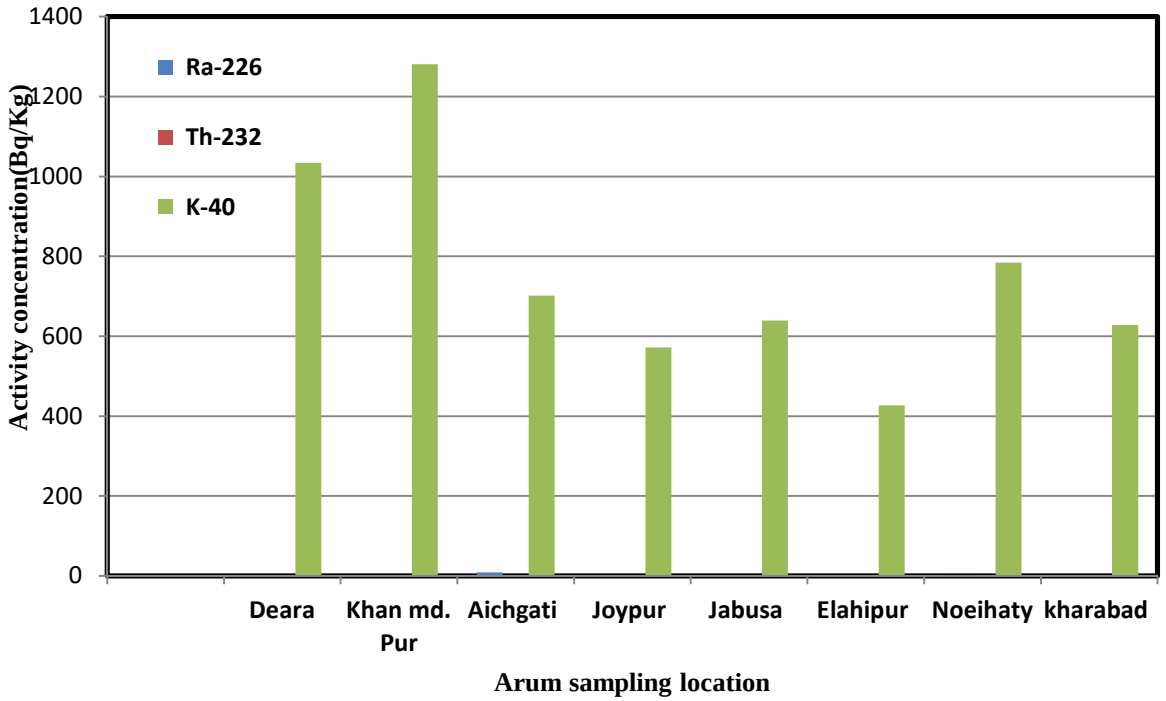

Fig. 4.9: Graphical representation of the activity concentrations of parents' nuclei ^{226}Ra, ^{232}Th and ^{40}K in all Arum samples.

4. 5 Radioactivity in Papaya samples

The activity concentration of all the daughter nuclides of ^{226}Ra & ^{232}Th series in Arum samples are given in Table 4.7. It is seen that the concentration of ^{214}Pb, ^{214}Bi, ^{212}Pb, ^{208}Tl and ^{228}Ac are found to be varied between 19.7±4.12 $Bqkg^{-1}$ to 61.07±6.82 $Bqkg^{-1}$, 6.89±15.15 $Bqkg,^{-1}$ to 97.13±34.82 $Bqkg,^{-1}$ BDL, BDL to 12.38±6.73 $Bqkg^{-1}$ and BDL to 26.2±17.27 $Bqkg,^{-1}$ respectively. Bar diagram in Fig: 4.10 and Fig: 4.11 shows the variation of activity concentrations all the daughter radionuclides present in the Papaya samples

On the other hand, The activity concentration of ^{226}Ra, ^{232}Th and ^{40}K in Papaya samples have been found to be varied between 13.295±9.64 $Bqkg^{-1}$ to 77.96±22.01 $Bqkg^{-1}$, BDL to 26.2±17.27 $Bqkg^{-1}$ and 1112.65±202.33 $Bqkg^{-1}$ to 1712.47±221.96 $Bqkg^{-1}$ respectively, with an average of 43.31±15.28 $Bqkg^{-1}$ of ^{226}Ra, 15.44±11.28 $Bqkg^{-1}$ of ^{232}Th and 1490.27±226.27 $Bqkg^{-1}$ of ^{40}K The highest activity concentration of 1712.47±221.96 $Bqkg^{-1}$ for ^{40}K has been found in Papaya sample (sample ID Papaya 3) collected from Aichgati.

Picture 4.7 Papaya Samples grown on the Bank of Rupsha River and picture 4.8 shows drying process of Papaya Sample in sun shine. The values of activity concentration in Papaya samples are shown in Table 4.8. Bar diagram in Fig: 4.12 shows the variation of activity concentrations of the Papaya samples. Table 4.9 represents the activity concentration (Bq/Kg) in Vegetables and Rice with different districts of Bangladesh and Table: 4.10 show the comparison of the present study with different parts of the world for radio nuclides in vegetables samples (Bq/Kg)

Picture 4.7: Papaya sample grown on the Bank of Rupsha River

Picture 4.8: Papaya Sample dry in sun shine

Table 4.7: Activity Concentrations of radioactive daughter elements of ^{226}Ra &^{232}Th radioactive series in papaya samples under study

Sl no.	Sampling Location	Sample ID	Activity concentration (Bq/kg)				
			Pb-214	Bi-214	Pb-212	Tl-208	Ac-228
1	Deara	papaya 1	23.82±5.59	11.96±21.89	BDL	BDL	BDL
2	Khan md.pur	papaya 2	58.79±9.19	97.13±34.82	BDL	BDL	BDL
3	Aichgati	papaya 3	51.46±6.47	33.9±20.79	BDL	BDL	26.2±17.27
4	Jabusa	papaya 4	47.74±5.83	41.77±7.58	BDL	BDL	9.54±14.73
5	Elahipur	papaya 5	38.79±5.7	27.29±19.46	BDL	12.38±6.73	8.75±19.52
6	Noeihati	papaya 6	61.07±6.82	86±23.04	BDL	BDL	BDL
7	Kharabad	papaya 7	19.7±4.12	6.89±15.15	BDL	BDL	BDL
Maximum			61.07±6.82	97.13±34.82	BDL	BDL	BDL
Minimum			19.7±4.12	6.89±15.15	BDL	12.38±6.73	26.2±17.27
Average			43.05±6.25	43.56±20.39	-	-	14.83±17.17

BDL: Below Detection Level

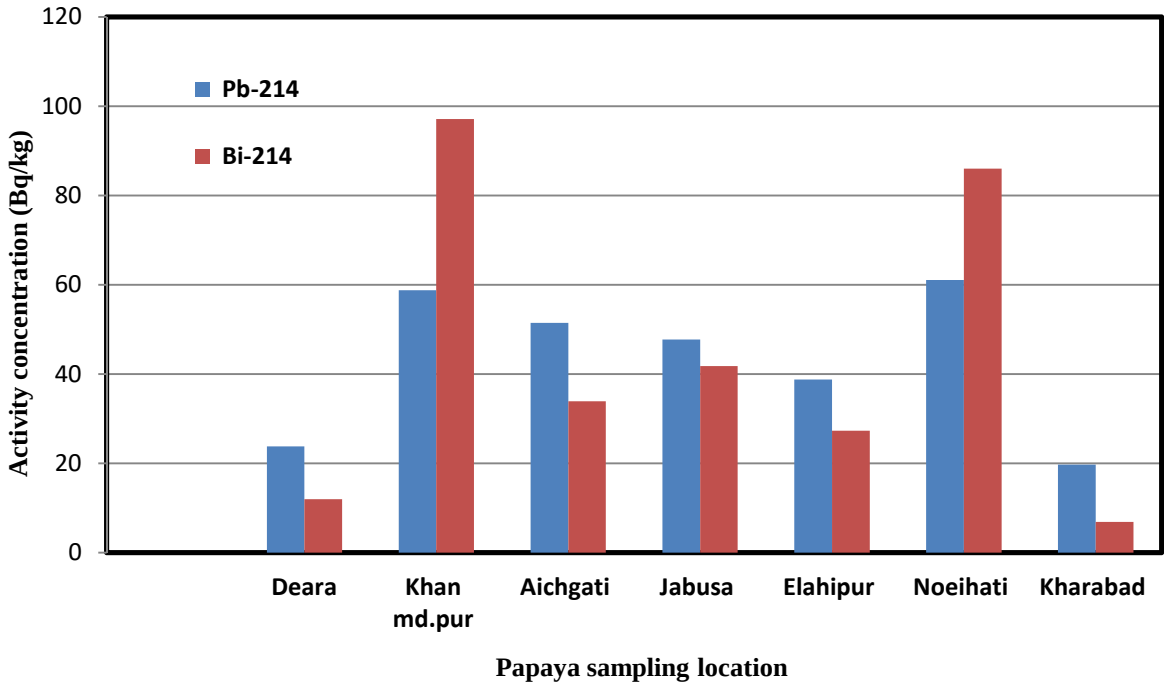

Fig. 4.10: Graphical representation of the activity concentrations of daughters (^{214}Pb, ^{214}Bi) of ^{226}Ra in all Papaya samples.

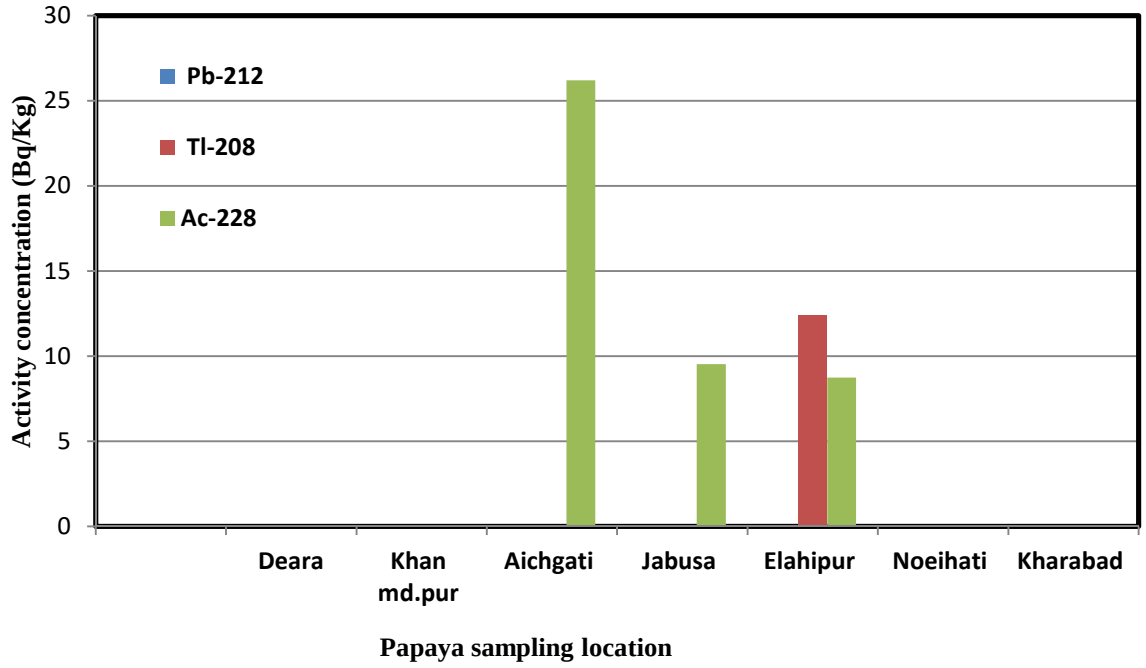

Fig.4.11: Graphical representation of the activity concentrations of daughters (^{212}Pb, ^{208}Ti, & ^{228}Ac) of ^{232}Th in all Papaya samples.

Table 4.8: Activity Concentration of radio nuclei Ra-226 &Th-232 and K-40 in Papaya

Sl no.	Sampling Location	Sample ID	Activity concentration (Bq/kg		
			Ra-226	Th-232	K-40
1	Deara	papaya 1	17.89±27.48	BDL	1455.38±238.57
2	Khan md.pur	papaya 2	77.96±22.01	BDL	1698.34±333.51
3	Aichgati	papaya 3	42.68±13.63	26.2±17.27	1712.47±221.96
4	Jabusa	papaya 4	44.76±6.71	9.54±14.73	1587.93±197.78
5	Elahipur	papaya 5	33.04±12.58	10.565±13.13	1112.65±202.33
6	Noeihati	papaya 6	73.535±14.93	BDL	1643.56±220.26
7	Kharabad	papaya 7	13.295±9.64	BDL	1221.53±169.49
Maximum.			77.96±22.01	26.2±17.27	1712.47±221.96
Minimum			13.295±9.64	BDL	1112.65±202.33
Average			43.31±15.28	15.44±11.28	1490.27±226.27

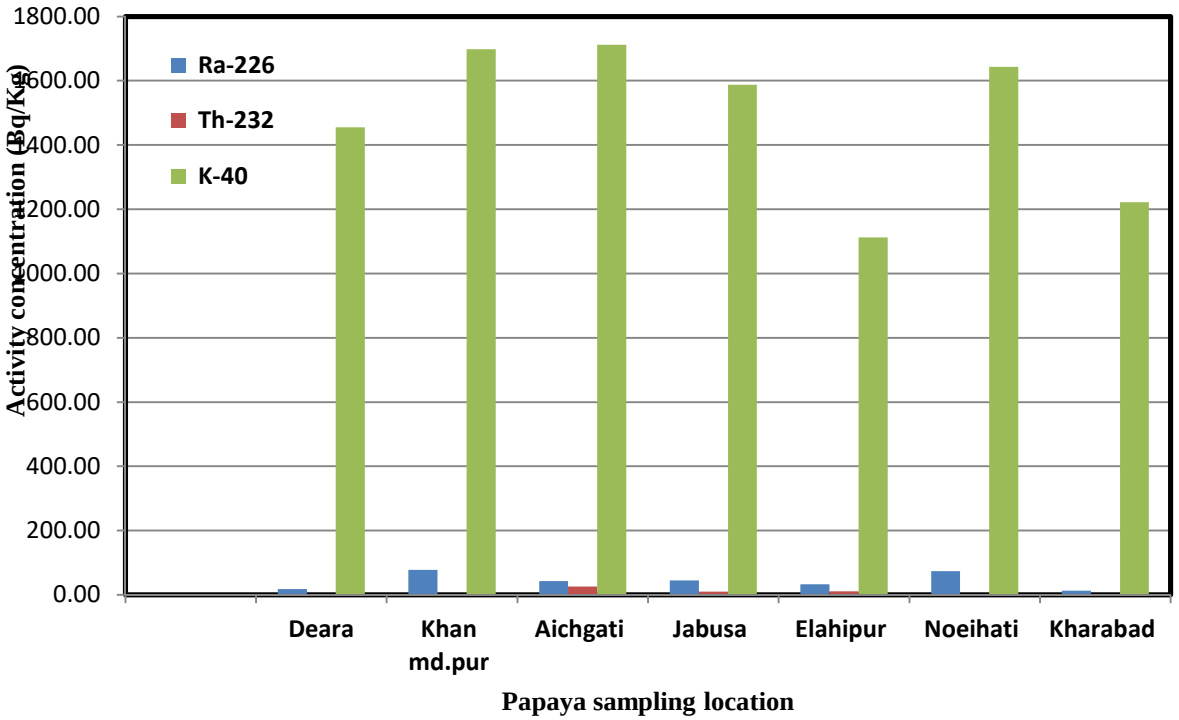

Fig. 4.12: Graphical representation of the activity concentrations of parents' nuclei ^{226}Ra, ^{232}Th and ^{40}K in all Papaya samples.

Table 4.9: Activity concentrations (Bq/Kg) in Vegetables and Rice with different districts of Bangladesh

Region	Samples name	^{226}Ra	^{232}Th	^{40}K	Reference
Jamalpur	Ladies finger	_	8 - 248	1274 - 4860	(Yeasmin and Begum, 2012)
Kustia	Redamaranth	_	5.5 - 23	870 - 1231	
Tangail	Redamaranth	_	9 – 23.6	1109 - 1383	
Jessore	Redamaranth	_	4 - 19	204 - 366	
Savar	Rice	2.86 – 26.61	1.93 – 42.63	307 - 498	(Imros, 2015)
World average value	Root vegetables/Fruits	0.03	0.0005	-	(UNSEAR,2000)
Khulna	Paddy	17.59 – 42.33	0 – 3.75	35.9– 170.12	Present study 2016
Khulna	Leafy vegetables	25.97-49.11	0- 17.08	625.88-1378.25	
Khulna	Arum	O – 8.78	0 – 2.53	426.91-1280.71	
Khulna	Papaya	13.29-77.96	0 -26.2	1112.65-1712.47	

Table 4.10: Comparison of the present study with different parts of the world for radio nuclides in vegetables samples ($BqKg^{-1}$).

Location	Radio-nuclides($BqKg^{-1}$)			Reference
	Ra-226	Th-232	K-40	
Bangladesh Cox's Bazar	80.95	83.53	1691.45	(Islam et al., 2014)
Malaysia	17.5	65.2	446	(Hariandra and Amin, 2008)
Nigeria	83.5	-	684.5	(Jibiri et al., 2007)
Iran	67	0.5	91.73	(Vahid et al., 2013)
China	0.32	-	111	(Tuo et al., 2016)
Bangladesh Khulna	24.83	2.048	93.96	Present study (paddy) 2016
Bangladesh Khulna	34.22	9.48	1110.50	Present study (Leafy vegetables) 2016
Bangladesh Khulna	5.77	-	758.29	Present study (Arum) 2016
Bangladesh Khulna	43.31	15.44	1490.27	Present study (papaya) 2016

4. 6 Annual Intake of Radionuclides and Estimation Annual effective Dose

Based on the samples consumption rates and radionuclide concentration given in Table 4.2, 4.4, 4.6, and 4.8 internal doses from the samples are estimated by multiplying the activity concentrations of ^{226}Ra, ^{232}Th and ^{40}K by the yearly food intake and ingestion dose coefficients. In this Study the annual consumption rate of papaya, Leafy vegetables, Paddy and Arum consumed by the adults was 20 kg y^{-1}, 36 kg y^{-1}, 196.6 kg y^{-1} and 15 kg y^{-1} (FAO, 2000). Annual intake of various radionuclides through the consumption of above mentioned samples (Paddy, Leafy vegetables, Arum and Papaya) are given bellow.

4. 6. 1 Annual Effective Dose in Paddy samples

The annual intakes of ^{226}Ra, ^{232}Th, and ^{40}K are estimated Annual Effective Dose with Paddy samples has been given in Table 4.11. It has been seen that the maximum annual effective dose of ^{226}Ra, ^{232}Th and ^{40}K are 51.58 µSv in sample ID Paddy-3 collected from Joypur, 544.84 µSv in sample ID Paddy-1 collected from Khan Md.pur, and 167.23 µSv in sample ID Paddy-6 collected from Kharabad. Bar diagram Fig. 4.13 shows Annual Effective Dose of ^{226}Ra, ^{232}Th, and ^{40}K in all Paddy samples collected from various locations in the banks of Rupsha River, Khulna.

4. 6. 2 Annual Effective Dose in Leafy vegetables samples

The annual intakes of ^{226}Ra, ^{232}Th, and ^{40}K are estimated annual effective Dose with Leafy vegetable samples is given in Table 4.12 It is seen that the maximum annual effective dose of ^{226}Ra, ^{232}Th and ^{40}K are found 494.98 µSv in sample ID Leafy veg.4 collected from Jabusa, 454.88 µsv in same sample ID Leafy veg.4 collected from Jabusa,, and 248.09 µsv in sample ID Leafy veg.5 collected from Elahipur. . Bar diagram 4.14 shows Annual effective Dose of ^{226}Ra, ^{232}Th, and ^{40}K in all Leafy veg. samples collected from various locations in the banks of Rupsha River, Khulna.

Table 4.11: Annual intake of radionuclides in the Paddy samples and estimated annual effective Dose

SI no.	Sampling Location	Sample ID	Annual Intake (Bq)			Annual effective dose (µSv)		
			^{226}Ra	^{232}Th	^{40}K	^{226}Ra	^{232}Th	^{40}K
1	Aichgati	Paddy 1	3457.21	736.27	16530.13	21.43	544.84	82.65
2	Joypur	Paddy 2	4398.93	137.62	23892.80	27.27	101.84	119.46
3	Jabusa	Paddy 3	8319.13	573.09	7071.70	51.58	424.09	35.36
4	Elahipur	Paddy 4	4399.91	473.81	13970.40	27.28	350.62	69.85
5	Noeihati	Paddy 5	4485.43	92.40	15926.57	27.81	68.38	79.63
6	Kharabad	Paddy 6	3752.11	0.00	33445.59	23.26	0.00	167.23
Average			4802.11	335.53	18472.86	29.77	248.29	92.36

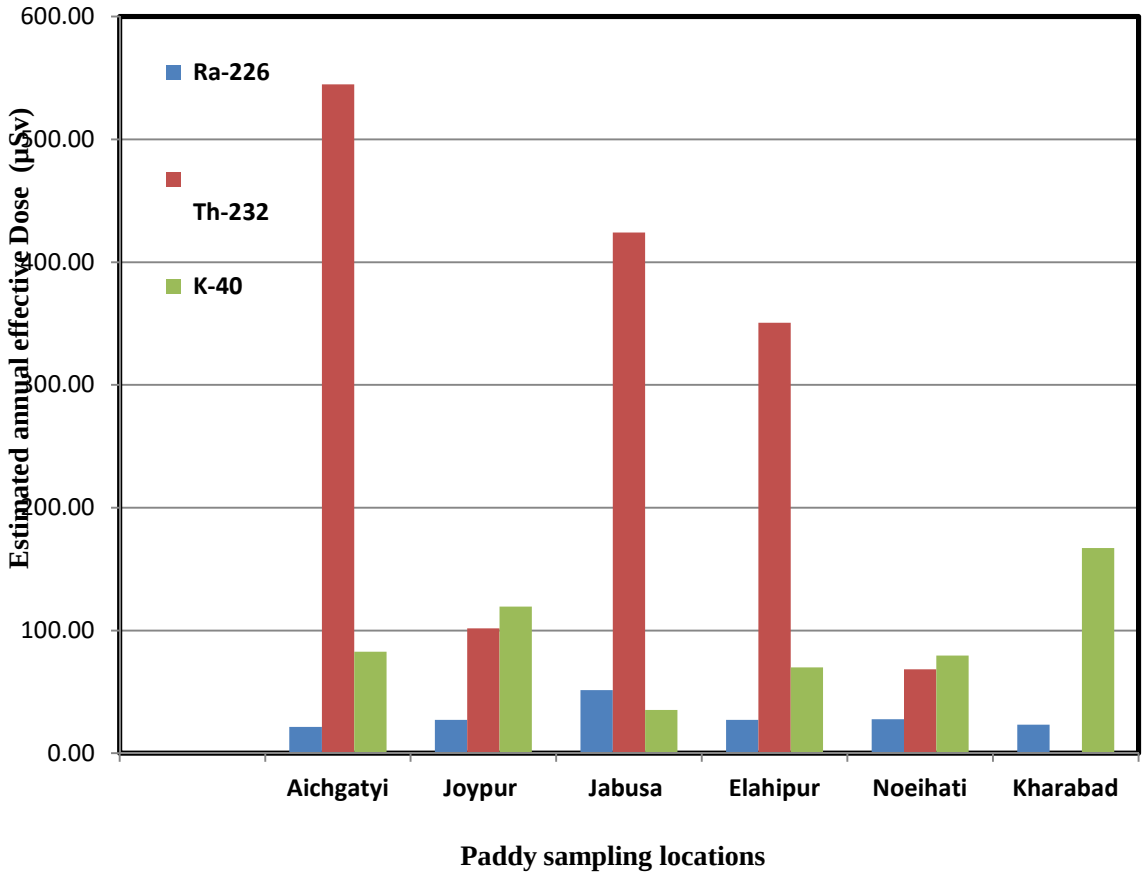

Fig 4.13: Variation of estimated Annual Effective Dose with all Paddy sampling locations.

Table 4.12: Annual intake of radionuclides in the Leafy vegetables samples and estimated annual effective Dose

Sl no.	Sampling Location	Sample ID	Annual Intake (Bq)			Annual effective dose (uSv)		
			^{226}Ra	^{232}Th	^{40}K	^{226}Ra	^{232}Th	^{40}K
1	Khan md.pur	Leafy veg. 1	33650.64	181.80	33293.16	261.73	134.53	166.47
2	Aichgati	Leafy veg.2	41996.88	156.24	22567.68	326.64	115.62	112.84
3	Joypur	Leafy veg. 3	53401.68	558.00	49431.96	415.35	412.92	247.16
4	Jabusa	Leafy veg. 4	63640.08	614.70	41734.08	494.98	454.88	208.67
5	Elahipur	Leafy veg. 5	38996.64	0.00	49617.00	303.31	0.00	248.09
6	Noeihati	Leafy veg. 6	36275.04	195.48	33768.00	282.14	144.66	168.84
7	Kharabad	Leafy veg. 7	42469.92	0.00	49433.76	330.32	0.00	247.17
Average			1231.86	243.74	39977.94	344.92	180.37	199.88

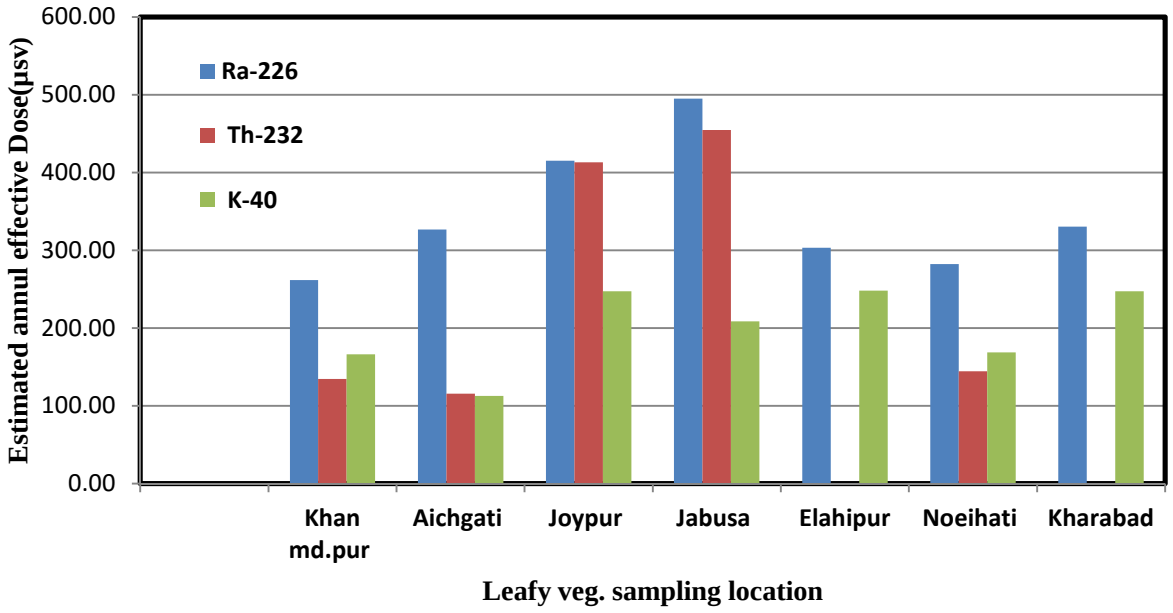

Fig.4. 14: Variation of estimated annual effective Dose with all Leafy vegetables sampling locations.

4. 6.3 Annual Effective Dose in Arum samples

The annual intakes of ^{226}Ra, ^{232}Th, and ^{40}K are estimated annual effective Dose with Arum samples has been given in Table 4.13. It has been seen that the maximum annual effective dose of ^{226}Ra, ^{232}Th and ^{40}K are 36.88 µSv in sample ID Arum 3 collected from Aichgati, 28.08 µSv in sample ID Arum 6 collected from Elahipur, and 96.05 µSv in sample ID Arum 2 collected from Khan Md.pur. Bar diagram 4.15 shows Annual effective Dose of ^{226}Ra, ^{232}Th, and ^{40}K in all Arum samples collected from various locations in the banks of Rupsha River, Khulna.

4. 6. 4 Annual Effective Dose in Papaya samples

The annual intakes of ^{226}Ra, ^{232}Th, and ^{40}K are estimated annual effective Dose with Papaya samples is given in Ttable 4.14 It is seen that the maximum annual effective dose of ^{226}Ra, ^{232}Th and ^{40}K are found 628.67 µsv in sample ID Papaya 2 collected from Khan Md.pur, 558.37 µsv in sample ID Papaya 3 collected from Aichgati, and 246.60 µsv in same sample ID Papaya 3 collected from Aichgati. Bar diagram 4.16 Shows Annual effective Dose of ^{226}Ra, ^{232}Th, and ^{40}K in all Papaya samples collected from various locations in the bank of Rupsha river, Khulna. Table 4.15 shows comparison of annual effective dose with World safe value and Table 4.16 presents annual effective dose data from foodstuffs for some countries.

Table 4.13: Annual intake of radionuclides in the Arum samples and estimated annual effective Dose

SI no.	Sampling Location	Sample ID	Annual Intake (Bq)			Annual effective dose (uSv)		
			^{226}Ra	^{232}Th	^{40}K	^{226}Ra	^{232}Th	^{40}K
1	Deara	Arum 1	0.00	0.00	15514.80	0.00	0.00	77.57
2	Khan md.pur	Arum 2	0.00	0.00	19210.65	0.00	0.00	96.05
3	Aichgati	Arum 3	131.70	0.00	10526.85	36.88	0.00	52.63
4	Joypur	Arum 4	0.00	0.00	8576.25	0.00	0.00	42.88
5	Jabusa	Arum 5	0.00	0.00	9584.10	0.00	0.00	47.92
6	Elahipur	Arum 6	0.00	37.95	6403.65	0.00	28.08	32.02
7	Noeihati	Arum 7	41.40	0.00	11759.85	11.59	0.00	58.80
8	Kharabad	Arum 8	0.00	0.00	9419.55	0.00	0.00	47.10
Average			21.63	5.42	11374.46	6.06	3.51	454.90

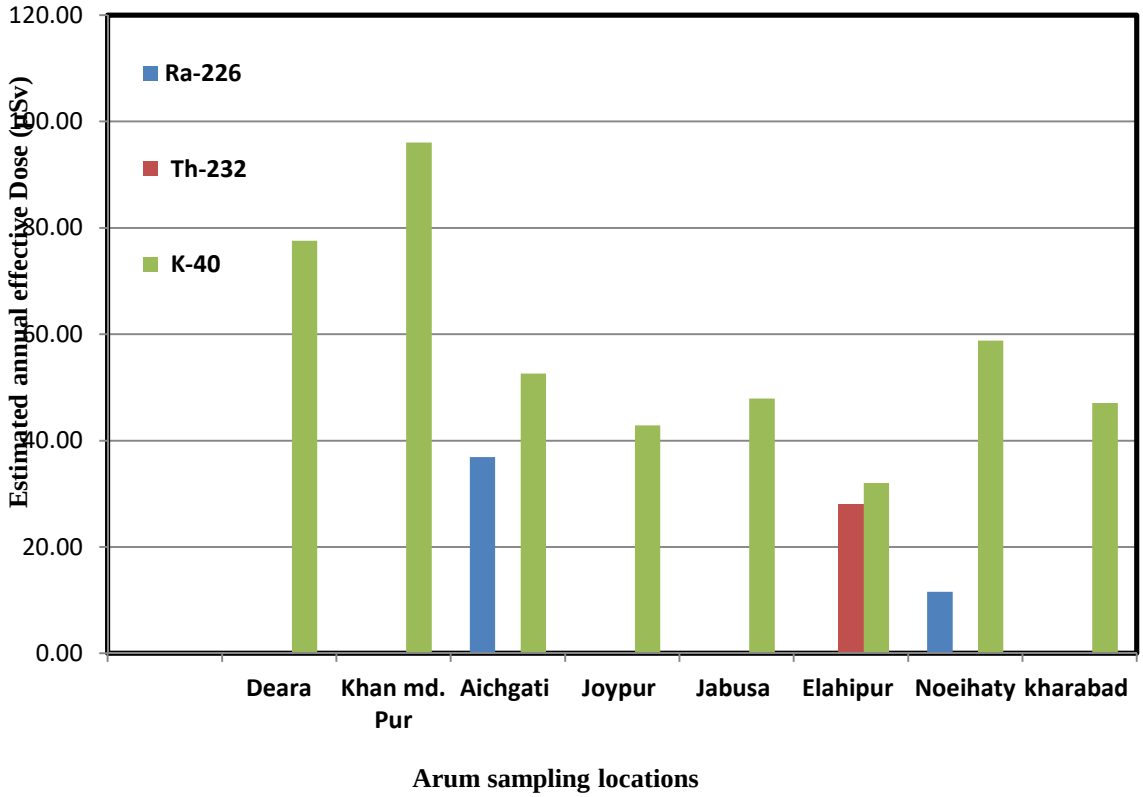

Fig 4.15: Variation of estimated annual effective Dose with all Arum sampling locations.

Table 4.14: Annual intake of radionuclides in the Papaya samples and estimated annual effective Dose

Sl no.	Sampling Location	Sample ID	Annual Intake (Bq)			Annual effective dose (uSv)		
			^{226}Ra	^{232}Th	^{40}K	^{226}Ra	^{232}Th	^{40}K
1	Deara	Papaya 1	515.23	0.00	41914.94	144.26	0.00	209.57
2	Khan md.pur	Papaya 2	2245.25	0.00	48912.19	628.67	0.00	244.56
3	Aichgati	Papaya 3	1229.18	754.56	49319.14	344.17	558.37	246.60
4	Jabusa	Papaya 4	1288.94	274.75	45732.38	360.90	203.32	228.66
5	Elahipur	Papaya 5	951.55	304.27	32044.32	266.43	225.16	160.22
6	Noeihati	Papaya 6	2117.81	0.00	47334.53	592.99	0.00	236.67
7	Kharabad	Papaya 7	382.90	0.00	35180.06	107.21	0.00	175.90
Average			1247.26	190.51	42919.65	349.23	140.97	214.59

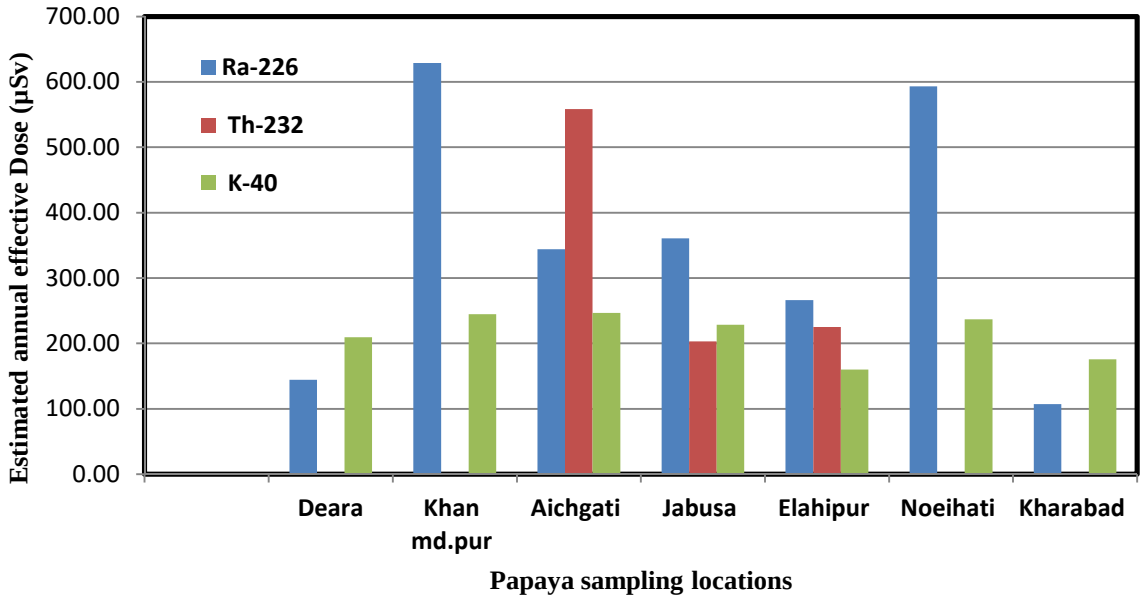

Fig 4.16: Variation of estimated annual effective Dose with all Papaya sampling locations.

4.7 Discussion

The average activity concentration of ^{226}Ra, ^{238}U, ^{232}Th and ^{40} K in all samples (Paddy, Leafy vegetables, Arum and Papaya) has been found in Table 4.2, 4.4, 4.6 & 4.6. Respectively, A comparison of the obtained value has been done with the activity concentration (Bq kg^{-1}) of the natural radio-nuclides in Rice and vegetables of different districts of Bangladesh which has also been given in Table 4.9. It shows that papaya of the study area has higher radioactivity concentration than the other parts of Bangladesh as well as than world average value for root vegetables and fruits suggested by (UNSCEAR, 2000).

Beside this, the activity concentration of ^{226} Ra in all samples (Paddy, Leafy vegetables, Arum and Papaya) of this area is higher than the other part of Bangladesh. According to a report by (UNSCER,2000) the total exposure per person resulting from ingestion of terrestrial radioisotopes should be 0.29 mSv, of which 0.17 mSv is from ^{40}K and 0.12mSv is from thorium and uranium series.

Annual effective dose of all samples (Paddy, Leafy vegetables, Arum and Papaya) has been found in Table 4.11, 4.12, 4.13 & 4.14. It shows that people intake high effective Dose of ^{226}Ra of 349.23µSvy^{-1} from Papaya samples and 344.92 µSv y^{-1} from leafy vegetables samples.^{232}Th of 248.29 µSvy^{-1} by Paddy samples & ^{40}K of 454.90 µSvy^{-1} by Arum samples. The effective dose of ^{226}Ra (0.39mSv) is high than world safe value (0.12mSv) in Papaya, The effective dose of ^{40}K (0.45mSv) is high than World safe value (0.17mSsv) in Arum and ^{232}Th (0.24mSv) is slightly than world safe value(0.12mSv) in Paddy samples ((UNSCEAR, 2000).

CHAPTER V

Conclusion

The activity concentrations and annual effective dose associated with Crops and vegetables (Paddy, Leafy vegetables, Arum and Papaya) samples collected from different locations on the Bank of Rupsha River, Khulna, Bangladesh have been investigated in the present study by using Gamma-ray spectrometry system using a Hyper-Pure Germanium (*HPGe*) detector which is a well-established and reliable method for radioactivity analysis, The results have been indicated that only the natural radionuclides (^{226}Ra, ^{232}Th and ^{40}K) are present in the samples and no artificial radionuclide has been detected in the samples. Radiological study has also been performed to obtain the annual effective dose of natural radionuclides (^{226}Ra, ^{232}Th ,^{40}K) in to human body due to intake of vegetables from high back ground radiation.

The natural radioactivity concentrations and annul effective dose of ^{226}Ra, ^{232}Th and ^{40}K for all samples (Paddy, Leafy vegetables, Arum and Papaya) are higher than the worldwide average values. The current results have been compared with the results of similar studies undertaken in other countries and in different places in Bangladesh. Average concentrations values of the radionuclides have been found in the present study are higher than those reported elsewhere. The annual effective doses due to the intake of radionuclides are also estimated using the measured activity concentration values. The estimated annual effective dose found in this study for an adult individual in Bangladesh is relatively higher than that of the world average value. However, these values of doses are much below the permissible level set by ICRP, and, therefore, there is no immediate health risk on workers and public due to natural radioactivity present in the samples of the study area.

The investigation conducted under the current study is very important concerning the radiological safety of the public and the environment in these areas. This study also provides current exposure level and base-line database for the development of future guidelines in the country.

References

Ajayi, O. S. and Owolabi, T. P., 2008: 'Determination of Natural Radioactivity in Drinking Water in Private Dug Wells in Akure, Southwestern Nigeria', Radiation Protection Dosimetry, Vol. 128, No. 4, pp. 477–484, doi:10.1093/rpd/ncm429.

Asimov and Isaac, B. 1976: "The Explosions within Us". Only A Trillion (Revised and updated ed.). New York: ACE books. pp. 37–39. ISBN 1-157-09468-6.

Balles, R. C. and Sallow, J. E., 1951: USAEC Report, "Health and Safety Information" USNR, vol. 123, pp 456-457.

Bhuiyan, M. R., 2009: Assessment of Radioactivity Releasing from Uranium, Thorium and their Daughters and 40K in Fertilizers and Soil using HPGe Digital Gamma Spectrometry System, M. Sc. Thesis. Department of Physics, Jahangirnagar University.

Bruzzi, L., Baroni, M., Mazzoti, G., Mele, R. and Righi, S., 2000: Radioativity in raw materials and end products in the Italian ceramincs industry, J. Environ. Radioact, 47, pp.171-181.

Canberra Product Catalog, Edition 12.(http://www.canberra.com/products/831.asp). PGT HPGe Detector Operating Manual, Princeton Gamma Tech. (PGT) Inc., U.S.A.

Cember, H., 1989: Introduction to Health Physics, second edition (revised), Northwestern University, Maxwell Macmillan International Editions, published by Pergamon Press.

Chang Kyu Kim, 1990: Radioanalytical and Environmental Studies on Long-Lived Radionuclides, D. Sc. Thesis, Department of Chemistry, University of Tsukuba.

Clark, S. P., Peterman, Z. E. and Heier, K. S., 1966: Abundance of Uranium, Thorium and Potassium, Handbook of Physical Contents,(revised edition) Grol, Soc, Am, Mem, vol. 97,pp 521- 541.

Debasish Paul, 2007: " Biological Effects of Ionizing Radiation" in the 49th training course on radiation protection for radiation control officiers (RCOs) of diagnostic X-ray installations held at the Atomic Energy Center(AEC) Audiotorium, BAEC,Dhaka.

Debertin, K. and Helmer, R.G., 1988: Gamma and X-ray Spectrometry with Semiconductor Detectors, North Holland Publishing Company, Elsevier Science Publishers B. V. Amsterdam, The Netherlands, . pp 16-22.

Ele Abiama, P., Ben-Bolie, G. H., Amechmachi, N., Najibb, F., El Khoukhi, T., and Owono Ateba, P., 2012: "Annual intakes of (226)Ra, (228)Ra and (40)K in staple foodstuffs from a high background radiation area in the southwest region of Cameroon." journal of Environmental Radioactivit.vol. 101, pp.59-63.

Eric, B., 1965: Radioactive Fallout, Soils, Plants, Foods, Man, Flower Amsterdam Elsevier,

FAO, 2000: Food Balance Sheets, Food and Agriculture Organization of the United Nations.

Harb, S., Din, K. S. and Abbady, A., 2008: Study of efficiency calibrations of HPGe detectors for radioactivity measurement of environmental samples. Preceding of the 3rd Environmental Physics Conference, Aswan, Egypt.

Hariandra, M., Amin, Y. M., 2008: "Transfer of Radionuclides K-40, Th-232 and Ra-226 from Mining Soil to Sawi (Japanese Mustard).CURRENT ISSUES OF PHYSICS IN MALAYSIA: National Physics Conference 2007 - PERFIK 2007. AIP Conference Proceedings, Volume 1017, pp. 245-249.

Hendry, Jolyon, H., Simon, Steven, L., Wojcik, Andrzej; Sohrabi, Mehdi; Burkart, Werner; Cardis, Elisabeth, Laurier, Dominique; Tirmarche, Margot; Hayata, Isamu, 2009: "Human exposure to high natural background radiation: what can it teach us about radiation risks?". Journal of Radiological Protection 29 (2A): A29–A42.

IAEA, 1989: Measurement of radionuclides in food and the environment. International Atomic Energy Agency, Technical Reports Series no 295, Vienna.

ICRP, 1977: Publication 26, Recommendations of the International Commission on Radiological Protection, Volume 1, No. 3, Published in the Annals of the ICRP, Pergamon Press, Oxford.

ICRP, 1996: Age-dependent Doses to the Members of the Public from Intake of Radionuclides Part5, Compilation of Ingestion and Inhalation Coefficients.International Commission of Radiological Protection Publication 72. Pergamon Press, Oxford.

ICRU, 1925: the International Commission on Radiological Units recommendation, Published in the Annals of the ICRU.

Imrose Jahan, 2015: "Study on the distribution of natural and probable artificial radioactivity in the environmental element in the low-land area of Ashulia, Saver". M .Sc Thesis, Department of Physics, Jhangirnagar University, Bangladesh.

Islam, A., Begum, A., Yeasmin, S. and Sultana, M. S., 2014: **"**Assessment of dose due to natural radionuclides in vegetables of high background radiation area in south-eastern part of Bangladesh". International Journal of Radiation Research, July, Volume 12, No 3.12 (3):271-275.

Jibiri, NN., Farai IP., Alausa SK., 2007: "Activity concentrations of (226) Ra, (228) Th, and (40) K in different food crops from a high background radiation area in Bitsichi, Jos Plateau, Nigeria." Radiation and Environmental Biophysics vol. 46,pp 53-59.

Johns, H.E. and Cunningham J.R., 1964: The Physics of Radiology, publication no. 743, American Lecture Series, published by Thomas C.C, vol. 24 pp 312-384.

Kannan, Rajan, V., Lyengar, M. P. and Ramesh, R., 2002: Distribution of natural and anthropogenic rodionuelides in soil and beach sand Samples of Kalpakkam (India), Appl. Rodiat. Isot. 57, 109-119

Kaplan Irving, 1964: Nuclear Physics, Department of Nuclear Engineering, MIT, 2nd Edition, Addison-Wesley Series in Nuclear Science and Engineering, Addison-Wesley Publishing Company, Inc.

Knoll, G. F., 1989: "Radiation Detection and Measurement", 3rd edition, John Wiley and Sons, 388-89.

Koddis, A., Rahman, M. M., Ali, M. L., Alam M. N., 1992: Characteristics of a Shielding Arrangement for a HPGe Detector Designed and Fabricated Locally at Health Physics & Radioactive Waste Management Unit, INST, AERE, Savar, Dhaka.

Kohman, T. P., 1959: Natural Radioactivity, Radiation Hygiene Hand-Book, Edited by H. Blatz, Mcgraw-Hill, , pp. 6-6 To 6-13.

Liton Miah, 2012: “Investigation of Natural and Probable Artificial Radioactivity in Marine Fish Samples after Nuclear Power Plant Accident in Japan and Comparison of the results with Fresh Water Fishes” M .Sc Thesis, Department of Physics, Jhangirnagar University, Bangladesh. pp 85-87.

Martin Alan and Samuel A. Harbison, 1979: An Introduction to Radiation Protection, 2nd Edition, published in the U.S.A. by Chapman and Hall in association with Meuthuen Inc., New York. pp. 18-88.

Muzibur Rahman, 1991: Fallout and natural radioactivity in the sand samples of coastal areas and in the rock samples of Northern-Eastern part of Bangladesh, M.Sc. Thesis, Department of Physics, Jahangirnagar University.

Nazrul Islam, K. M., 2009: Natural Environmental Radiation Studies on Sand and Soil Samples from Kuakata Sea Beach of Patuakhali, M.Sc. Thesis, Dept. of Physics, Jahangirnagar University.

NCR, 1994: Report No. 58, A Hand Book of Radioactivity Measurements Procedures, 2nd Edition, Published by National Council on Radiation Protection and Measurements, 1994, 7910 Woodmount Avenue.

Nusrat Jahan Shirin, 2013: “Study on natural and artificial radioactivity in sand and adjacent soil samples collected from the Patenga Sea Beach, Chittagong”. M .Sc Thesis, Department of Physics, Chittagong University, Bangladesh.

Quindos, L. S., Rodenas, C., Fernandez, L. And Soto, J., 1992: Estimate Of External Gamma Exposure Outdoors in Spain, Radiation Protection Dosimetry, Volume 45 (1992), pp. 527, MerrilEisenbud, Environmental Radioactivity from Natural, Industrial and Military Sources, 3rd Edition (1987), Academic Press Inc.

Roessier, C. E., Smith, Z. A., Bloch, W. E. and Prince, R. J., 1970: Uranium and radium in Floride phosphate materials. Health Physics, vol. 37, pp. 269-277.

Roy. P. K., 1991: Radioactivity in soil of Chittagong hills, M.Sc. Thesis Department of Physics, Chittagong University, Bangladesh.

Rubin, P. and Casarett, G. W., 1968: Clinical Radiation Pathology (Philadelphia: W. B. Sa radiation protection groups unders.).

Shahbazi-Gahrouei, D., Gholami, M., Setayandeh, S., 2013: “A review on natural background radiation.” J. Advanced Biomedical Research, vol. 2, pp. 65 DOI: 10.4103/2277-9175.115821.

Strom, P.O., 1958: Long Lived Cobalt Isotopes Observed in Fallout, Science, Volume 128 pp. 417.

Sullivan, S., 1957: Trilinear Chart of Nuclides, Government Printing Office, Washington D. C.

Tuo, F., Zhang, Q., Zhou, Q., Xu, C., Zhang, J. Li. W., Zhang, J., Su, X., 2016: “Measurement of (238)U, (228)Ra, (226)Ra, (40)K and (137)Cs in foodstuffs samples collected from coastal areas of China.” ;111:40-4. doi: 10.1016/j.apradiso.

UNSCEAR, 2000: Sources and effects of ionizing radiation, Report of the United Nations Scientific Committee on the Effects of Atomic Radiation to the General Assembly, United Nations, New York, USA, Annex.

Usif, M.A. and Taher, A. E., 2008: Radiological assessment of Abu-Tartur phosphate, western desert Egypt, Radiation Protection Dosimetry, vol.130, pp.228-235.

Vahid CHANGIZI, Elham SHAFIEI, and Mohammad Reza ZAREH, 2013: “Measurement of ^{226}Ra, ^{232}Th, ^{137}Cs and ^{40}K activities of Wheat and Corn Products in EIlam Province – Iran and Resultant Annual Ingestion Radiation Dose” .Iran J Public Health. 2013 Aug; 42(8): 903–914.

Wilkinson, D.W., 1950: ‘Semiconductor Detectors Spectrometer”. Proc-phil, Soc.46, pt.3,pp. 508.

Yeasmin, S. and Begum, A. 2012: Distribution of radioactive levels of environmental samples from different upazilla of Bangladesh, Bangladesh Journal of Physics,II.

Zhang, S. P., 2012: "Mechanism study of adaptive response in high background radiation area of Yangjiang in China". Zhonghua Yu Fang Yi Xue Za Zhi (Europe PubMed Central) 44: 815–9. PMID 21092626.